

University of Denver

Digital Commons @ DU

Electronic Theses and Dissertations

Graduate Studies

1-1-2011

Solar Power System Modeling and Performance Analysis

Jiaqi Wang

University of Denver

Follow this and additional works at: <https://digitalcommons.du.edu/etd>



Part of the [Power and Energy Commons](#)

Recommended Citation

Wang, Jiaqi, "Solar Power System Modeling and Performance Analysis" (2011). *Electronic Theses and Dissertations*. 689.

<https://digitalcommons.du.edu/etd/689>

This Thesis is brought to you for free and open access by the Graduate Studies at Digital Commons @ DU. It has been accepted for inclusion in Electronic Theses and Dissertations by an authorized administrator of Digital Commons @ DU. For more information, please contact jennifer.cox@du.edu, dig-commons@du.edu.

Solar Power System Modeling and Performance Analysis

A Thesis

Presented to

The Faculty of Engineering and Computer Science

University of Denver

In Partial Fulfillment

of the Requirements for the Degree

Master of Science

by

Jiaqi Wang

August 2011

Advisor: Prof. WenZhong Gao

©Copyright by Jiaqi Wang 2011

All Rights Reserved

Author: Jiaqi Wang
Title: Solar Power System Modeling and Performance Analysis
Advisors: WenZhong Gao
Degree Date: August 2011

Abstract

At present the main source of our power and energy needs are from fossil fuel; almost all transportation tools and nearly 70% of electrical power are produced by fossil fuel. But unfortunately these materials are limited in our planet, with obvious drawback such as pollution. So looking for new kinds of energy supply is an urgent matter. Solar-powered photovoltaic system provides a clean energy solution to this problem. It is developing fast all over the world in terms of both research work and actual applications. It is estimated that the power supplied by solar energy can provide 10 percent of United States power needs. This thesis mainly discusses photovoltaic system modeling from the beginning of site selection to system sizing. Some tools are used during the project. A GIS application is used to help developers in the preliminary studies. Photovoltaic system simulation software PVsyst involves the system components setting and sizing process. Two types of systems are built in this study: stand-alone system and grid connected system; the location is set at Denver, Colorado. For each system the array mounting, analysis of loads and modules selection are studied. The simulation is performed after the system model is completed, the results includes loss diagrams, system energy yields and system efficiencies. At last the economic analysis and comparison between the two types of PV systems is analyzed.

Acknowledgments

I would like to thank Professor Wenzhong Gao for his guidance during the thesis completion. He gave me the direction and ideas about the study of photovoltaic system as a topic of the thesis. I get not only the theoretical knowledge but also spirit when doing research. To Dr. Yunbo Yi and Dr. Mohammad Matin, thanks them for serving as my thesis committee members. I also would like to thank my parents for their support and help during my study.

Table of Contents

Chapter one: Solar radiation	1
1. Solar radiation	1
1.1 Basic concepts of solar radiation.....	1
1.2 Tilt and azimuth angle of the panel.....	8
1.3 Solar radiation calculation.....	10
Chapter two: GIS implementation for estimating photovoltaic system	14
2.1 Introduction.....	14
2.2 Introduction of PVGIS.....	15
2.2.1 Database and models of PVGIS	16
2.3 Web applications.....	21
2.4 Using online calculators.....	28
2.5 Example and results	29
2.6 Conclusion	32
Chapter Three: Stand alone system design principles	33
3.1 PV modules.....	33
3.1.1 I-V curve	33
3.1.2 Device response	34
3.1.3 Module connections.....	36
3.1.4 Bypass diodes	37
3.1.5 PV module modeling	38
3.1.6 PV cell materials	40
Chapter four: Photovoltaic System components.....	42
4.1 batteries	42
4.1.1 Introduction.....	42
4.1.2 Battery capacity.....	43
4.1.3 Battery types	44
4.1.4 Battery selection	45
4.2 Battery charge controllers	48
4.2.1 Overcharge protection	48
4.2.2 Overdischarge protection.....	48
4.3.3 Charge controller setpoints	49
4.4 Type of charge controllers	53
4.4.1 Shunt charge controller	53

4.4.2 Series charge controllers	54
4.4.3 Maximum power point tracking (MPPT) charge controllers	55
4.4 Loss in PV systems	57
4.4.1 Array incidence loss (IAM loss).....	57
4.4.2 Array mismatch loss	57
4.4.3 Wiring loss	58
4.4.4 Array thermal losses.....	58
4.4.5 Soiling loss	59
4.5 Inverters	59
4.5.1 DC-DC converters:	60
4.5.2 Maximum power point trackers (MPPT)	60
4.5.3 Inverter characteristics.....	60
Chapter five: Stand-alone system design using PVsyst software	67
5.1 Introduction of PVsyst Software	67
5.2 Geographical and meteorological data	69
5.3 Orientation:	73
5.4 Stand-alone system sizing	77
5.4.1 Load analysis	77
5.4.2 Array and battery sizing.....	83
5.4.3 Charge controllers	95
5.4.4 Array losses in PVsyst.....	97
Chapter six: Grid connected system design	102
6.1 Grid-connected system sizing.....	102
6.1.1 Insolation.....	103
6.1.2 System AC energy needs	103
6.1.3 Inverter sizing	103
Chapter seven: Simulation using PVsyst.....	106
7.1 Simulation process	106
7.2 Results	108
7.2.1 Stand-alone system results.....	108
7.2.2 Grid-connected system simulation results	112
Chapter eight: Economic analysis.....	120
8.1 Cost analysis	120
8.1.1 Initial costs.....	121
8.1.2 Maintenance costs	121
8.1.3 Energy costs.....	122

8.1.4 Repair and replacement costs	122
8.1.5 Salvage value	122
8.2 Life-cycle cost analysis.....	122
8.3 Economic evaluations by using SAM (System Advisor Model).....	125
8.3.1 Financing settings.....	125
8.3.2 Annual system performance	126
8.3.3 PV system costs	126
8.3.4 Solar array inputs	127
8.3.5 Electric load	128
8.4 economic results	128
Chapter nine: Conclusion	131

List of figures

Figure1. 1: Solar radiation from sunrise to sunset.....	2
Figure1. 2: Average photovoltaic resource of United States [1].....	2
Figure1. 3: Radiation constituents: direct, diffuse and reflected	4
Figure1. 4: Schematic diagram of AM (air mass).....	5
Figure1. 5: Declination angle.....	6
Figure1. 6: Altitude angle and azimuth angle	7
Figure1. 7: Altitude angle calculation [5]	8
Figure1. 8: optimal tilt angle due to time variation of year	9
Figure 2. 1: solar radiation map in Europe	23
Figure 2. 2 application inputs window	24
Figure2. 3: estimated PV output for the same location	31
Figure2. 4: estimated solar irradiation for the same location	31
Figure 3.1: I-V curve of PV modules	33
Figure3.2: solar irradiance response	35
Figure3.3: voltage will drop due to temperature increase.....	36
Figure 3.4: current output for similar devices and dissimilar devices.....	37
Figure3.5: I-V curves of modules in parallel	37
Figure3.6: Bypass diode	38
Figure3.7: One diode model.....	38
Figure4. 1: relationship between capacity and temperature	43
Figure4. 2: batteries are connected in series	46
Figure4. 3: batteries are connected in parallel.....	47
Figure4. 4: series and parallel connections are combined together.....	48
Figure4. 5: Voltage regulation and array reconnect setpoint.....	51
Figure4. 6: low-voltage disconnect setpoint and reconnect voltage setpoint	53
Figure4. 7: Shunt Interrupting Controller.....	54
Figure4. 8: Series Controller Design	55
Figure4. 9: Maximum power point tracking.....	56
Figure4. 10: Current voltage curve of mismatch effect.....	58
Figure4. 11: Inverters limit the power output by reducing voltage	61
Figure4. 12: The operating input range and their maximum power point.....	63
Figure4. 13: The relationship of utility and array voltage	64
Figure4. 14: Input currents are reduced when voltage rises.....	65
Figure4. 15: Inverter efficiency of different power rating	66
Figure5. 1: system components selection in project design	68
Figure5. 2: Locations of TMY3 ground stations [26].....	70
Figure5. 3: Setting Albedo values	73
Figure5. 4: fixed mount array	74
Figure5. 5: Adjustable tilt mounting.....	75
Figure5. 6: vertical axis tracking	75
Figure5. 7: one axis tracking.....	75
Figure5. 8: two axis tracking mounting	76
Figure5. 9: two axis horizontal axis N-S east to west	76
Figure5. 10: plane optimization for yearly irradiation yield	77
Figure5. 11: domestic appliance power consumption settings for January.....	82

Figure5. 12: loads energy consumption for July.....	82
Figure5. 13: Loss of load probability can be roughly determined by insolation and autonomy. ...	84
Figure5. 14: DC system voltage and Current	85
Figure5. 15: battery capacity is affected by discharge rate and temperature.....	87
Figure5. 16: Battery basic parameters sizing.....	87
Figure5. 17: battery discharge rate	89
Figure5. 18: choosing PV modules	92
Figure5. 19: I/V characteristics given under irradiance of $1000\text{W}/\text{m}^2$, temperature 25°C	93
Figure5. 20: ND-72 ELU I-V curve under different irradiance.....	94
Figure5. 21: PV module behavior with different temperature.....	95
Figure5. 22: wiring loss setting.....	98
Figure5. 23: mismatch loss of PV module: ND-72 ELU of Sharp.....	99
Figure5. 24: array losses effect.....	100
Figure 6. 1: Array voltages setting	105
Figure 6. 2: Array Ohmic loss for grid-connect system.....	105
Figure7. 1: loss diagram of stand-alone system	111
Figure7. 2: normalized productions of the stand-alone system.....	112
Figure7. 3: loss diagram of grid-connected system	116
Figure7. 4: Grid-connected system normalized production	117
Figure8. 1 Financing setting page.....	125
Figure8. 2 PV system costs setting page.....	127
Figure8. 3 Operation and maintenance costs	127
Figure8. 4 The total cost of a PV system.....	129

List of tables

Table1. 1 Albedo of different ground surface.....	12
Table2 1: System energy production estimate	30
Table3.1: gap energy for different materials [20].....	39
Table3.2: PV material efficiencies.....	41
Table4. 1: lead-acid batteries characteristics [22].....	45
Table4. 2: Battery selection criteria.....	45
Table4. 3: voltage regulation setpoint for different type of batteries [23]	49
Table5. 1:Date: June 21 st :	71
Table5. 2: Date: December 21 st :	71
Table5. 3: AC loads analysis of July:.....	79
Table5. 4: Critical design analysis	81
Table5. 5: Battery sizing parameter.....	88
Table5. 6: array sizing parameters.....	91
Table5. 7: module selection	92
Table5. 8: charge controller setpoints	96
Table5. 9: Losses effect.....	101
Table6. 1: PVIN02KS main parameter.....	104
Table 6. 2: Array sizing.....	104
Table 6. 3: operating conditions	104
Table7. 1: Meteorological and irradiation data	108
Table7. 2: Battery bank performance:.....	109
Table7. 3: system energy production and consumption	109
Table7. 4: Inverter performance.....	113
Table7. 5: Energy yield of grid-connected system	114
Table7. 6: System efficiency	115
Table7. 7: Stand-alone system normalized performance coefficients.....	118
Table7. 8: Grid-connected system normalized performance coefficients.....	118
Table8. 1: Life-cycle costs of stand-alone system	123
Table8. 2: life cycle costs of grid-connected system:.....	124
Table8. 3 Results of the PV system simulation	128

Chapter one: Solar radiation

1. Solar radiation

Choosing a suitable location is the beginning step of a photovoltaic system design and is very important. Even a well-established solar system with good component parameters and configuration cannot have desired power output if it is not installed at an appropriate place. Generally speaking, the solar panels should insolate under sunlight for at least six hours each day; so the study of solar radiation and its properties is essential.

1.1 Basic concepts of solar radiation

1.1.1 Definition of solar irradiation

Solar irradiation is the product of solar irradiance (Watts per square meter) and time (hour). So solar irradiation has a unit of Watt-hours per square meter. It can also be denoted by insolation. The figure below shows the variation of solar radiation during a certain day.

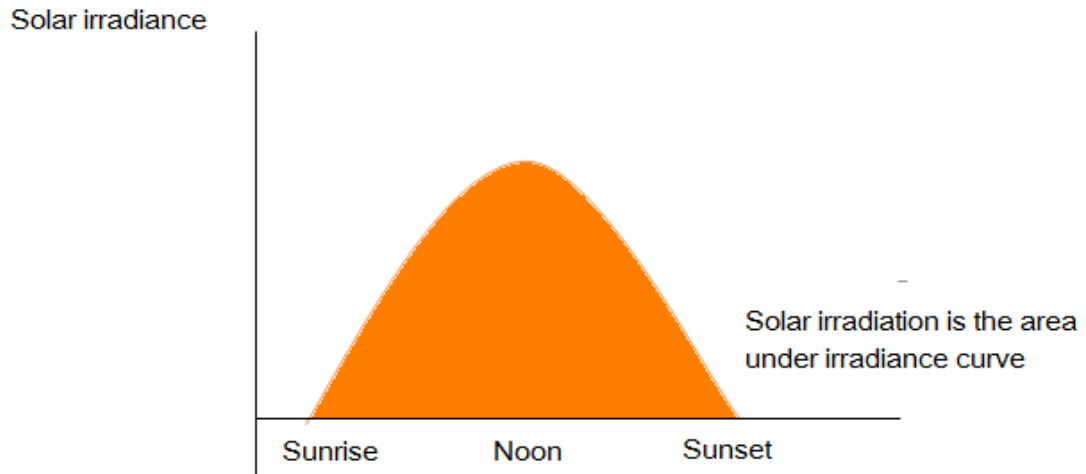


Figure1. 1: Solar radiation from sunrise to sunset

Peak sun hour is the total number of hours of a day that can receive radiation; it is an equivalent form of insolation and most radiation data is represented using either of these units expressed as kWh/m²/day. The figure below shows the annual insolation map of the United States.

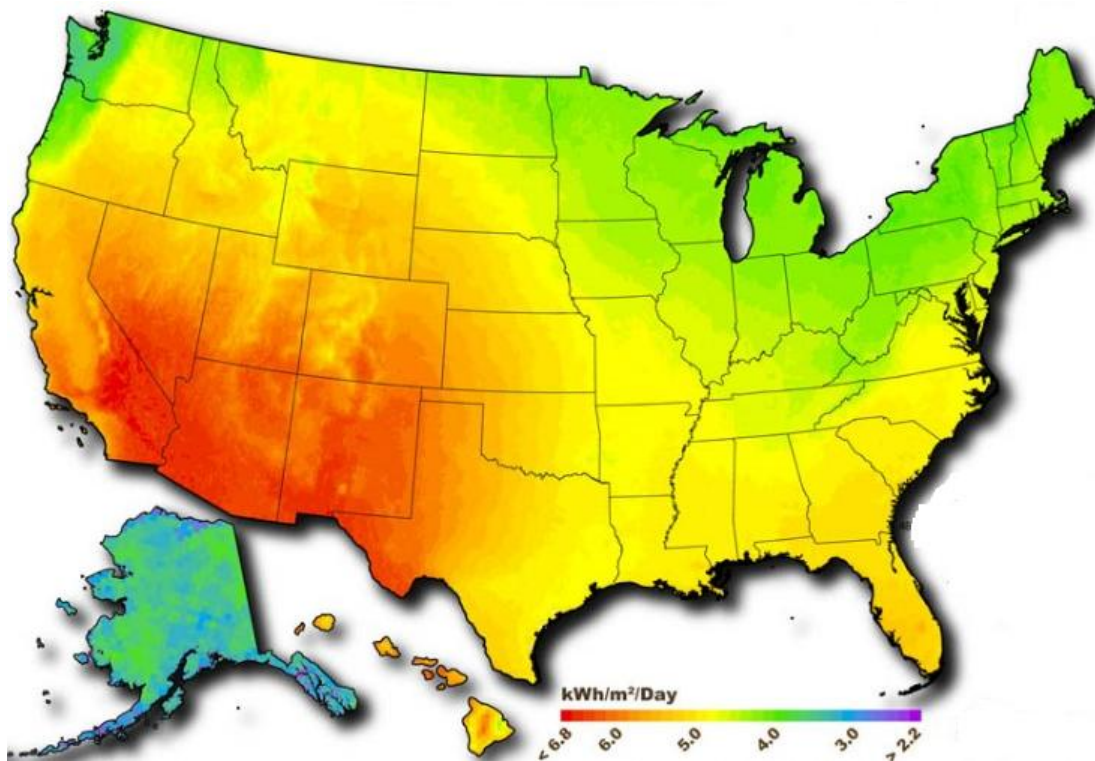


Figure1. 2: Average photovoltaic resource of United States [1]

1.1.2 Direct, diffuse and reflected radiations

In photovoltaic technologies people are more interested in terrestrial radiation which is the amount of radiation reaching the ground surface. The radiation originating from the sun will be affected by some factors while traveling through earth atmosphere.

When sunlight passes through the atmosphere, attenuation will be caused by the following phenomena:

- a. Rayleigh scattering [2] by small particles in the atmosphere;
- b. Scattering by aerosols and dusts;
- c. Absorption in the atmosphere, such as ozone absorbs at high energies and water vapor, carbon dioxide absorb infrared [3].

The original radiation is divided into direct, diffuse and reflected radiation after scattering and absorption [2]. Direct radiation is the radiation that reaches the earth surface without scattering; diffuse radiation is scattered by atmosphere and clouds, and the radiation reflected from ground features is called reflected radiation. The summation of these three kinds of radiation composes global radiation. In practice, reflected radiation is much less than the other ones, so usually it can be ignored.

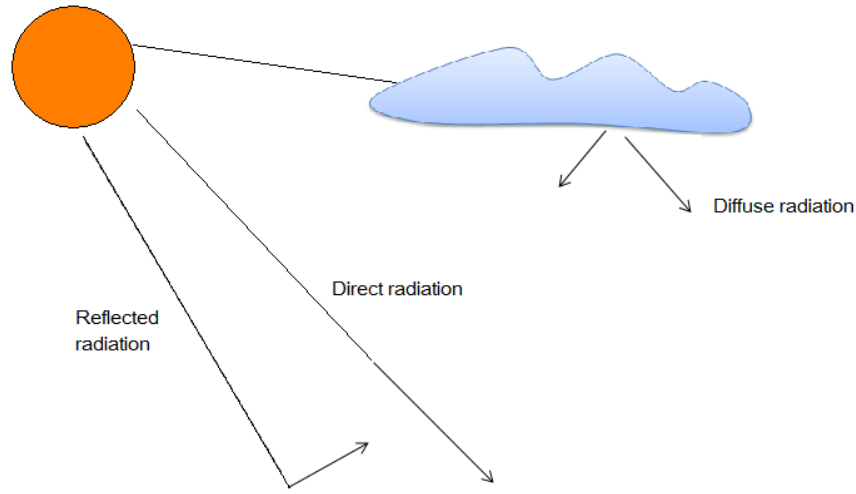


Figure1. 3: Radiation constituents: direct, diffuse and reflected

1.1.3 Air mass

If the sky is clear, the maximum radiation will be received by the ground when the sun is directly overhead or called zenith; in this case the sunlight has the shortest pathlength. This pathlength is approximated as $1/\cos\theta$; θ is the angle between the actual position of the sun and the position when the sun is directly overhead. The pathlength is called air mass represented by AM and thus is determined as:

$$AM=1/\cos\theta \quad (1-1)$$

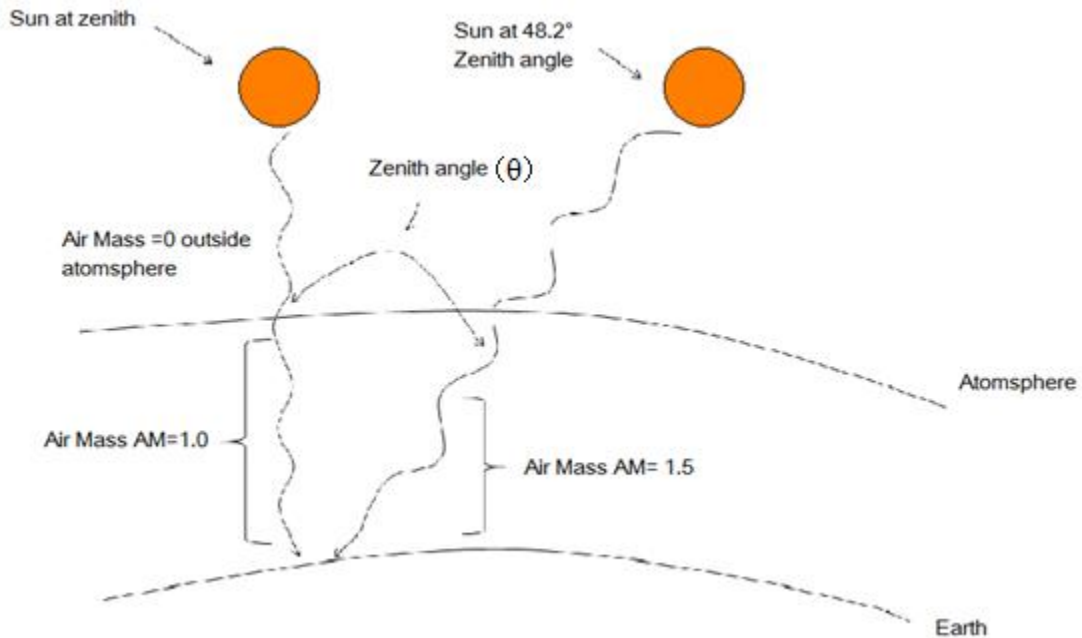


Figure 1. 4: Schematic diagram of AM (air mass)

When $\theta=48.2^\circ$ the air mass equals 1.5; AM1.5 is the standard terrestrial solar spectrum.

1.1.4 Angular influence in solar radiation

Besides atmosphere factors that affect radiation, there are other movements affecting the results. They are angular considerations caused by the rotation of earth around the sun and the axis of itself. When earth rotates around the sun, it forms two planes due to the difference of its orbit around the sun and its tilted axis. The plane of the orbit around the sun is called ecliptic plane and the plane parallel with equator is called equatorial plane. Therefore the angle between ecliptic plane and equatorial plane is declination angle.

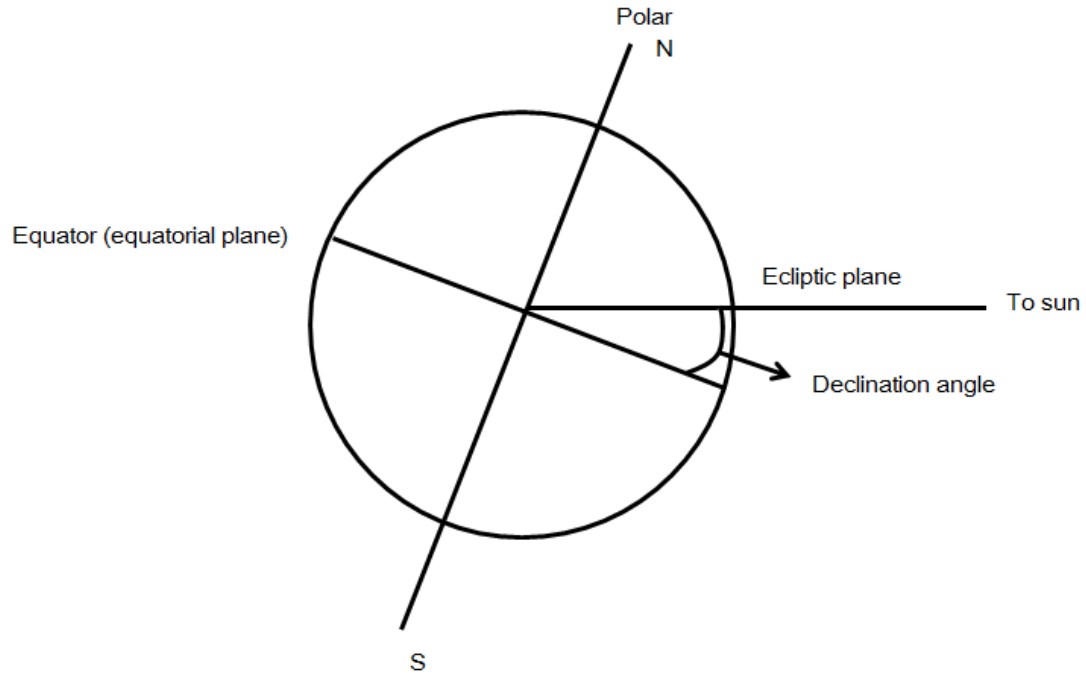


Figure1. 5: Declination angle

The declination angle is changes periodically through a year due to the movements of the earth. The maximum and minimum value of declination occurs at summer and winter solstice with the angle of 23.45° and -23.45° , respectively. It can be calculated in the following equation [4]:

$$\delta = 23.45 \sin \left(360 \frac{284+n}{365} \right) \quad (1-2)$$

Where n is the number of day from 1 (Jan 1st) to 365 (Dec 31st). On equinoxes the declination will get the value of zero.

The altitude angle (elevation angle) is the angle between the sun and the horizon. It varies through the day which equals 0° at sunrise and reaches its maximum value at solar noon. Azimuth angle is the horizontal angle between the sun and a reference direction. Normally the reference direction is north or south.

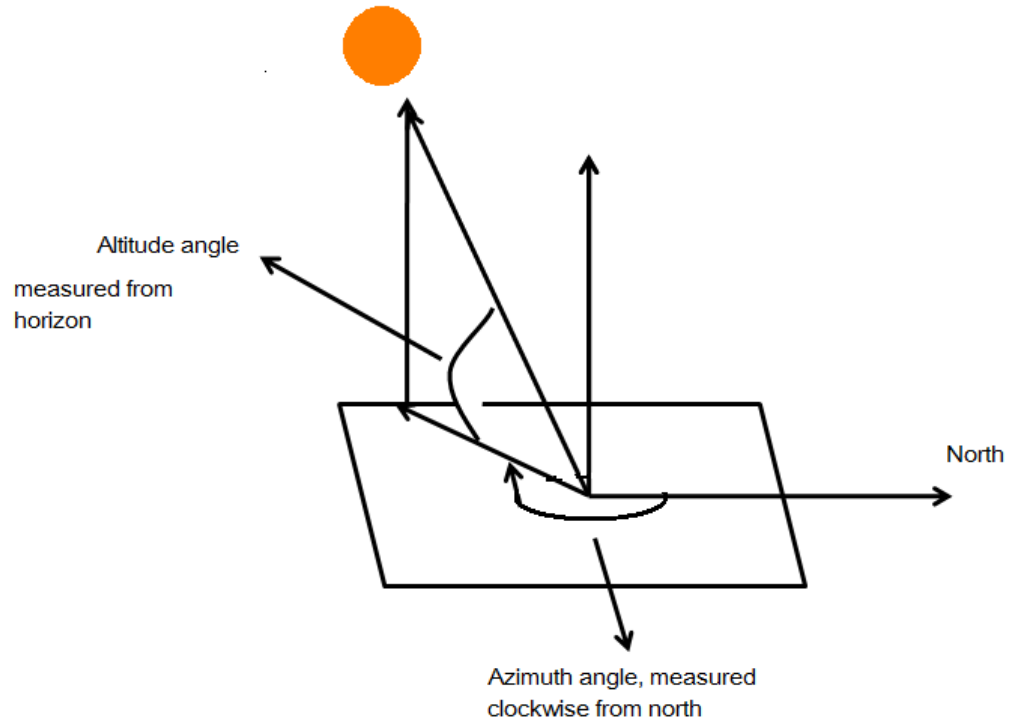


Figure1. 6: Altitude angle and azimuth angle

The value of altitude angle depends on latitude and time of year. The following equation can be used to determine the altitude angle [3]:

$$\alpha = 90^\circ + \varphi - \delta \quad (1-3)$$

where: δ is the declination angle derived from equation (2), φ is the latitude and α represents altitude angle.

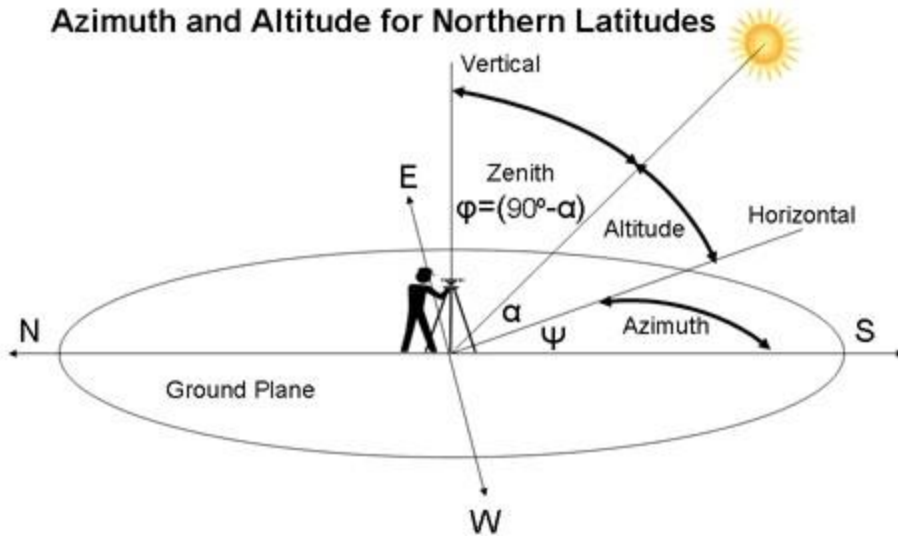


Figure1. 7: Altitude angle calculation [5]

The azimuth angle can be calculated as follows [6]:

$$\Psi = \arcsin \left(\frac{\cos \delta \sin \omega}{\cos \alpha} \right) \quad (1-4)$$

where δ is the declination angle and ω is the solar hour angle with negative value in the morning and positive value in afternoon, α is altitude angle.

Solar zenith angle is the angle between the sun and the vertical axis from the earth; it can be calculated by the equation below:

$$\cos \theta_z = \sin \delta \sin \phi + \cos \delta \cos \phi \cos \omega \quad (1-5)$$

where δ is declination angle and ϕ the latitude, ω is the solar hour angle.

1.2 Tilt and azimuth angle of the panel

The orientation of the solar panel is a very important factor for determining the electrical power output. There are two parameters affecting orientation: array tilt angle and array azimuth angle. Tilt angle is the angle between the panel plane and the horizontal surface. Azimuth angle is the angle between the reference direction (typically south in northern hemisphere) and array facing direction.

Generally speaking, the optimal tilt angle of an array should be the latitude of where it is located, so in high latitude area the array tilt angle is larger than low

latitude areas, however, due to the variation of climate and solar declination angle, there is often an adjustment of the tilt angle. For instance, on summer solstice the tilt angle should decrease because the declination achieve a maximum value of 23.5° while on winter solstice the tilt angle increases.

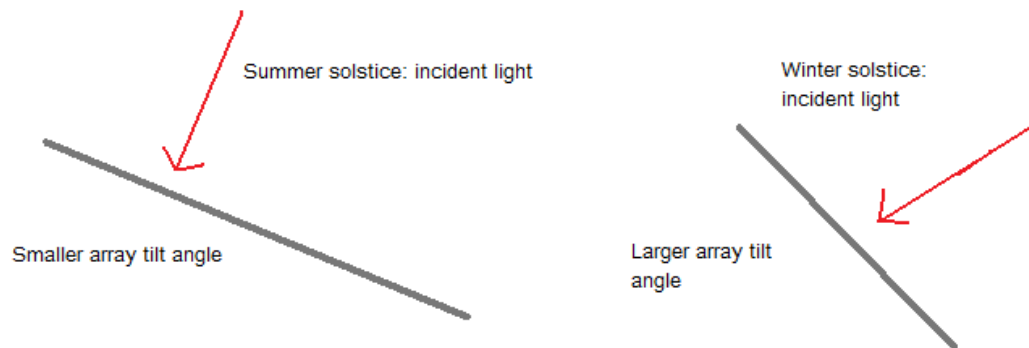


Figure1. 8: optimal tilt angle due to time variation of year

The optimal azimuth angle for northern hemisphere is due south. Deviation from south direction will result in decrease of solar power production and this decrease becomes worse with larger tilt angles, so it should be noted when building PV system in high latitude areas. In lower latitude area this reduction is in an acceptable range.

The collector will have maximum radiation when incident light is perpendicular to the panel, but with the change of the position of the sun, a fixed mounted solar panel can only get maximum insolation during part time of a day. To get higher radiation levels, tracking systems is introduced. It uses axis to fix the solar panel an then it allows the panel to adjust the tilt and azimuth angle according to the current position of the sun. In one-axis tracking system, the panel can rotate around the vertical axis to change its azimuth. Two-axis tracking can make the panel facing the sun by adjusting two axes simultaneously to receive better radiation.

1.3 Solar radiation calculation

1.3.1 Sunset hour angle

Sunset hour angle is the angle at the time of sunset. It is represented by ω_s and can be calculated by the following equation [7]:

$$\cos\omega_s = -\tan\phi\tan\delta \quad (1-6)$$

where ϕ is the latitude of the location and δ is the declination angle.

1.3.2 Extraterrestrial radiation

Extraterrestrial radiation is solar radiation outside Earth's atmosphere. It is required to know the quantity and characteristics of extraterrestrial radiation. Daily value of extraterrestrial radiation is calculated as follows:

$$H_0 = \frac{86400G_{sc}}{\pi} \left[1 + 0.033 \cos \left(2\pi \frac{n}{365} \right) \right] (\cos\phi\cos\delta\sin\omega_s + \omega_s\sin\phi\sin\delta) \quad (1-7)$$

In the above equation, G_{sc} is the solar constant with the value of 1367W/m^2 , ϕ is the latitude of calculated position, δ is the declination angle and ω_s is sunset hour angle.

Another important parameter that needs to be introduced is called clear sky index, it is the ratio between terrestrial radiation and extraterrestrial radiation.

According to this definition, it is represented as:

$$K_T = H/H_0 \quad (1-8)$$

where K_T is clear sky index and H is terrestrial radiation on horizontal surface.

1.3.3 Solar radiation on tilted plane

As mentioned before, due to its low value, ground reflected radiation is neglected in the following calculation.

To calculate average daily diffuse radiation a model from [21] is used and can be expressed as:

$$\frac{\overline{H_d}}{\overline{H}} = 1.391 - 3.560K_T + 4.189K_T^2 - 2.137K_T^3, \text{ or}$$

$$\frac{\overline{H_d}}{\overline{H}} = 1.391 - 3.560K_T + 4.189K_T^2 - 2.137 \quad (1-9)$$

$\overline{H_d}$ in the above equations is average daily value of diffuse radiation which is calculated from average daily global radiation \overline{H} .

The first formula is used in the case of sunset hour angle is less than 81.4° and the second one is used when this angle is greater than 81.4° . K_T is the clear sky index calculated in equation (7).

Then for global irradiance the hourly values of radiation can be derived through the calculation below:

$$r_t = \frac{\pi}{24} (b + c \cos \omega) \quad (1-10)$$

In the above formula, the coefficients b and c is expressed as:

$$b = 0.409 + 0.5016 \sin \left(\omega_s - \frac{\pi}{3} \right) \quad (1-11)$$

$$c = 0.6609 - 0.4767 \sin \left(\omega_s - \frac{\pi}{3} \right) \quad (1-12)$$

where r_t is the ratio of hourly radiation to daily global radiation, ω is solar hour angle and ω_s is the sunset hour angle.

Similarly, for diffuse irradiance the following equation is given [8]:

$$r_t = \frac{\pi}{24} \frac{\cos \omega - \cos \omega_s}{\sin \omega_s - \omega_s \cos \omega_s} \quad (1-13)$$

where r_t is the ratio of hourly diffuse radiation value to daily value. Therefore

the hourly global radiation and diffuse radiation for each day can be derived by:

$$H = r_t \overline{H} \quad (1-14)$$

$$H_d = r_d \overline{H_d} \quad (1-15)$$

So the direct radiation H_b is further given by:

$$H_b = H - H_d \quad (1-16)$$

1.3.4 Calculation of solar irradiance on the PV array

To get the hourly irradiance of the PV array, a model from [Duffie and Beckman] is used to describe it. It can be expressed as below:

$$H_t = H_b R_b + H_d \left(\frac{1 + \cos \beta}{2} \right) + H \rho \left(\frac{1 - \cos \beta}{2} \right) \quad (1-17)$$

where ρ is called diffuse reflectance or ground albedo: it is set to different values according to ground types. Generally the values of 0.15 to 0.2 are most commonly used in practice. Table below shows albedo of various ground types[9].

Table1. 1 Albedo of different ground surface

Surface	Albedo
Grass	0.25
Macadam	0.18
Asphalt	0.15
Snow	0.45-0.9
Dark soil	0.08-0.13
Savanna	0.16-0.21
Dry sand	0.35
Concrete	0.25-0.35
Red tiles	0.33
Aluminum	0.85

where β in equation (16) is the slope of the array surface and R_b is the ratio of direct radiation of the PV array to the radiation on horizontal plane and is given as:

$$R_b = \frac{\cos\theta}{\cos\theta_z} \quad (1-18)$$

where θ is the incident angle and θ_z is solar zenith angle given by equation (5).

By using this model the change of the position of the sun as well as solar array can be determined for more accurate estimation.

After all values of H_t are obtained, they are added together to get the daily irradiance $\overline{H_t}$. Here is the summary of the whole calculation process:

- a. Compute the hourly direct and diffuse radiation H_b and H_d based on the data of global radiation.
- b. Continue to calculate hourly global radiation H_t on a tilt surface.
- c. Through summation of the results of the second step, the final daily irradiance can be obtained.

Chapter two: GIS implementation for estimating photovoltaic system

2.1 Introduction

Solar power has competitive advantages in the fields of sustainable development and environmental protection. However, there are still many obstacles to apply PV generation at large scale so far; one of the main reasons is the initial costs., Due to this point the preliminary investigation and site selection are crucial for PV power station; these factors must be taken into consideration carefully.

When assessing solar radiation of a certain area, in order to consider landscape features it is ideal to build solar radiation model integrated with Geographic information system (GIS). This kind of model can provide fast, low-cost and precise solar radiation result that covers large area. It also has the capability of analyzing the effects of slope, orientation and shadowing. So integrating solar radiation model with GIS and image processing software is very helpful for analysis and improvements of application.

2.2 Introduction of PVGIS

PVGIS is a program developed by European Commission Joint Research Center [10]. The model can be used to calculate the solar radiation potential of a certain area, based on solar radiation map. It can be generally categorized as a database with web application and can be used to provide PV system development information for decision-makers, researchers and industry in a region. It can also be used to observe solar distribution and do some simple calculation such as estimating solar radiation of a region. The PVGIS can be accessed from <http://re.jrc.ec.europa.eu/pvgis/index.htm>.

The unique solar irradiation database includes the solar radiation map of Europe and Africa. This database is developed by using r.sun command which is integrated into GRASS GIS software [11] [12]. The database contains raster map of monthly average and annual horizontal surface. In addition, it considers the situation of slope of 15°, 25° and 40°. It can be used to estimate diffuse and reflected components of clear and overcast sky. Daily irradiation is then calculated through the integration of collected solar irradiation at different time intervals of a day.

To build the database of solar radiation, the first step is to compute the global surface solar radiation under clear sky condition [12]. There is a parameter called Linke turbidity, which is based on several global information including clear sky irradiation, perceptible water vapor, aerosol optical depth and ground information from aerosol measurement. The root mean square error is set to be 0.7 in this case. Then the clear sky irradiation is computed.

Next phase is the interpolation of clear sky index and computation following

with the raster map of surface solar irradiation. In this step, the clear sky irradiation G_{hc} and clear sky index K_c are computed respectively. K_c is computed as the ratio of real sky radiation and clear sky radiation. This parameter is calculated in GRASS GIS, a solar radiation model built in GIS software. After that, the overcast global irradiation is computed and the raster map can be obtained.

The third step is the calculation of diffuse and beam components of overcast condition and the radiation raster map of inclined surface. To achieve this purpose, a new parameter, of inclined surface is introduced, which is denoted as G_i . The value can be obtained using the same way as calculating K_c (clear sky index).

PVGIS model is built by r.sun model which is built into GRASS GIS software to create the database. In r.sun model the three kinds of radiation— direct, diffuse and reflected radiations are derived under clear sky condition and finally the global radiation is obtained.

2.2.1 Database and models of PVGIS

As a solar power radiation database, PVGIS has the following features: open source data and software structure; integration of high resolution meteorological and geographical environmental data into GIS system; understandable map-based results, and user-friendly interface access. The database is built by using solar radiation model r.sun which is integrated into GRASS GIS software and other related programs. As a result, PVGIS combines the conclusions from laboratory, observation station and geographical testing. It is used as a research tool of solar technology performance assessment from geographical aspect; the web interface can be used to provide interactive access between data, map and tools.

The database of PVGIS is mainly used to evaluate the potential electricity

generation of PV modules that are built on horizontal, vertical and optimal surfaces. Horizontal structure is not common unless under integration considerations. However, it may be used as baseline estimate. One reason is that many radiation data are measured under horizontal surface condition. So it will be helpful to estimate tilted surface results by comparing with the data of horizontal surface. For most widely used PV technology, installation in existing infrastructure in residential area, the annual electricity generation E from a PV system is calculated by the following equation: [13]

$$E = P_k PR G \quad (2-1)$$

where P_k is unit peak power, PR is the ratio of system performance, and G is the annual radiation sum measured under horizontal, vertical or inclined surface.

The capacity of PV system is given by W_p ; it represents the nominal power output under standard test condition of 1000 W/m^2 irradiance and environmental temperature of $25 \text{ }^\circ\text{C}$. The advantage of this measurement is that it does not require the knowledge of PV conversion efficiency or module attributes. Theoretically PR in equation (1) is 1 if the system operates normally under standard test condition. In practice, the system output is lower than peak value even if the radiation value is 1000 W/m^2 . One reason is that the operation temperature is often higher than $25 \text{ }^\circ\text{C}$ and leads to reduced PV efficiency. Other reasons include angular and spectrum uncertainty and power loss in inverters and cables. So a parameter gross is used to represent the ratio between actual output and nominal power. This ratio of a typical module of mono crystalline or poly crystalline installed on the rooftop is 0.75. [13]

The database is connected with web-based interactive application; this web-based access is designed to evaluate solar radiation and PV system performance by

using some maps and diagrams. The specific evaluation location can be decided by directly choosing from the map; choosing the name of a city or a country or entering the latitude and longitude of the area. The monthly and yearly solar radiation estimation results will be displayed in new windows. A basic map and special meteorological solar radiation distribution map can give the user a geographical comprehension of the data.

2.2.1.1 Solar radiation models and database:

R.sun [10] model has three dataset as its input:

A. Digital Elevation Model (DEM), in GRASS GIS the data used for calculating main database and spatial analysis comes from SRTM-30 (Shuttle Radar Topographic Mission) [14]. It calls for high resolution SRTM-30 dataset of global dataset in the web-application, but for those areas beyond 60 degrees north latitude, there is only SRTM-30 database available.

B. Linke Turbidity Factor [15], it provides the optical status of monthly clear atmosphere. This dataset has 12 10-km resolution grids [14]. By combining data source of different points and grid the raster map is drawn. The initial data in SRTM-30 DEM is reduced to 1-km resolution grid.

C. Clear sky coefficients K_{cb} and K_{cd} , they are used to convert the clear sky beam and diffuse radiation, which are calculated in the r.sun model, into practical values. These two coefficients are obtained by observation results of average daily value of beam and diffuse radiation from 566 meteorological stations in the region. These data records observation or estimated values from a 10-year period of 1981-1990. In addition, some information is obtained from Europe Solar Radiation Atlas

(ESRA) [16] as supplement for remote areas or areas without observation stations. Through multivariate spline interpolation method the monthly average values of K_{cb} and K_{cd} are converted into grid cells of 2 by 12. Moreover, those results that are attenuated higher than 15 percent due to shadowing effects caused by terrain feature are excluded from the data collection.

Another input parameter called surface albedo, it is the part of solar radiation that reflected from earth surface back to space, usually for ground it takes the value of 0.2. It can also use other data source as the spatial distribution value of each grid cell to improve the estimation accuracy.

The above three database are converted to Lambert azimuth equal area map projection and are integrated in to GRASS GIS software for simulation and calculation. For PVGIS web-application, the following data layers are compiled and optimized to achieve the purpose of fast saving and reading: linke atmosphere turbidity factor and clear sky coefficients are stored in 1km grid resolution format; this database also contains land coverage and other geographical information.

For desired locations, SRTM-3 elevation and related data are stored in 100m grid resolution. Interactive tools read these data and reduce the 1km resolution of neighboring area.

Under the time interval of every 15 minutes, r.sun model uses three input parameters to run the estimation of beam, diffuse and reflected radiation of horizontal and inclined surface from sunrise to sunset, respectively. The three parameters are elevation, atmosphere turbidity factor and surface albedo as mentioned above. Clear sky coefficients K_{cb} represents the ratio of monthly daily sum and daily sum of beam

radiation, K_{cd} represents the ratio of monthly daily sum and daily sum of diffuse radiation. They are used to predict the radiation for a particular day. The model assumes that these coefficients are obtained from meteorological stations and are interpolated into the algorithm structure. Also the model can use the data measured from satellite.

Only the average value of K_{cb} and K_{cd} can be used as inputs in PVGIS. Practical radiations of a certain day in a month are calculated according to these inputs, and thus the monthly and yearly radiation results can be obtained. PVGIS uses the terrain shadowing derived by SRTM-3 digital elevation model as obstacle factor. With the use of `r.horizon` command to precalculate the terrain elevation and optimize overall operation procedure, elevation level data is read in `r.sun` model and used to compute shadow effects of beam component of radiation.

Besides `r.sun` model, there are some other GIS programs related with photovoltaic. They are: `r.sunyear` for calculating the optimal inclination angle of mounted PV module; `r.suntrack` for the simulation of two-axis tracking PV system and `r.pv` for the simulation of silicon crystalline PV system with the consideration of temperature, respectively. User can estimate the radiation or output of flat-plate PV through integrated application of these programs. In the web application these programs are embedded for the convenience of user to perform analysis for a region.

The accuracy of model outputs is evaluated by actual measurements of ground stations. Having the results of 539 ground stations and after the analysis of these results, it is found that among these stations there are 92% of them with output errors less than 5% between the simulation results and practical measurements. And twelve

stations have the error of 8% which take the 2.2% of all stations. In addition, these results are based on the analysis after obtaining actual measurement results. For the regions without ground stations the uncertainty concept should be built. Cross validation is used to predict the error of these areas that are far away from ground stations. However, the conclusion of cross validation does not give the geographical distribution of error, 90% of test areas have an error less than 7.2%, while in 19 locations this number raises to 10%.

2.2.1.2 Air temperature

The creation of temperature database is through the collection of seven monthly averages during different time point of each day; they are maximum value, minimum value, and five values measured through a 3-hour interval from six am to six pm. The measurements come from European Meteorological Monitoring Infrastructure (EMMI) [17]. In GRASS GIS, elevation are taken into account through multivariate spline interpolation method using `v.vol.rst` command and thus a better temperature estimation of mountainous region is obtained.

The five measurements obtained by 3-hour interval from 6 am to 6 pm are used to build monthly daytime air temperature results and simulate the performance of silicon crystalline PV modules through `r.pv` command. The daytime air temperature results are obtained by a polynomial representing each grid cell. Similar method can be used to calculate average temperature, maximum air temperature and time of appearance.

2.3 Web applications

For the purpose of providing this solar radiation evaluation tool to the public,

a web application was built and was put into use in 2002. Afterwards, it was updated for several years with a big upgrade in the year of 2007. The user interface of this web application is programmed by PHP and JavaScript and uses Google map as media. The basic tools for performing calculation process are compiled in C language. Global radiation, temperature and other geographical data are stored in the server end as binary files to guarantee fast accessing calculation program.

The new user interface is composed by a map window and some application parts, the map window is shown in fig.2.1 and its calculation parts are shown in fig.2.2.



Figure 2. 1: solar radiation map in Europe

PV Estimation
Monthly radiation
Daily radiation

Performance of Grid-connected PV

Radiation database: Classic PWGIS [\[What is this?\]](#)

PV technology: Crystalline silicon

Installed peak PV power 1 kWp

Estimated system losses [0;100] 14 %

Fixed mounting options:

Mounting position: Free-standing

Slope [0;90] 35 ° Optimize slope

Azimuth 0 ° Also optimize azimuth

(Azimuth angle from -180 to 180. East=-90, South=0)

Tracking options:

Vertical axis Slope [0;90] 0 ° Optimize

Inclined axis Slope [0;90] 0 ° Optimize

2-axis tracking

Horizon file Browse

Output options

Show graphs Show horizon

Web page Text file PDF

Calculate
[help]

Figure 2. 2 application inputs window

Through this user interface there are four applications:

- 1). Querying local monthly average meteorological information

Solar radiation, temperature and other related information of long term monthly average observation results of different regions can be selected. Terrain shadowing caused by high elevation surface of each month can be calculated, as along with the yearly loss of horizontal radiation. The following results can be derived by using this function:

Global radiation of horizontal and inclined surface

Optimal angle of mounted PV installed at south-faced inclined surface

The ratio of diffuse radiation and global radiation on horizontal surface

Linke turbidity factor

The air temperature of all day and the time period between sunrise and sunset

2). the simulation for a typical day of each month

User can obtain monthly average values of radiation and temperature. The radiation data contains average global radiation; diffuse and real sky radiation of mounted surface and two-axis tracking system for given angle and orientation. Radiation profile is calculated from the clear sky values between sunrise and sunset which is adjusted by the clear sky index coefficients K_{cb} and K_{cd} . Therefore the radiation profile is symmetrical with the sun at noon unless the radiation is affected by shadowing effects. The time interval used to compute radiation profile is 15 minutes.

A monthly average daytime radiation value profile is calculated by the observation results derived from 6:00 to 18:00 divided by three hours interval. These values are computed through a polynomial which can help calculate the temperature of any time during a time period. Outside the time period, the accuracy of these results decreases fast, so it is only valid within time period from 6:00 to 18:00. This application also can show horizontal elevation changing with sun track at summer and winter solstice.

3).estimate of PV system performance

This function can be used to estimate the performance of PV system that is

connected to grid. Only a few information needs to be provided by the user: system nominal peak power; system loss estimation (including inverter and cable loss with a default value of 14 percent); the orientation and inclined angle of fixed-mounted PV module; installation method - fixed or two-axis tracking; and PV technology used - crystalline silicon or thin film.

When entering installation angle, user can let the application calculate optimal orientation and inclined angle, or compute the optimal inclined angle under given orientation. The calculation method used in this application is the same as the model of solar radiation estimation. In the calculation the terrain shadowing effect and high reflectance under shallow solar radiation incident angle are also considered.

The choice of different PV technology is used to determine the complexity of model. For crystalline silicon a model that uses a function of temperature and radiation is introduced to calculate conversion efficiency of PV module.

Compared with the actual results obtained from instantaneous radiation and temperature, those results based on monthly averaged values have a acceptable accuracy [18][19]. Right now the database only has long-term 15 minutes averaged profiles of radiation and temperature for a typical day of each month. Since the relationship of PV modules energy production and radiation is not linear, this simplification will result in error. A preliminary study shows that due to the positive correlation between radiation and air temperature, the yearly energy is overestimated by 1 to 1.5 percent. Because most radiation is absorbed when the sky is cloudless, the clear sky radiation model is used to replace real sky radiation when calculating PV conversion efficiency. The overestimation can be reduced to less than 1 percent in

this way. Adding time series of radiation and temperature can further reduce the error.

The model of thin film is still under development; the energy production estimation accuracy of this kind of technology is difficult, since it largely depends on the solar spectrum; its performance is closely related to long-term radiation effect and the period with high temperature.

4).PV potential of different regions

This tool shows the yearly global radiation and solar source of different countries and regions in Europe. It is used for regional planning and policy making; in addition, it also gives the solar source of fixed mount PV module in different inclined conditions and PV potential.

For each region, there will be an average potential value from CORINEL and Cover and Global Land Cover databases which is based on residential areas. By doing this remote areas such as mountain are avoided and more emphasis is put to those locations that are more frequently used for PV module installation, like the rooftop of buildings and vicinities, for the needs of connecting to the grid.

Compared with other applications, this program uses previous map instead of Google map. It has zoom function and the regions can be selected from list.

For these four applications, the related data will be calculated first, the data defined by the user is run as request. Due to the complicated calculation procedure, the following measures are taken to reach optimal calculation speed. First, all calculation process are run at the server end, therefore the calculation time will not be determined by the computer of user end. The program are compiled using C language to ensure faster running speed than those programs compiled in scripting language,

such as PHP or Perl. Data that is necessary in calculation is saved in binary form, each grid use fixed capacity, so the read and write operation of input data is independent of the size of data set.

For the estimation of PV capacity, the user can choose to run the program under optimal inclined angle and orientation conditions (east-west direction). The data storage in the server is 7 GB. Besides the program for solar radiation calculation, other parts of application are mostly written by scripting language at server end, mainly in PHP. The scripting language Java is minimized to make it convenient for those users who do not have related programming background.

2.4 Using online calculators

The user input has been shown in figure 2.2. Some of the input parameters are listed below.

a. Mounting position

For fixed mounting PV modules, installation method will influence the temperature of modules and then affect the efficiency. Experiments show that if the air flow around the module is limited, module will become hotter. There are two options in the application. The first one is called free standing where the module is installed on a plane allowing air flowing around the module. The second way is building integrated where, the module will be built completely inside the structure of the building, such as the wall or rooftop. In this way, the air flow is restricted. There are some other installation methods besides these two ways, for instant, the module is mounted on the curved roof tiles allowing air flow. In this case, the performance will be somewhere between the two results mentioned above.

b. Tilt and azimuth angle

c. Tracking options

For some systems, the PV modules can be moved to track the sun in the sky to better absorb the sunlight. There are several different ways of tracking:

(1) Vertical axis

Module is mounted on a vertical rotating axis at a certain angle. It is assumed that the axis rotates at daytime so that the angle between module and the sun is always as small as possible. This means that it will not keep a constant value of rotating speed during the day. The angle is determined by module and ground surface, or it can be calculated to get the optimal value.

(2) Inclined axis

The module is installed on an axis that has an angle with horizontal surface and faces south-north direction. The plane of module is assumed to be parallel with the rotating of axis. Same as the vertical axis, user can directly enter this angle or calculate it from application provided by program.

(3) Two-axis tracker

The module is put on a system that can move the module in east-west direction and so there is an angle with ground to make sure it always points to the sun. The module not only collects radiation directly from the sun, but also uses reflected light from other part of the sky.

2.5 Example and results

Table 2.1 shows the estimated PV output of application for a selected location. The parameters are as follows, user needs to input the location, mounting method and PV technology.

Location: 40 °48'9" North, 1 °13'49" West, Elevation: 1249 m

Solar radiation database used: PVGIS-classic

Fixed mounting with tilt angle of 35 ° and azimuth angle due to south

Nominal power of the PV system: 1.0 kW (crystalline silicon)

Estimated losses due to temperature: 9.6% (using local ambient temperature)

Estimated loss due to angular reflectance effects: 2.6%

Other losses (cables, inverter etc.): 14.0%

Combined PV system losses: 24.3%

Table 2 1: System energy production estimate

Fixed system: tilt angle = 35 °, Azimuth angle = 0 °				
Month	E_d (kWh)	E_m (kWh)	H_d (kWh/m ²)	H_m (kWh/m ²)
January	2.75	85.2	3.41	106
February	3.18	89.1	4.00	112
March	4.19	130	5.44	169
April	4.24	127	5.58	167
May	4.55	141	6.13	190
June	4.64	139	6.39	192
July	4.78	148	6.65	206
August	4.64	144	6.42	199
September	4.38	131	5.91	177
October	3.56	110	4.67	145
November	2.77	83.0	3.48	104
December	2.39	74.2	2.96	91.9
Yearly average	3.84	117	5.09	155
Total for year	1400		1860	

In the table:

E_d : Average daily electricity production from the given system (kWh)

E_m : Average monthly electricity production from the given system (kWh)

H_d : Average daily sum of global irradiation per square meter received by the modules of the given system (kWh/m²)

H_m : Average sum of global irradiation per square meter received by the modules of the given system (kWh/m²)

Figure 2.3 shows the graph of the estimated monthly PV output:

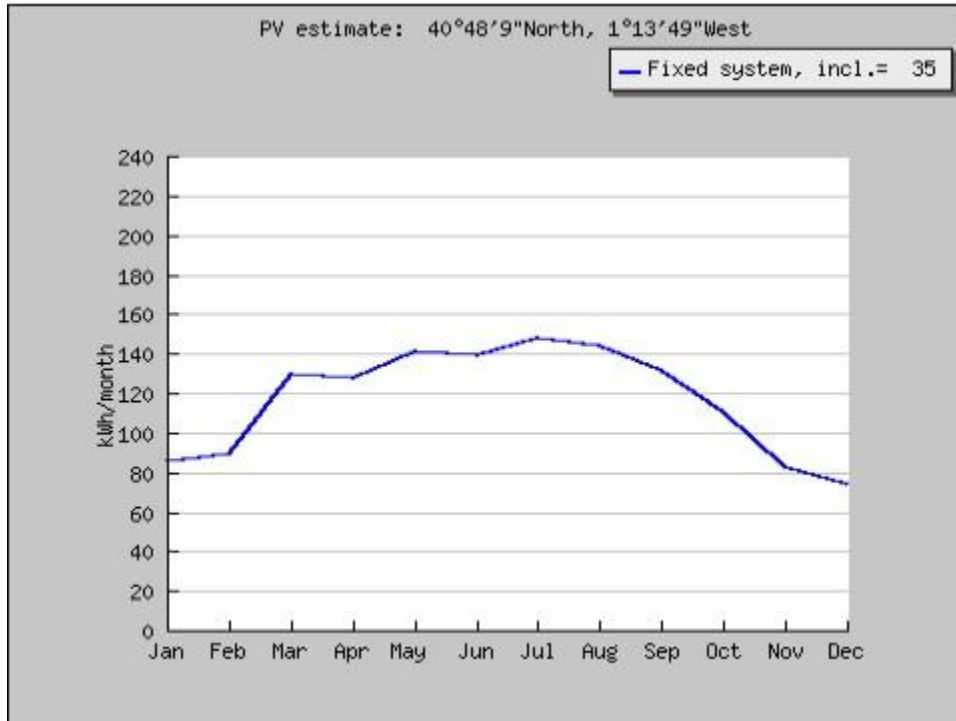


Figure2. 3: estimated PV output for the same location

Figure 2.4 shows estimated solar irradiation graph for the same location:

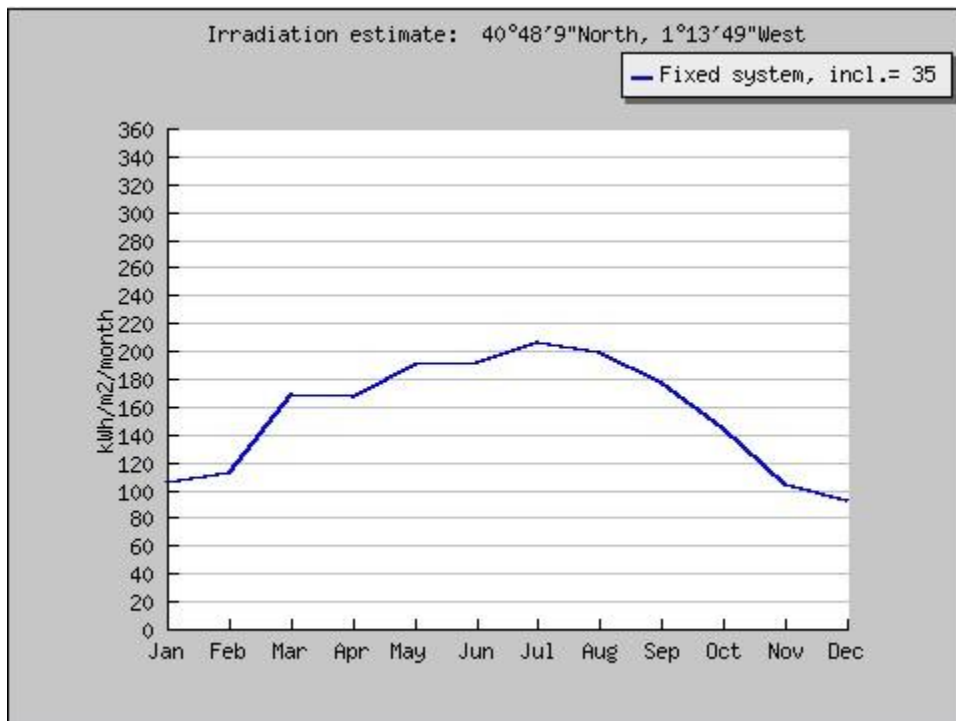


Figure2. 4: estimated solar irradiation for the same location

2.6 Conclusion

The development of PVGIS is for assisting policy making, research and education. Its goal is to increase the understanding of PV technology and other solar related technologies in Europe. The map-based instantaneous analysis tool is useful for both professionals and public at preparation stage of PV project, especially for prefeasibility study and site selection analysis.

When comparing the output of PVGIS with other simulation model, the errors exist due to the different sources of database development. In addition, different simulation methodology also leads to the error. Only through comparison it can be decided that which model is better for different project.

Chapter Three: Stand alone system design principles

3.1 PV modules

3.1.1 I-V curve

PV cells are the basic elements of a PV system; through series or parallel connection they form PV modules to produce desired voltage; PV modules are further connected together to constitute PV arrays for practical use. To describe the characteristics of a PV module, I-V curve is a fundamental way to show the performance of the PV module, and through it some important parameters of modules can be obtained.

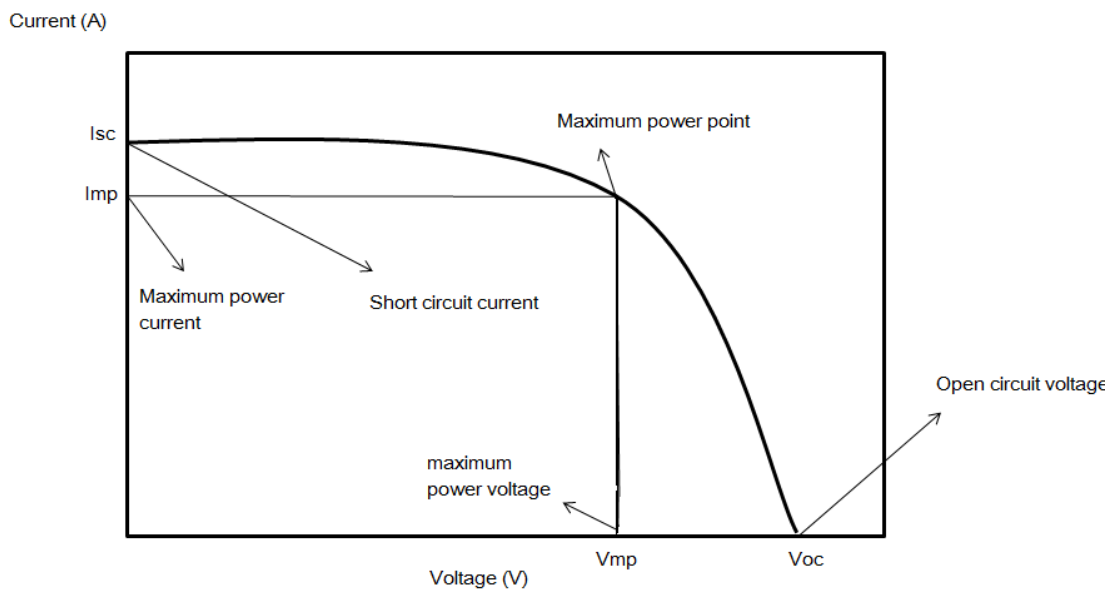


Figure 3.1: I-V curve of PV modules

Graph in Fig. 3.1 is a basic I-V curve. It shows parameters including short-circuit current, open-circuit voltage, maximum power current and voltage and maximum power point. These parameters depend on the irradiance and temperature of PV modules.

In the I-V curve figure, the maximum power point is the module operating point at which the power output of modules reaches maximum value; the corresponding current and voltage are called maximum power current and maximum power voltage respectively. This value of maximum power point can be used to evaluate performance of PV modules under standard test condition or other circumstances.

3.1.2 Device response

I-V curves vary with different modules, but the magnitude and position of the curve still changes even for the same module because of irradiance and temperature variation.

3.1.2.1 Solar irradiance response

Solar irradiance variation has small influence on voltage but bigger influence on current., it is proportional to the solar irradiance increasing, therefore the output power also follows a similar change with irradiance, as shown in Figure 3.2.

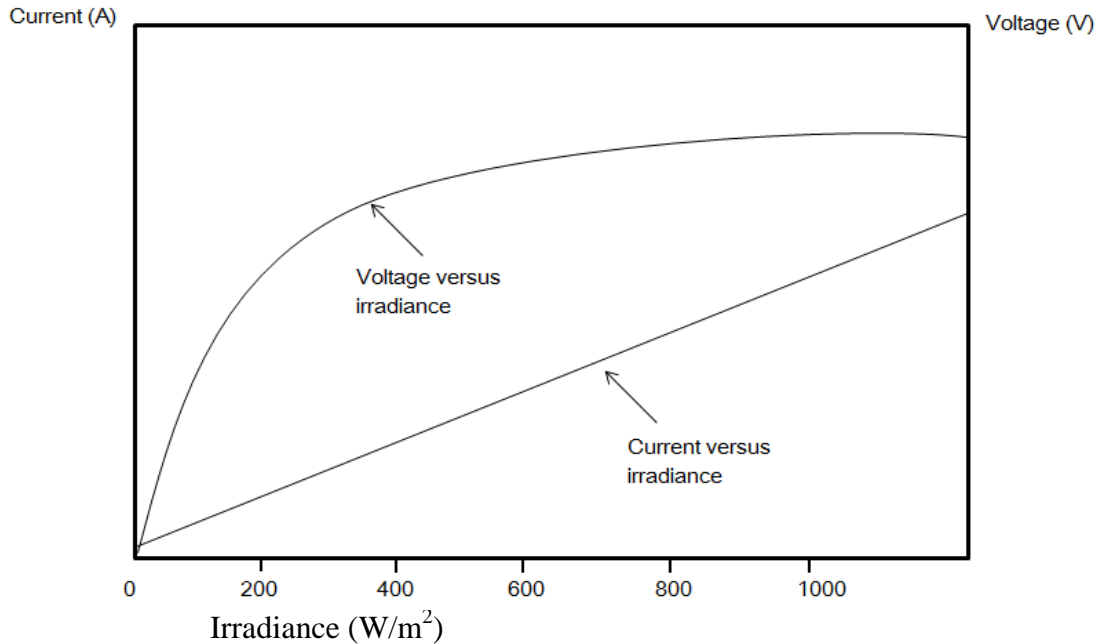


Figure3.2: solar irradiance response

3.1.2.2 Temperature response

The rise of temperature will cause a dramatic fall of voltage but only a little increase of current, thus higher operation temperature reduces power output and module efficiency. Long duration high temperature environment also leads to damage of PV modules. So it is desired to install modules in a place where is cool enough. Temperature affection on modules are shown in the figure below. Refer Fig. 3.3?

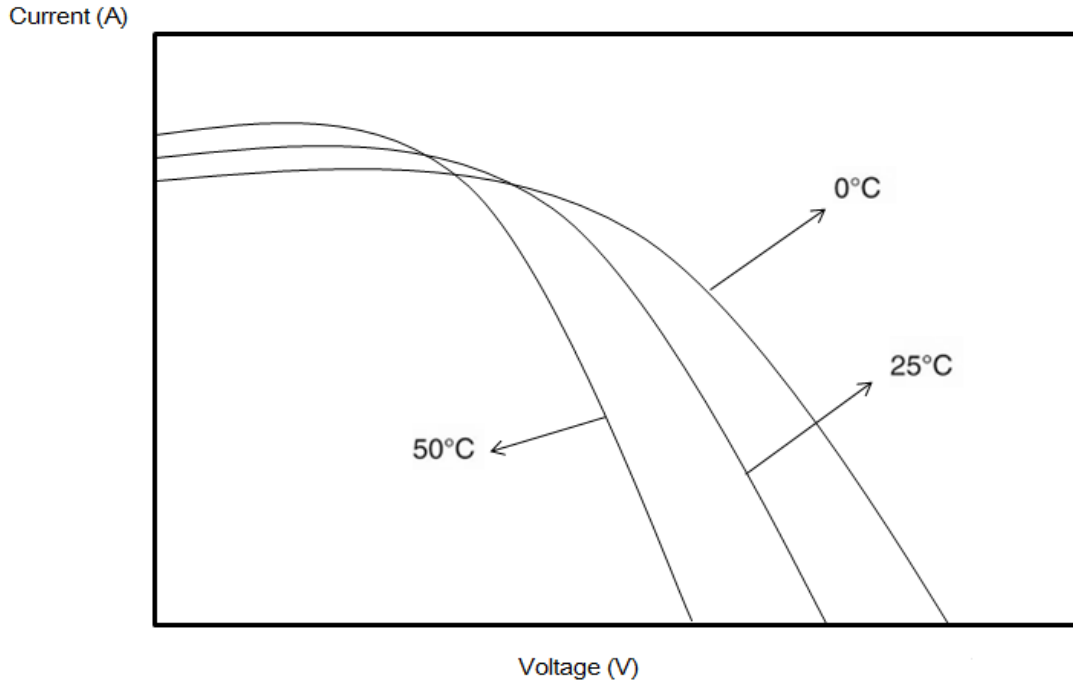


Figure3.3: voltage will drop due to temperature increase

3.1.3 Module connections

First the modules will be connected in series to get desired voltage, and then they are connected in parallel for current and power requirements.

3.1.3.1 Series connection

For series connection, it is critical to use the same type of modules. When identical modules are connected together, the voltage will be the sum of each individual module's voltage while current remains the same. If modules with different I-V curve are connected together power loss will occur, because only the lowest current can be the output of the entire module. However, modules with different voltages can be connected in series if their output currents are the same. In this case it will not have power loss.

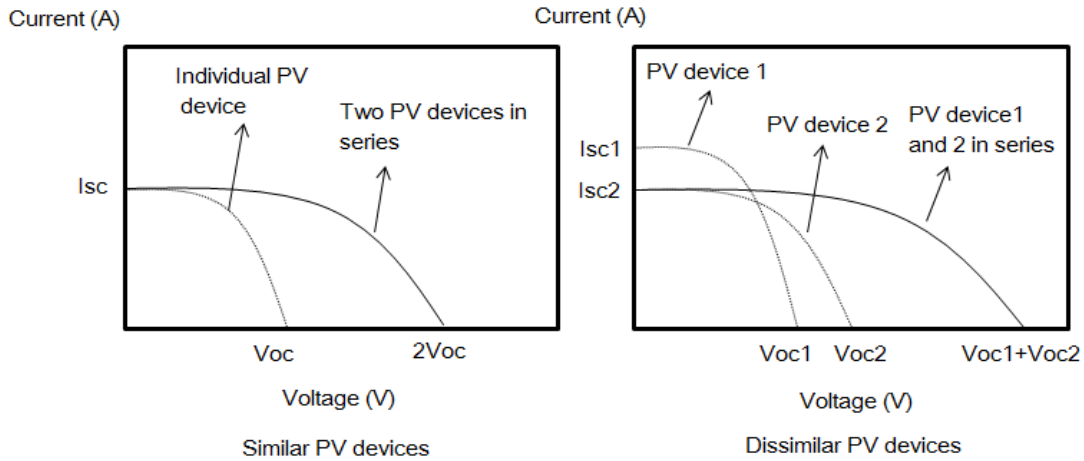


Figure 3.4: current output for similar devices and dissimilar devices

3.1.3.2 Parallel connections

When connected in parallel, if the module of the same type, the current is the sum of each branch's current and voltage remain the same as individual module's voltage. Different modules can also be connected in parallel. In this case the voltage will be the average value between two output voltages.

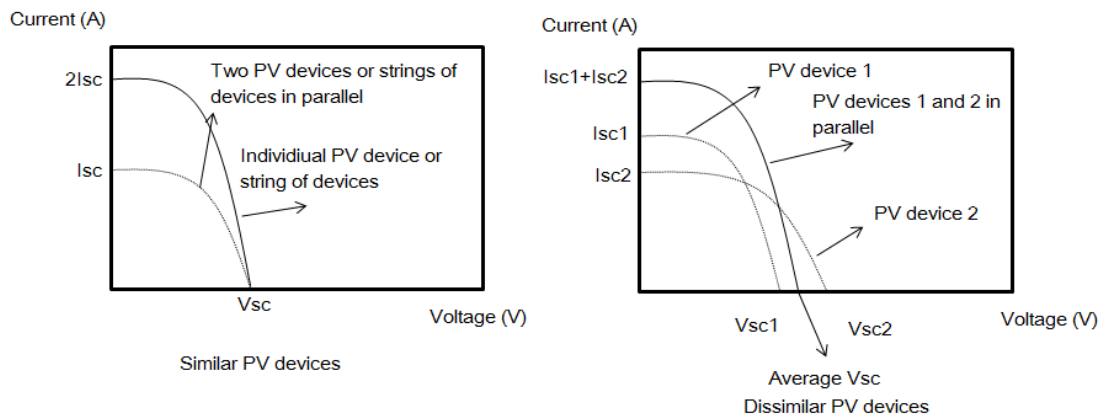


Figure 3.5: I-V curves of modules in parallel

3.1.4 Bypass diodes

Sometimes PV modules will experience reverse-bias situations. Under this state, negative voltage will be generated instead of normal positive voltage. It is caused by open-circuit or broken cells. A bypass diode is used to prevent this

phenomenon. It is connected in parallel with PV cells, in normal conditions the current will flow through cells and in the case of a broken cell, current can still pass through bypass diode to charge the battery. Without bypass diode the reverse voltage will reach breakdown voltage and finally damage the modules. Usually a bypass diode will limit the breakdown voltage to 0.7 V [20].

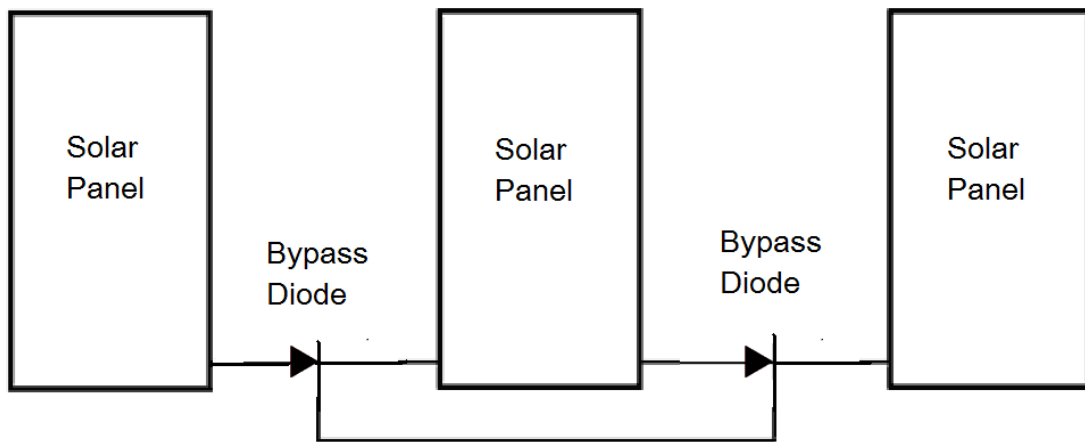


Figure3.6: Bypass diode

3.1.5 PV module modeling

The simulation in later chapters uses a PV model called one diode model [21].

The model has the following equivalent circuit for a PV cell.

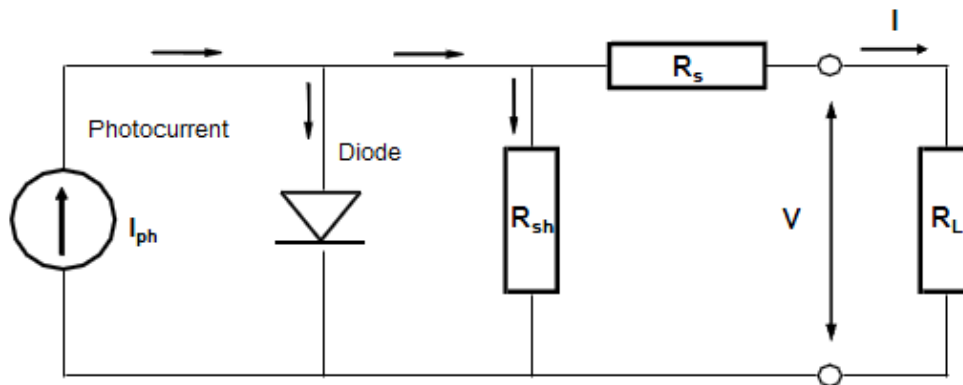


Figure3.7: One diode model

This model is at first designed to describe single PV cell. Assuming that every cell is the same, the model can be expressed by the following equation:

$$I = I_{PH} - I_o e^{\frac{q \cdot (V + I \cdot R_s)}{N_{cs} \cdot \gamma \cdot k \cdot T_c}} - (V + I \cdot R_s) / R_{sh} \quad (3-1)$$

where I is the current produced by the module;

I_{PH} is phototcurrent which is proportional to the irradiance;

I_o is the inverse saturation current depending on temperature;

V is the voltage at terminal of the module and q the charge of a single electron;

R_s and R_{sh} is series resistance and shunt resistance respectively;

K is bolzmann's constant and γ represents diode quality factor which often falls between 1 and 2.

N_{cs} is the number of cells in series.

T_c is the effective temperature of modules.

In the above equation, photocurrent depends on the irradiance and temperature of the PV cells; it can be determined as follows:

$$I_{ph} = \left(\frac{G}{G_{ref}} \right) \cdot [I_{phref} + \mu_{ISC}(T_c \cdot T_{cref})] \quad (3-2)$$

where G is real irradiance and G_{ref} is the irradiance under standand test condition with 1000 w/m².

T_c and T_{cref} is the real temperature and temperature under standand test condition which is 25 °C.

μ_{isc} is temperature coefficient of the photocurrent.

The diode reverse saturation current I_o in equation (3-1) are expressed below:

$$I_o = I_{Oref} \left(\frac{T_c}{T_{cref}} \right)^3 \cdot e^{\left(\frac{q \cdot E_{gap}}{\gamma k} \right) \cdot \left(\frac{1}{T_{cref}} - \frac{1}{T_c} \right)} \quad (3-3)$$

where E_{gap} is the gap energy of the material. This number vaies with different materials.

Table3.1: gap energy for different materials [20]

Material	Gap energy
Crystalline silicon	1.12 eV
CIS	1.03 eV
Amorphous silicon	1.7 eV
CdTe	1.5 eV

3.1.6 PV cell materials

By far the most commonly used for PV cell industry is crystalline silicon (c-Si). Other semiconductors like gallium arsenide (GaAs) and amorphous silicon are also used for different kinds of PV modules. Crystalline silicon materials are dominant in PV cells market because it is more cost-effective than other materials. Gallium arsenide materials have higher efficiency; however, the price is also expensive compared with crystalline silicon. In addition, the toxicity is another factor that limits the use of gallium arsenide. GaAs can be mixed with indium, phosphorus and aluminum to produce semiconductor. The alloy can receive solar radiation components with different wavelength through sunlight. Therefore they are highly efficient and are ideal for concentrating applications. Thin-film technologies are also widely used today. Thin-film module can be obtained by putting a thin layer of semiconductors on the plane through chemical vapor deposition techniques. Then using laser to divide cells and make electrical connection between them. Usually the materials for thin-film technology are amorphous silicon (a-Si), copper indium gallium selenide (CIGS) and cadmium telluride. Compared with crystalline silicon, they are less expensive but the efficiency is lower. Other PV materials include multijunction and photoelectrochemical cells such as dye-sensitized cells and polymer cells. The table below shows efficiencies of some mainly used materials [22].

Table3.2: PV material efficiencies

Material	Typical efficiencies in percent	Best laboratory efficiency in percent
Gallium arsenide	20	32
Monocrystalline silicon	14 to 17	25
Polycrystalline silicon	11.5 to 14	20
Ribbon silicon	11 to 13	16.5
Copper indium gallium selenide	9 to 11.5	19
Cadmium telluride	8 to 10	16.5
Amorphous silicon	5 to 9.5	13
Dye-sensitized	4 to 5	11
Polymer	1 to 2.5	5

PV modules fabrication involves producing wafers and assembling them into cells and modules. Wafer is semiconductor material in the form of flat sheet. They are typically 180 μ m to 350 μ m thick and made from p-type silicon. Generally crystalline silicon wafers have three forms: monocrystalline silicon, polycrystalline silicon and ribbon silicon. Each of them are different in efficiency and cost. Monocrystalline silicon have an efficiency of 14% to 17% while some laboratories can produce samples with efficiency of 25%. Polycrystalline silicon have relatively small efficiency compared with monocrystalline silicon but their cost is lower and the denser packing in modules also make them attractive. Ribbon silicon has the lowest efficiency among the three types with the cheapest price, because during manufacturing there is less material waste.

Chapter four: Photovoltaic System components

4.1 batteries

4.1.1 Introduction

In the simplest stand-alone system design, PV arrays connect directly to the loads and it is called direct-coupled systems. It is very easy to design and build such a system. However, in practice this kind of design is not easy to use. Because there are many factors that affect the performance and power output of the PV system, like temperature, solar radiation and load variation during peak hour and off-peak hour. A system with simple structure does not have the capability to operate properly according to different conditions. So designing direct-coupled system requires accurate system parameters to satisfy different considerations.

Due to the difficulties described above, in fact most stand-alone PV system will have batteries for the purpose of energy storage to better face the situation of demand fluctuations during certain period.

4.1.2 Battery capacity

Capacity measures energy storage capability of batteries and is expressed as ampere hour. Capacity can be influenced by several parameters including temperature, charge and discharge and age. Usually batteries will have better capacity under higher temperature than cold conditions, but excessive high temperature also reduces the battery life. Next figure shows the relationship between temperature and battery capacity. It can also be read from the figure that capacity is affected by discharge rate.

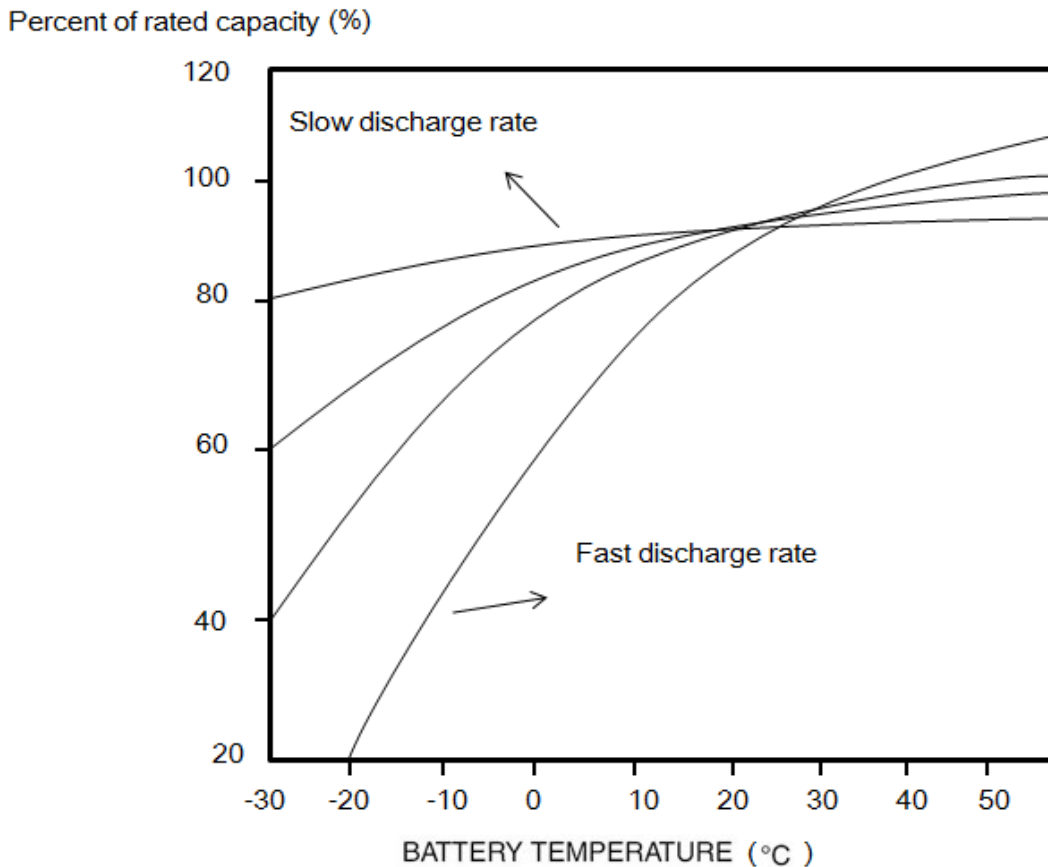


Figure4. 1: relationship between capacity and temperature

4.1.3 Battery types

4.1.3.1 Flooded-electrolyte batteries

For this type of batteries the electrolyte is liquid. The constituents change according to different battery chemistry. In lead-acid cells the electrolyte is diluted sulfuric acid and in nickel-cadmium cells it is potassium hydroxide solution. Flooded-electrolyte batteries can be divided into open-vent type and sealed-vent type.

Open-vent batteries: there is a way for air flow and water supply, because it is necessary to add water against water loss and maintain the correct concentration. It has a removable cap through which water can be added.

Sealed-vent batteries: in contrast with open-vent batteries, there is no way for gas escape and water supply.

4.1.3.2 Captive-electrolyte batteries

Captive-electrolyte is the electrolyte in the form of solid. Captive-electrolyte cannot be replenished from outside, but it can combine the oxygen produced from positive plates and hydrogen from negative plates to create water and thus provide supplement internally. Due to this feature, it is an ideal choice to use captive-electrolyte batteries for stand-alone system that is located in remote areas.

4.1.3.3 Lead-acid batteries

Lead-acid batteries are by far the most commonly used in PV systems. They are low cost and have the capacity ranging from 10 Ah up to 1000 Ah. The deep cycle characteristics make them appropriate for PV installations. But there are still some

limitations of lead-acid batteries. They are sensitive to harsh temperature and need to be maintained frequently. The table below shows characteristics of different lead-acid batteries.

Table4. 1: lead-acid batteries characteristics [22]

	Type	Cost	Availability	Deep cycle performance	Temperature tolerance	Maintenance
Flooded electrolyte	Lead-antimony	Low	Very good	Good	Good	High
	Lead-calcium open-vent	Low	Very good	Poor	Poor	Medium
	Lead-calcium sealed-vent	Low	Very good	Poor	Poor	Low
	Lead-antimony/lead-calcium	Low	Limited	Good	Good	Medium
Captive electrolyte	Lead-calcium sealed-vent	Medium	Limited	Fair	Poor	Low
	Lead-antimony/lead-calcium	Medium	Limited	Fair	Poor	low

Lead-acid batteries can be divided according to the elements alloyed in the plate. Three major types are lead-antimony, lead-calcium and hybrids.

4.1.4 Battery selection

Choosing batteries for PV systems involves many considerations and a balance needs to be found between desired and undesired properties. Two main parts to be considered are system requirements and battery characteristics. Table below shows some key properties that need to be considered when selecting batteries.

Table4. 2: Battery selection criteria

System requirements	Battery characteristics
system configuration	energy storage density
discharge current	allowable depth of discharge
daily depth of discharge	charging characteristics
autonomy	life cycles
accessibility	electrolyte specific gravity
temperature	freezing susceptibility
	sulfation susceptibility
	gassing characteristics
	self-discharge rate

4.1.4.1 Battery bank

In practical use batteries are usually connected together to provide required capacity and voltage. They can be connected either in series or in parallel. In most cases the voltage of a battery bank is 12V, 24V or 48V. The figure below shows the capacity and voltage of a battery bank in series and in parallel, respectively.

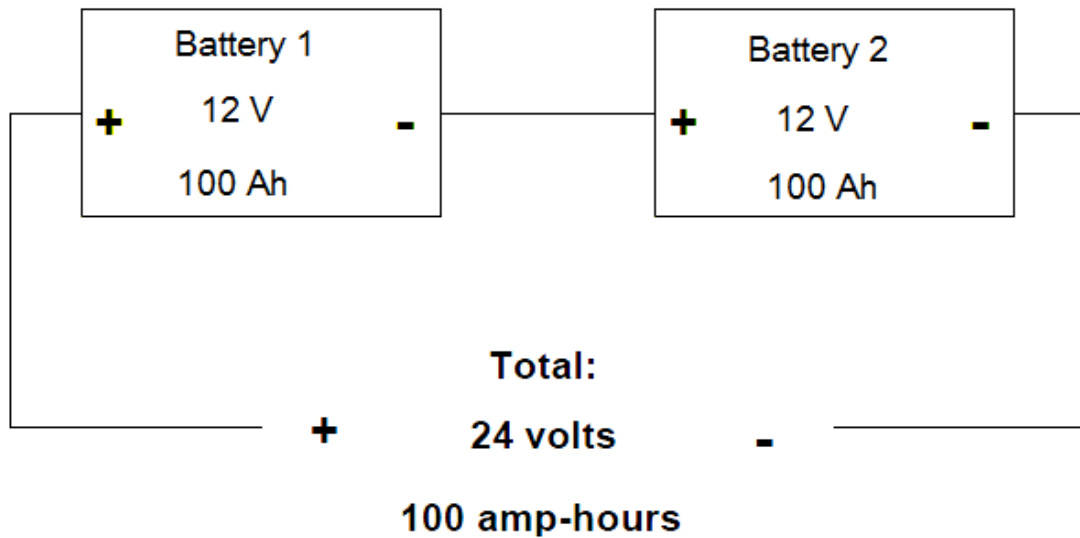


Figure4. 2: batteries are connected in series

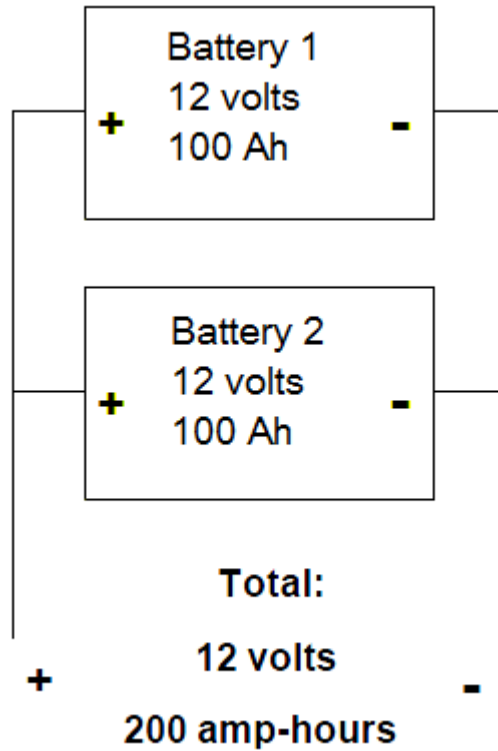


Figure4. 3: batteries are connected in parallel

It is recommended to connect batteries in series rather than in parallel, because when batteries are connected in parallel, the small difference due to resistance, length and integrity will lead to inequality of electricity for batteries. To overcome this deficit, when connected in parallel the external connection should be made from positive and negative terminals on opposite sides of the PV bank. The connection is presented in figure 4.4

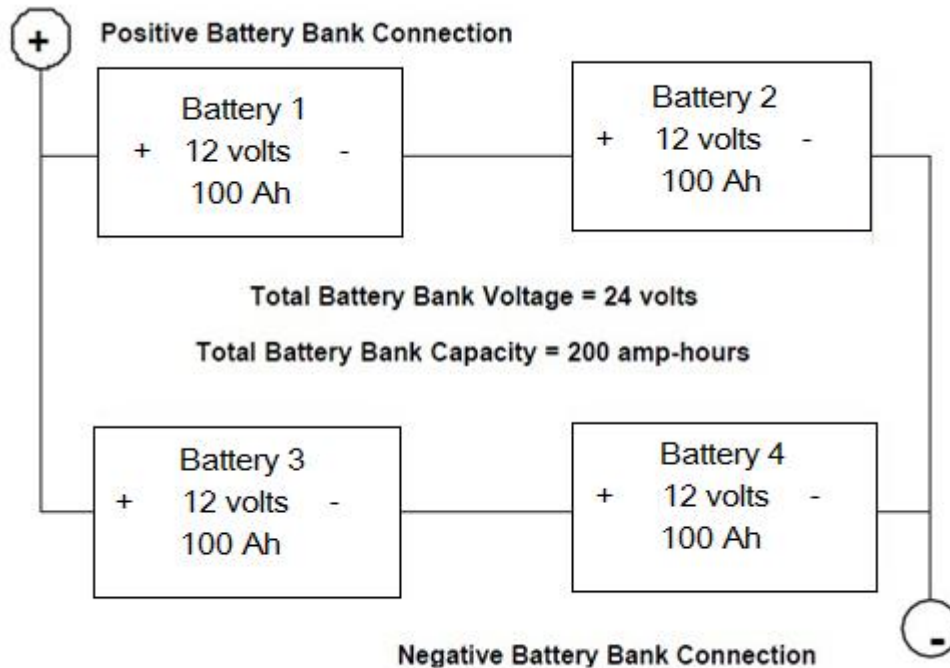


Figure4. 4: series and parallel connections are combined together

4.2 Battery charge controllers

A charge controller is an essential component of stand-alone PV systems. It is used to protect the batteries from overcharge and discharge in order to get higher capacity and extend cycle life.

4.2.1 Overcharge protection

If a battery without a charge controller is fully charged, the charging process will continue and leads to an excessive voltage, and then it may result in battery damage including gassing, electrolyte loss, internal heating and grid corrosion. A Charge controller prevents a battery from overcharge by interrupting or limiting the current flow when a battery is at full state of charge. To achieve this purpose, a voltage regulation setpoint is employed.

4.2.2 Overdischarge protection

When the load's demand exceeds the supply of PV arrays in peak hours or the

irradiance is insufficient, the batteries may be in the status of overdischarge which can cause reduction of battery life and performance. To prevent overdischarge a charger controller is used to disconnect the load from the battery if the voltage of the battery reaches a predetermined value.

4.3.3 Charge controller setpoints

Charge controllers need to operate under some particular situations; typically these situations are defined previously and are setpoints. They can be divided into charge regulation setpoints and load control setpoints.

4.3.3.1 Voltage regulation (VR) setpoints

Voltage regulation setpoint is used to describe the maximum voltage that a battery should reach when charging. Once the battery voltage reaches charge regulation setpoints, it means the battery is fully charged. A Charge controller will disconnect the array and battery or limit the current to the battery. It is critical to choose an appropriate setpoint for charge controllers and it depends on factors like battery type, size of array and load, temperature and electrolyte losses. The next table lists setpoints for different kinds of batteries.

Table4. 3: voltage regulation setpoint for different type of batteries [23]

Battery type	Interrupting charge controller		Linear charge controller	
	Per cell	Per nominal 12V battery	Per cell	Per nominal 12V battery
Flooded open vent lead-acid	2.43 – 2.47	14.6-14.8	2.40-2.43	14.4-14.6

Sealed valve-regulated lead-acid (VRLA)	2.37-2.40	14.2-14.4	2.33-2.37	14.0-14.2
Flooded pocket plate nickel-cadmium	1.45-1.50	14.5-15.0	1.45-1.50	14.5-15.0

When define setpoints for stand-alone system practically it is often to set them higher than manufacturer's recommendation. The reason is that batteries need to be charged in a short time period due to limitation of real conditions. So a higher voltage regulation setpoint can reduce the charging time.

4.3.3.2 Reconnect voltage of array

If the voltage reaches voltage regulation setpoint the charge controller will disconnect array and battery, current will stop from flowing into the battery and then battery begins to discharge with the decrease of battery voltage. Again when this number reaches a predetermined value then array will reconnect battery and continue charging. This predefined value is called array reconnect voltage.

Without setting array reconnect voltage, the battery will not be charged again and remain at a low level state of charge condition. Reconnect voltage ensures battery in a normal cycle of charging and discharging. Figure below shows voltage regulation and array reconnect setpoints.

Battery bank voltage

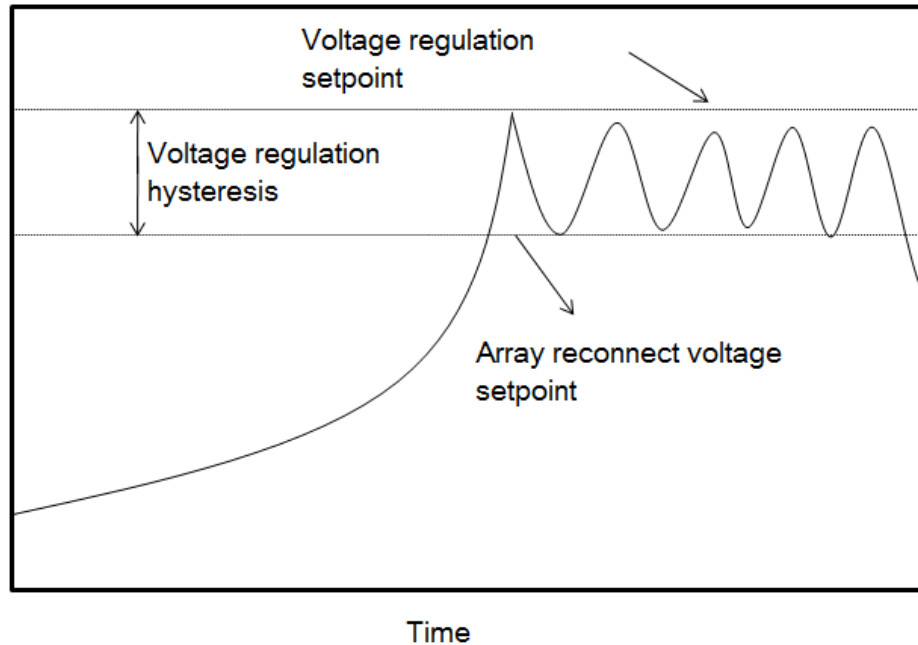


Figure4. 5: Voltage regulation and array reconnect setpoint

From figure 4.5, noted that voltage regulation setpoint and array reconnect voltage setpoint are not equal. The voltage difference between them is called voltage regulation hysteresis (VRH). It is an important parameter for interrupting type controllers, if the VRH is too large it will be more difficult to charge the battery and cause low energy utilization. For small VRH the battery will change the status of charging and discharging frequently which will damage the charge controller. Most interrupting charge controllers use a VRH of 0.4 V to 1.4 V.

4.3.3.3 Low-Voltage Disconnect Setpoint

In practical use if the battery voltage drops to a low level its performance and life will be shortened. A device is used to achieve the function of disconnecting the load from batteries. It can either be a single unit or be integrated into charge controllers. To achieve this function a low-voltage disconnect (LVD) setpoint is

established. The setpoint also defines depth of discharge and available capacity of the battery.

Choosing a proper disconnect voltage need to take into account both battery life and load needs. If the value is too low, load demand can be satisfied but the battery will experience high depth of discharge and reduce battery life. For high LVD batteries can perform well but limit the load availability.

Generally speaking, LVD setpoints are located at the position where the depth of charge of battery is less than 75% to 80% [22]. Usually the LVD setpoint for lead-acid batteries with nominal voltage of 12V is 11.2V to 11.5V. A lower setpoint is given for high discharge rate in order to achieve the same depth of discharge.

4.3.3.4 Load reconnect voltage (LRV) setpoint

Similar to the array reconnect voltage setpoint, after disconnection of the load and battery, the battery voltage will rise to open circuit voltage and due to the power supply from the array or other backup generators, the voltage are increasing gradually until some particular values. At that value the controller will reconnect the load with the battery; this value is load reconnect voltage setpoint.

When choosing LRV setpoint, it is important to select a value high enough to ensure the battery is charged to a certain level, while not too high considering load availability. The values are often set between 12.5V to 13.0V for nominal 12V lead-acid batteries. And the batteries often reach 25% to 50% state of charge when they are reconnected with loads.

Battery voltage (V)

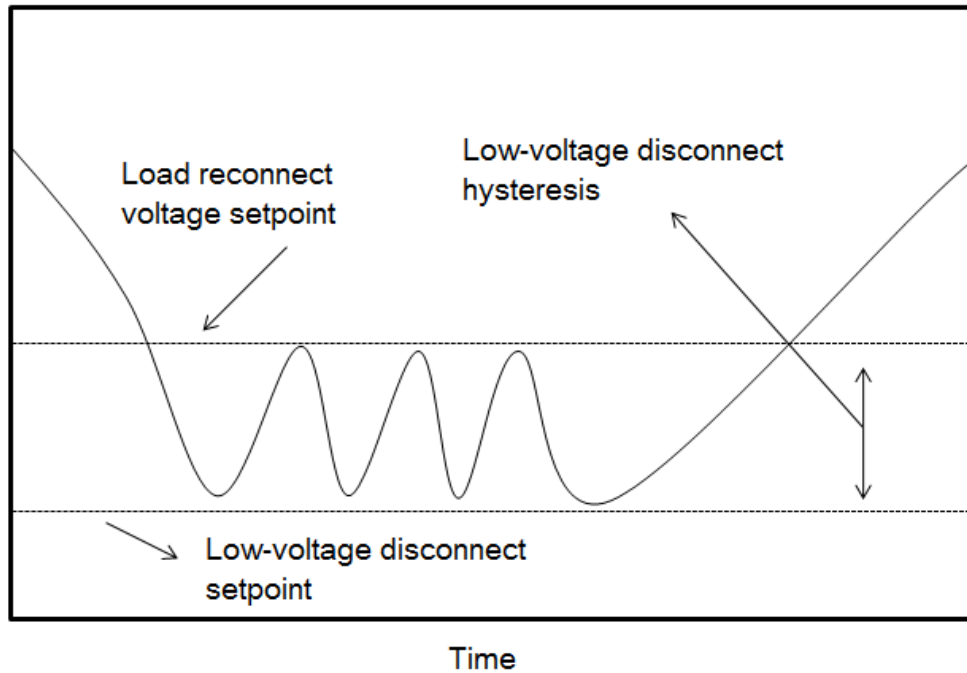


Figure4. 6: low-voltage disconnect setpoint and reconnect voltage setpoint

There is also a difference between voltage disconnect setpoint and reconnect point, it is called low-voltage disconnect hysteresis (LVDH). A proper LVDH selection will take the consideration of both battery and loads. Larger LVDH will make the battery to get fully charged which is beneficial to battery life but give up loads availability. Small LVDH ensures loads to work more efficiently but the battery will rapidly change the status of charge and discharge so shorten its life.

4.4 Type of charge controllers

Charge controllers often use switch elements to regulate current, they can be either interrupting or linear type. The first type regulates current by an ON/OFF switch and linear type use a more consistent way by lowering current gradually.

4.4.1 Shunt charge controller

Shunt charge controller regulates the current flow by short-circuiting the array through an element inside the controller. A blocking diode is used to prevent the

battery from short-circuit. Due to the voltage drop existed in the array components which is caused by resistance, a heat sink is required for controllers.

Usually a power transistor or MOSFET is used as the control element. The simplest and cost-effective design is interrupting type controllers. It can perfectly disconnect array and battery by an ON/OFF switch. After voltage reaches the reconnect value, the switch will close to charge the battery. Shunt interrupting controllers can be widely used in PV systems and especially suitable for small stand-alone system. Next figure shows a graph of shunt interrupting controllers.

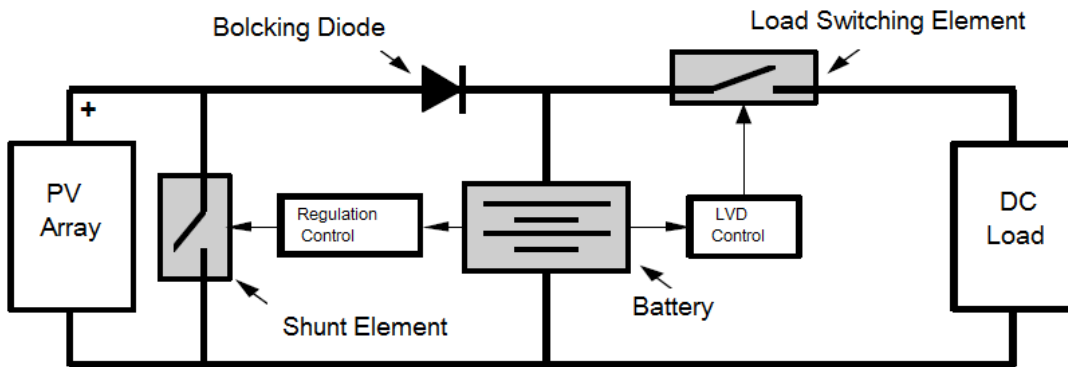


Figure4. 7: Shunt Interrupting Controller

Shunt linear controllers limit the current when the battery reaches full state of charge by gradually reducing the resistance. When selecting voltage regulation setpoints interrupting controllers requires higher values than linear controllers in order to make the battery fully charged.

4.4.2 Series charge controllers

Series charge controllers regulate current by open-circuiting the array. The control elements are in series rather than in parallel as shunt control. There is also a switch or a relay that can open the circuit to stop charging current flowing when the battery voltage reaches voltage setpoints. Compared to shunt controller design, there

is no need to put blocking diode to prevent battery short-circuiting. Figure shows series charge controller.

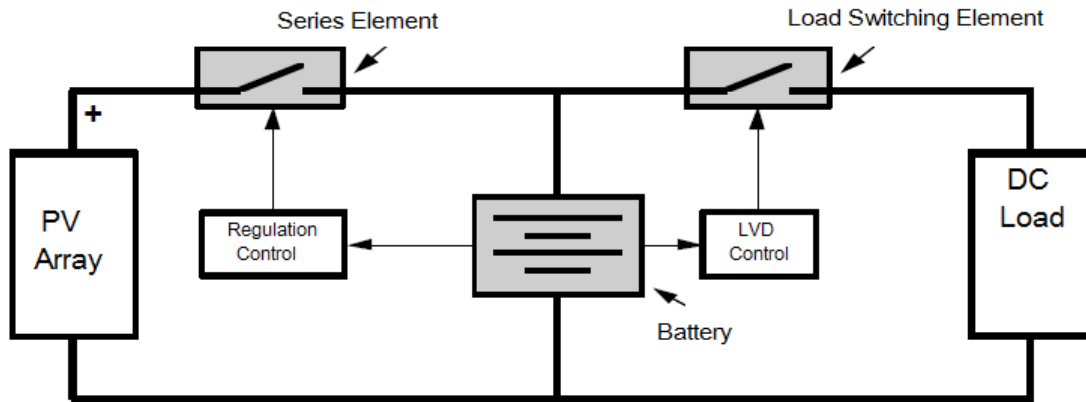


Figure4. 8: Series Controller Design

Series interrupting charge controllers are the most basic design forms. Similar to shunt interrupting controllers, it contains a switch to open or close the circuit. If the battery voltage achieves the voltage regulation setpoint the controller will open circuit to cut the current, after a time period when the voltage drops down to the voltage reconnect setpoint then array will connect battery again to charge. As battery becomes more fully charged, it takes less time to reach voltage regulation setpoint for each charging and discharging cycle. And the current also reduces for each time. So full charge is achieved by small intervals which is analogous to the shunt controller.

4.4.3 Maximum power point tracking (MPPT) charge controllers

This kind of charge controllers can make system operating as close as possible to the maximum power point on I-V curve through monitoring the circuit and changing the resistance or input voltages dynamically.

Array current (A)

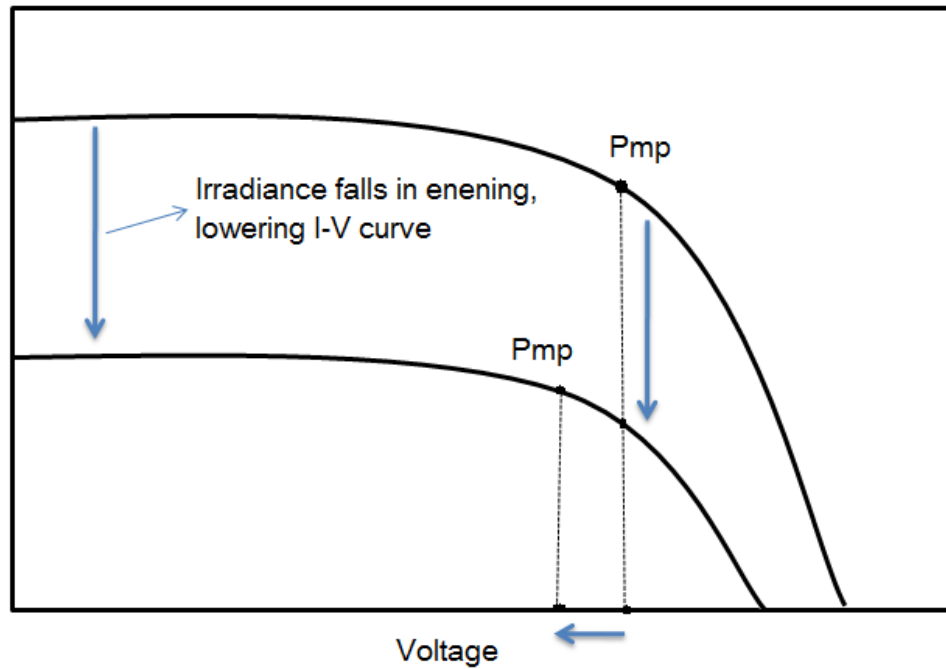


Figure4. 9: Maximum power point tracking

When external condition changes as irradiance reduction as shown in the figure, the I-V curve has a new pattern as well as the position of maximum power point. MPPT controller can adjust voltage according to current conditions to continue get maximum power. MPPT charge controllers improve battery charging performance effectively. Without MPPT control the array will operates at low battery voltage with a power loss of about 20%.

4.4 Loss in PV systems

In ideal conditions, the array should yield 1KWh under standard test conditions with irradiance of 1kW. However, there are some unavoidable factors that reduce the efficiency of PV system; they are losses existing widely among system components. System losses are caused by many kinds of reasons, like the resistance of electronic circuits and units aging. Major loss includes irradiance loss, mismatch loss, wiring loss soiling loss and thermal loss.

4.4.1 Array incidence loss (IAM loss)

The incident light will be weakened when it reaches the surface of the PV array surface compared with STC. The loss follows Fresnel's law of transmission and reflection of the outside layer of solar panel and cell surface. The effect of IAM loss can be described by the following parameter [20]:

$$F_{IAM} = 1 - b_0 \left(\frac{1}{\cos i} - 1 \right) \quad (4-1)$$

Where i is the incident angle. Coefficient b_0 is determined by different modules, for single-glazed thermal module, b_0 is 0.1. For crystalline modules with high refraction index the b_0 take the value of 0.05.

4.4.2 Array mismatch loss

Mismatch loss are mainly caused by the connection of cells with different characteristics. A PV module that constituents with different cells may result in power loss and reliability degradation due to the abnormal operating state of single cell. This loss is more severe for series connection when a certain cell is shaded or broken. Next figure shows the effect of mismatch cell.

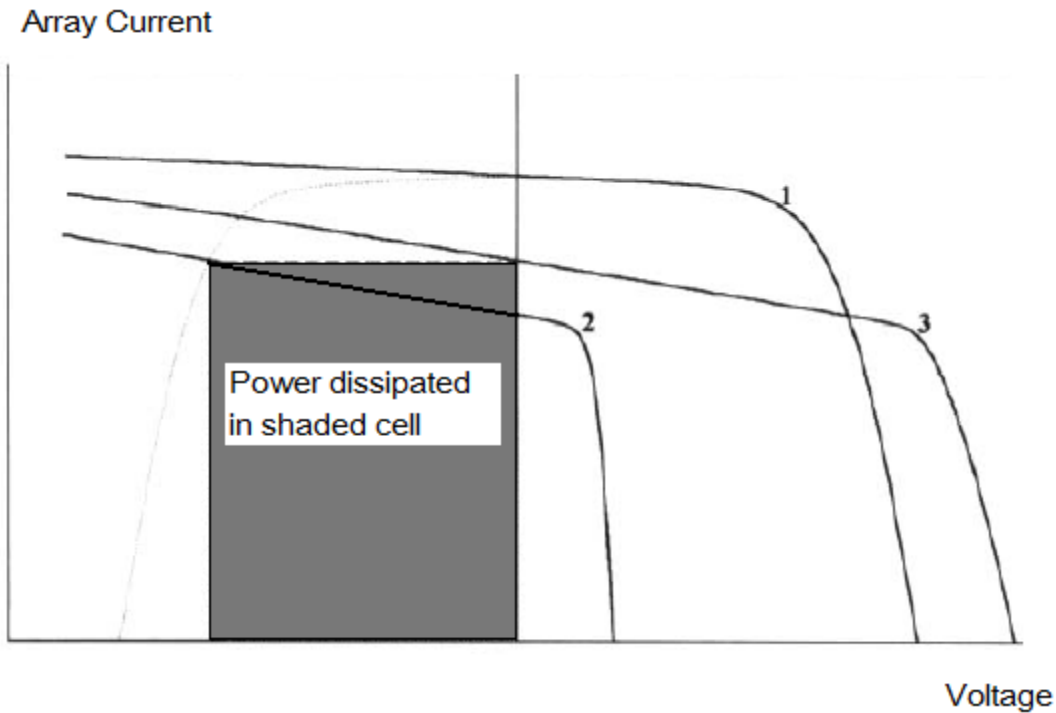


Figure4. 10: Current voltage curve of mismatch effect

In the above figure, curve 1 presents several identical cells connection and 2 shows a shaded cell. When they are connected together from the result of curve 3 it is clear that current reduction appears. So the power output also decreases, sometimes can drop to zero. In this case if the array is short-circuited, the shaded cell is reverse-biased and other cells operate at their maximum power point. All power generated by other cells will cumulate at the shaded cell and cause damage. Bypass diodes are used against these results.

4.4.3 Wiring loss

Wiring loss are existing modules and terminals of the array. These losses can be characterized by the resistance R .

4.4.4 Array thermal losses

In practical the modules often operates at higher temperature than STC conditions which will decrease their performance and further the power output. This kind of loss is called thermal loss. For crystalline silicon cells, the thermal loss will

result 0.4% of power output reduction from maximum power point with each degree Celsius rise.

4.4.5 Soiling loss

Soiling loss are those losses caused by the coverage of external objects that can block the insolation such as snow and pollutant. The influence of dirt depends on location and weather condition, for industrial or urban areas, the effect of dirt accumulation will be higher as well as droughty weather. In winter season snow also cause soiling loss, the duration of snow coverage on module surface is the main factor that affects energy yield. It will depends on the ambient temperature and module tilt angle, when it is below zero degree Celsius snow will remain on the surface for long time. A small tilt angle also prevents snow from sliding off the surface. A PV module with lower tilt angle can experience 30% more energy [24] reduction compared with a module that has higher tilt angle.

4.5 Inverters

The function of an inverter is to transform DC power to AC power; it is widely used in the systems that contain AC appliances. In real system design the inverters also integrates other components to form power conditioning unit (PCU) [22]. Power conditioning units can act as DC to DC converters and maximum power point trackers.

PV inverters can be divided into stand-alone inverters and grid-connected inverters.

Stand-alone inverters connect with batteries and operate independently from PV array. Grid-connected inverters connect PV array and operate in parallel with utility grids.

4.5.1 DC-DC converters:

DC-DC converters are used to change the voltage of DC power from one to another. They can achieve this function through high frequency switching and transformers. Transformers can also provide circuit isolation. Buck converter and boost converter are used as step down converter and step up converter, respectively.

PV inverters often use DC-DC converters to change voltage before the inverting process. For battery-based system, converters can provide other voltages rather than battery nominal voltage. Parameters of DC-DC converters are power rating, input and output voltages and conversion efficiency.

4.5.2 Maximum power point trackers (MPPT)

Maximum power point trackers are a form of DC-DC converter. It uses electronic components to adjust PV outputs and make it operate at its maximum power point under changing irradiance and temperature. Interactive inverters often contain MPPT circuits.

For large PV system with multiple PV arrays, individual MPPTs are designed to connect each array, in this way it is more efficient for MPPTs to operate at maximum output with each array that has different characteristics. So the total performance of PV system improves.

In some system, battery charge controllers have the function of MPPT, so there is no need to contain MPPT circuits in inverters.

4.5.3 Inverter characteristics

Main parameters that describe inverters include power, voltage and current ratings and efficiency.

4.5.3.1 Power ratings

Power ratings mainly affect power output of an array. Grid-connected inverters have a power ratings ranging from 700 W to 500 kW for large utility needs. Stand-alone inverters are smaller in range from 3 kW up to 6 kW.

Temperature limitation is the major factor that restricts power ratings. Usually inverters can operate at temperature from $-20\text{ }^{\circ}\text{C}$ to $50\text{ }^{\circ}\text{C}$. Inverters can use heat sinks or ventilation fans against excessive high temperature.

Grid-connected inverters limit temperature by control the power delivered to inverter. It can make the voltage rises and operating away from maximum power point. When the temperature drops, it can again operate at maximum power point. Next figure illustrate this process.

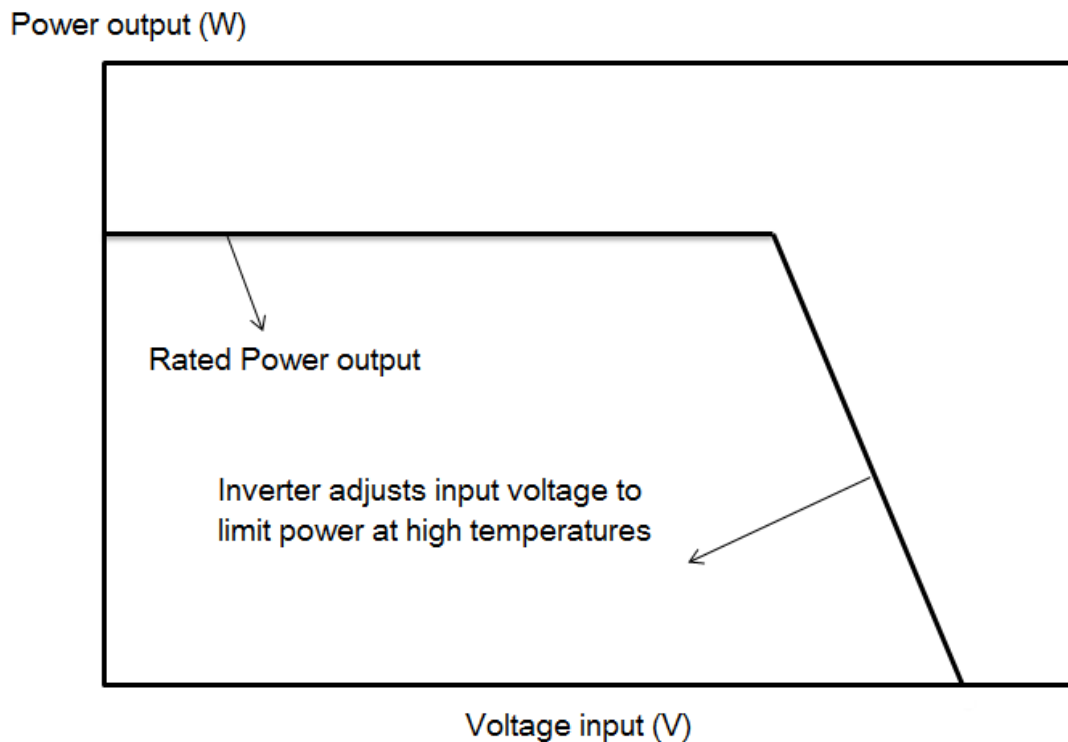


Figure4. 11: Inverters limit the power output by reducing voltage

4.5.3.2 Voltage ratings

Voltage ratings of inverters refer to AC output voltage and DC input voltage. The AC output for smaller inverters typically produces 120 V or 240 V. Larger inverters have the voltages of 208 V, 277 V or 480 V three phase AC output. For grid-connected inverters the voltage output should be within -10% to 5% of nominal voltage.

DC input voltage depends on the type of inverter. For stand-alone inverters it is based on battery characteristics while for grid-connected inverters it is determined by PV arrays. Stand-alone systems with lead-acid battery of 12 V have a voltage range from 11 V to 16 V [22]. And for larger systems the range also changes.

For grid-connected inverters, there are minimum operating voltages to ensure inverters normal performance and produce desired peak and RMS value of output voltage. On the other hand, a maximum voltage is also required to prevent inverters operate at excessive voltage. Figure below shows the operating voltage range.

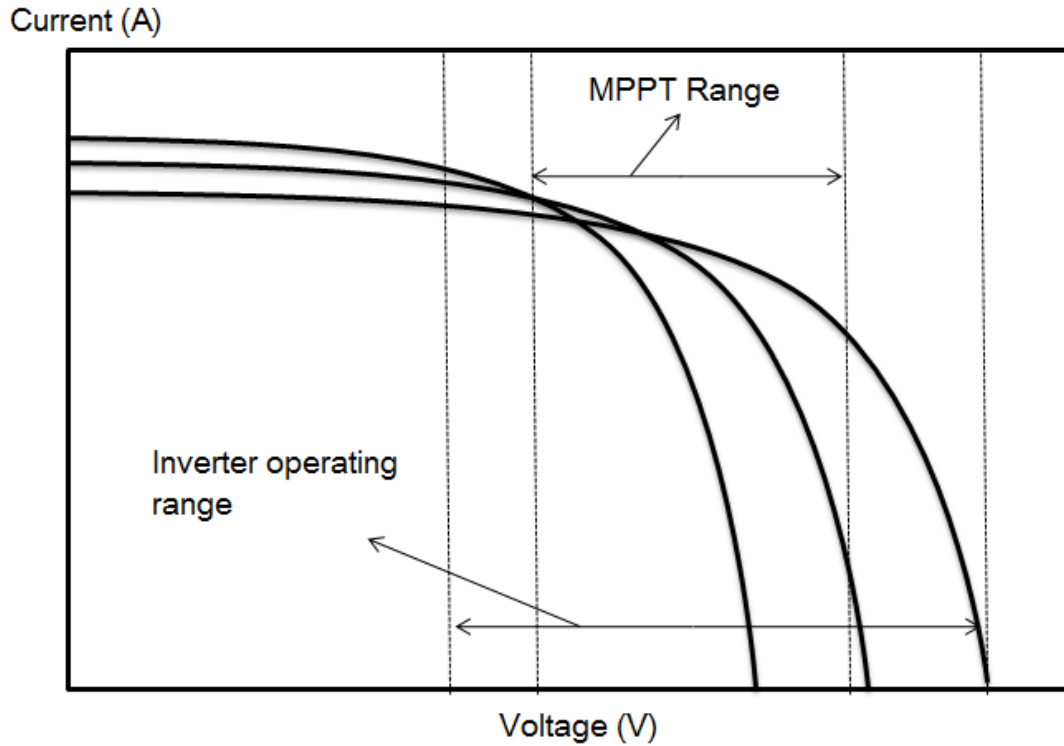


Figure4. 12: The operating input range and their maximum power point
 Array voltage increases with increasing grid voltage, in order to have a
 desired range of output AC voltage the DC input voltage must meet has a certain
 minimum values. Next figure illustrate this.

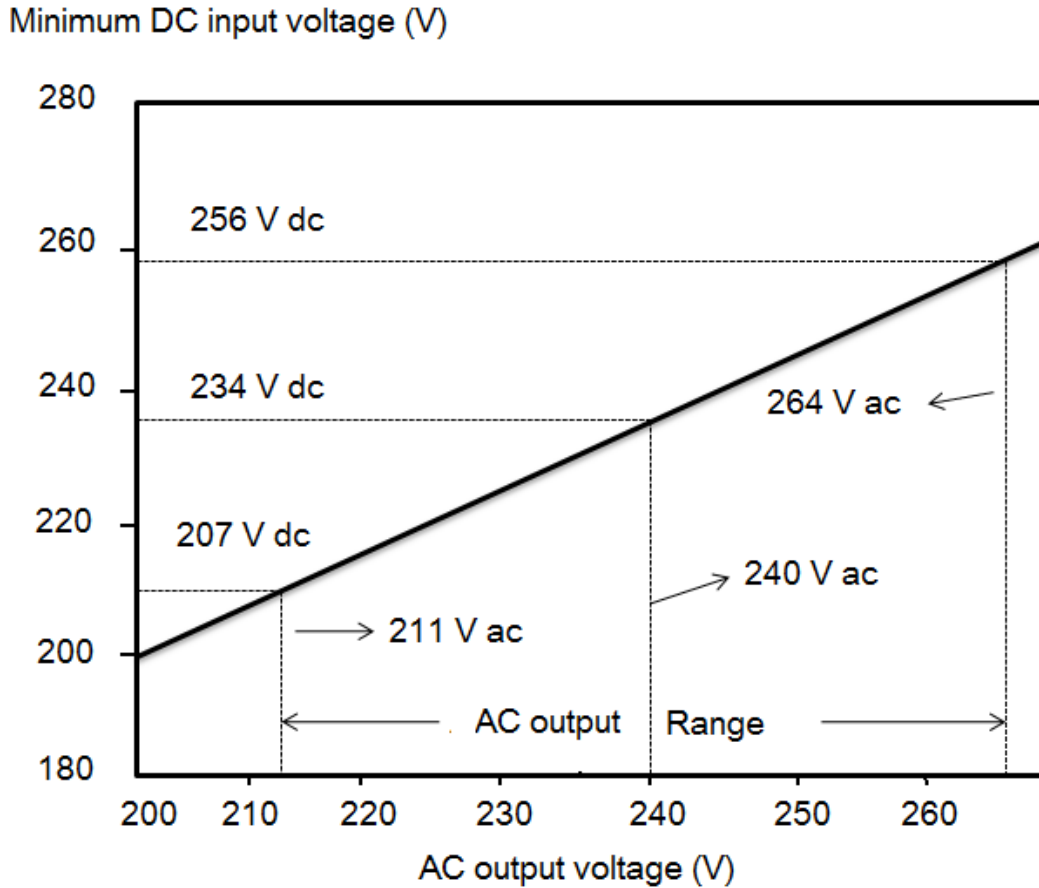


Figure4. 13: The relationship of utility and array voltage

DC input voltage for grid-connected inverters is affected by temperature. And some inverters have a wide range of input voltages which allows different array sizes and configurations.

4.5.3.3 Current ratings

Current ratings is responsible for the current value of both input and output side. For DC side, current ratings decide the maximum input current under normal inverter operation. For output current the loads and magnitude of current are concerned.

The output AC current is affected by ambient temperature. DC input current decreases with the increasing of input voltage to give a constant power output as the

figure shows below:

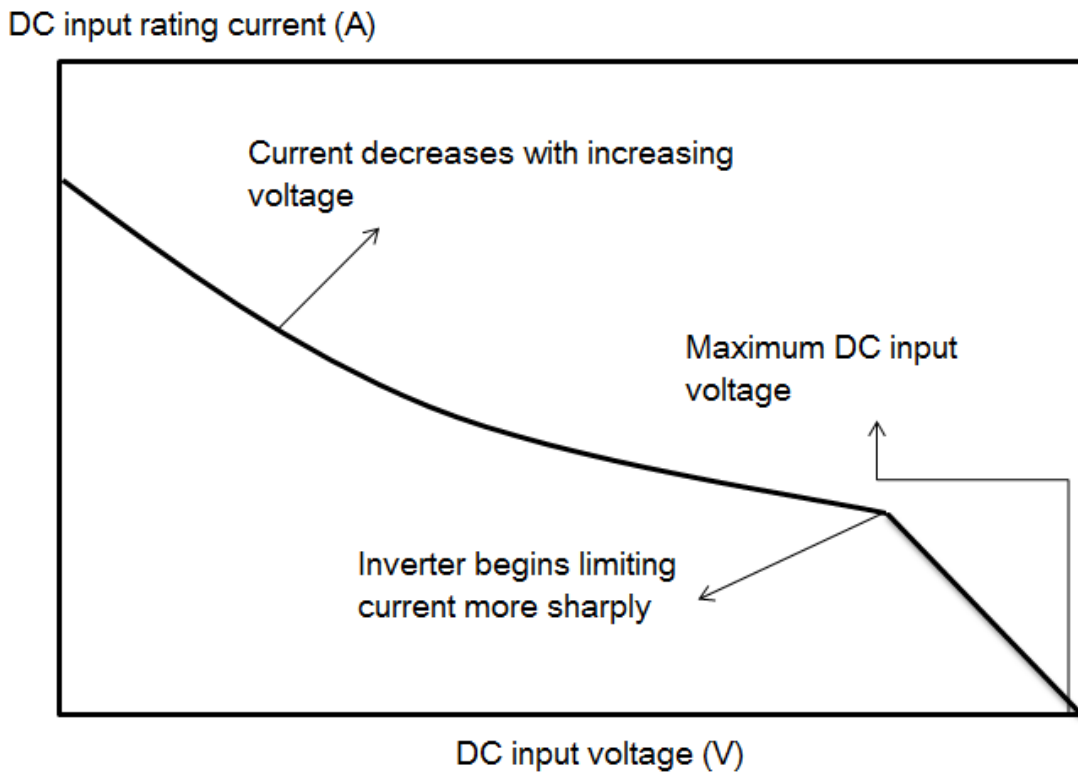


Figure4. 14: Input currents are reduced when voltage rises.

Maximum outputs AC current are also monitored and protection devices are used to prevent over current. They are integrated within the inverters.

4.5.3.4 Efficiency

During inverting process, there are some power losses due to operation needs and heat loss caused by circuit resistance. The efficiency of an inverter can be described by the following equation:

$$\eta_{inv} = \frac{P_{AC}}{P_{DC}} \quad (4-2)$$

Where η is inverter efficiency and P_{AC} is output power, P_{DC} is input power.

Most grid-connected inverters have an efficiency of 90% to 95%. Stand-alone inverters have peak efficiency of 90%. Generally inverters with high frequency and

voltage are more efficient than those lower ones. The efficiency is mainly affected by the load, inverter temperature and DC input voltage. Next figure shows inverter efficiencies for grid-connected inverters.

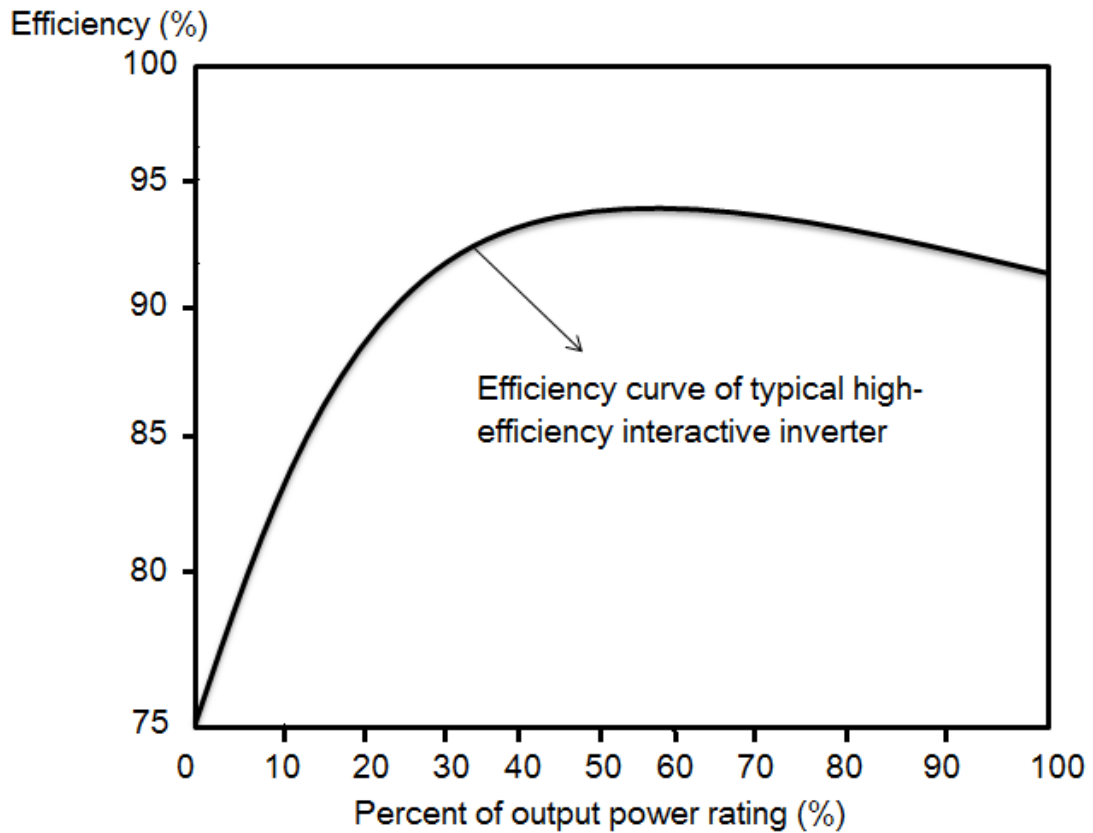


Figure4. 15: Inverter efficiency of different power rating

Chapter five: Stand-alone system design using PVsyst software

5.1 Introduction of PVsyst Software

The modeling process, simulation and results analysis are based on PVsyst. It is a software package used to study, size and analyzing data of different types of photovoltaic system including stand alone system, grid-connected system, water pumping system and DC grid system. The first three kinds of systems contain a preliminary design and a detailed project design.

The preliminary design uses monthly values of meteorological data and just few key parameters of system component for simulation process and obtains a rough estimation of the project. For grid-connected systems, it gives array orientation and system specification settings, including module type and technology, mounting and ventilation property.

For stand-alone systems, user can define module orientation, loads monthly or yearly total consumption, in the results array nominal power, battery capacity and other required system parameters can be obtained such as autonomy and system voltage.

In project design provides comprehensive system configurations. At first user choose the project location to get meteorological data. Then select the plane orientation type of fixed plane or tracking options. And a detailed system components dataset is given for defining PV module and array connection, loads, batteries, inverters and charge controllers as shown in figure below.

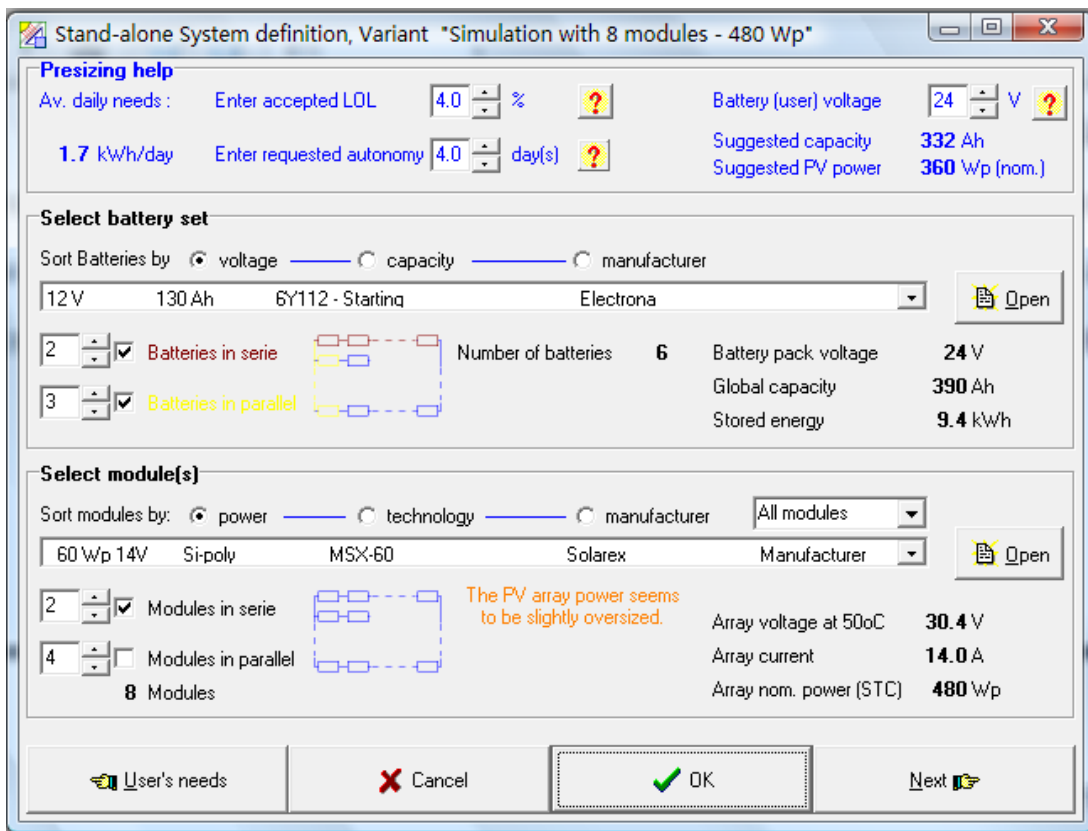


Figure5. 1: system components selection in project design

After that user can set detailed loss parameters like thermal loss, wiring loss, mismatch loss, soiling loss and incident angle loss. Simulation results are categorized by several aspects. Users can view irradiation, energy output, battery performance,

loads availability through the results. And a detailed loss diagram to visualize all the loss factors of the entire system. There is also a economic evaluation for financial analysis.

5.2 Geographical and meteorological data

PVsyst provide two kinds of meteorological data for users: monthly and hour data. When defining geographical site, the monthly meteorological data of horizontal global irradiation, diffuse irradiation, ambient temperature and wind velocity are given at the same time. However, for detailed simulation purpose, the hourly value of irradiation and temperature are needed. Synthetic hourly data can be generated automatically from monthly values of global irradiation and temperature when the site is confirmed. For more accurate simulation results PVsyst support external data sources to be imported for project.

The location of the project is chosen to be at Denver. Users can choose the location by selecting country and region, further location definition can be obtained through entering latitude, longitude and altitude directly. For meteorological data at least the global irradiation and temperature should be included in dataset to ensure the running of the simulation while the diffuse horizontal irradiation and wind velocity are optional.

In the project the data files of US Typical Meteorological Year (TMY3) data are used. It is a data file contains meteorological data from 1961-1990 and 1991-2005 National Solar Radiation Data Base and developed by National Renewable Energy Laboratory. (NREL)[25] In TMY3 the data are collected from 1020 sites of the US. Next figure shows the locations.

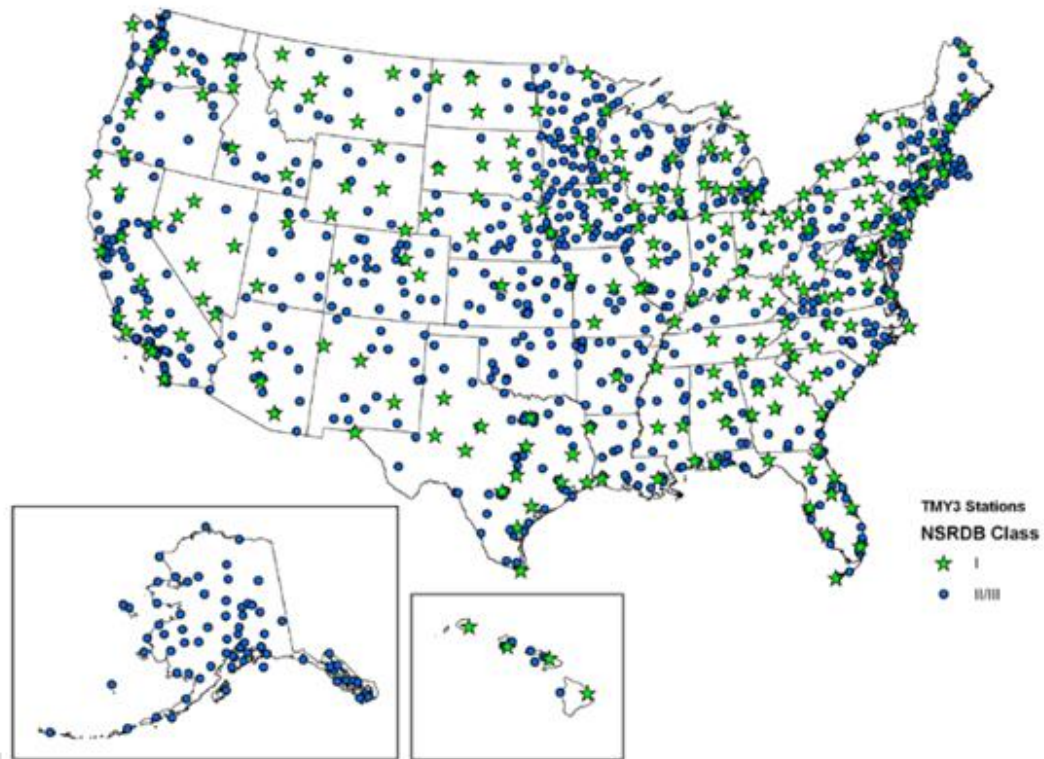


Figure5. 2: Locations of TMY3 ground stations [26]

The TMY3 datasets contains hourly values of solar insolation and climate data of one-year period. It is an external data source so user should get it freely from the web and import it into PVsyst. Next table shows hourly value during one year with two different days of December 21st and June 21st, respectively.

Table5. 1:Date: June 21st:

Time interval beginning	Global irradiation (W/m ²)	Diffuse radiation (W/m ²)	Temperature (°C)	Wind velocity (m/s)
00:00	0	0.0	17.20	3.10
01:00	0	0.0	16.70	4.10
02:00	0	0.0	16.70	1.50
03:00	0	0.0	15.60	1.50
04:00	4	3.0	16.10	1.50
05:00	76	64	17.20	2.10
06:00	123	96.0	18.30	3.10
07:00	382	136.0	20.60	2.10
08:00	634	119.0	22.20	2.60
09:00	702	159.0	24.40	2.10
10:00	870	207.0	26.10	3.60
11:00	946	180.0	27.20	2.10
12:00	723	460.0	26.70	0.00
13:00	569	298.0	26.70	5.20
14:00	429	317.0	26.10	2.60
15:00	402	254.0	23.90	1.50
16:00	337	144.0	24.40	2.60
17:00	117	117.0	23.90	1.50
18:00	38	38.0	19.40	6.70
19:00	3	3.0	18.30	3.60
20:00	0	0.0	17.80	2.60
21:00	0	0.0	17.20	2.60
22:00	0	0.0	17.20	2.60
23:00	0	0.0	17.20	2.10

Table5. 2: Date: December 21st:

Time interval beginning	Global irradiation (W/m ²)	Diffuse radiation (W/m ²)	Temperature (°C)	Wind velocity (m/s)
00:00	0	0.0	-1.10	1.50
01:00	0	0.0	-1.70	2.10

02:00	0	0.0	-1.70	2.10
03:00	0	0.0	-2.20	2.60
04:00	0	0.0	-2.20	2.10
05:00	0	0.0	-2.20	2.10
06:00	0	0.0	-2.80	2.10
07:00	20	9.0	0.60	3.10
08:00	148	32.0	3.90	5.20
09:00	294	44.0	8.30	4.10
10:00	404	53.0	12.20	4.10
11:00	461	57.0	15.00	3.10
12:00	457	57.0	16.10	1.50
13:00	395	52.0	15.60	2.10
14:00	279	43.0	15.60	2.10
15:00	130	32.0	14.40	1.50
16:00	13	9.0	9.40	2.10
17:00	0	0.0	4.40	2.10
18:00	0	0.0	4.40	2.10
19:00	0	0.0	3.90	3.60
20:00	0	0.0	3.30	3.60
21:00	0	0.0	2.20	3.60
22:00	0	0.0	2.80	4.10
23:00	0	0.0	2.20	1.50

Then Albedo values are needed to be set. It is the fraction of global irradiation reflected by the ground and received by PV array. It is zero for horizontal plane and increases with tilt angle. Program allows adjusting the albedo values for each month for the consideration of snow coverage. Usually the values range from 0.14 to 0.22 and up to 0.8 for snow situation. In the simulation this it is set to be a default value of 0.2.

Albedo Values

Monthly values

Jan.	<input type="text" value="0.20"/>	July	<input type="text" value="0.20"/>
Feb.	<input type="text" value="0.20"/>	Aug.	<input type="text" value="0.20"/>
Mar.	<input type="text" value="0.20"/>	Sep.	<input type="text" value="0.20"/>
Apr.	<input type="text" value="0.20"/>	Oct.	<input type="text" value="0.20"/>
May	<input type="text" value="0.20"/>	Nov.	<input type="text" value="0.20"/>
June	<input type="text" value="0.20"/>	Dec.	<input type="text" value="0.20"/>

Set a common value

Common value

(Default: albedo = 0.2)

Figure5. 3: Setting Albedo values

5.3 Orientation:

In photovoltaic system design the orientation should be taken into consideration because they will affect the performance of photovoltaic systems. To receive the maximum amount of solar radiation the photovoltaic panel needs to be placed at a certain angle.

There are different ways of array mounting and the simplest one is fixed-tilt mounting type. It is also the most commonly used way by far. In this way the array are permanently installed at an angle and face one direction according to its location, for northern hemisphere it faces south and opposite in southern hemisphere. It is cost-effective and is easily for installation and maintenance. However, due to the limitation of sunlight absorption, the energy collection is rather low. An improved way for this kind of mounting is using an adjustable tilt structure. The tilt angle can be adjusted manually to better receive sunlight; in summer season when the sun is higher the tilt angle is decreased while it is raised to catch the sun in lower position of the sky.

Although adjustable tilt angle mounting is an improvement to fixed-tilt array mounting. It is still cannot get the maximum power output because only by adjusting

tilt angle is not enough to ensure the PV panel to work at a desired orientation. By using tracking system this drawback can be overcome. Sun-tracking system can make the array orient to the sun according to its changing position and so the panel will face the sun at all time during daytime. Compared with fixed mounting, the array can produce up to 40% more power. According to the number of axis used and way of rotation, tracking systems are classified into different types.

Single-axis tracking use one axis and the array can rotate through it to follow the sun path. The array rotates either around the vertical axis to change the azimuth angle or rotate east-west. Both of these two ways can also adjust tilt angle simultaneously.

Two axis tracking are further used to catch the sun position more accurately. The two axes rotate independently. One configuration is altitude-azimuth tracking, one axis rotates to change the azimuth angle and another axis is tilt axis used to follow the sun's altitude. Equatorial tracking uses north-south axis to rotate the array in an east-west way and tilt axis change the tilt angle periodically over one year.

PVsyst gives numerous orientation schemes for photovoltaic modules installation including the mounting methods mentioned above. They are:

- a. Fixed tilted plane: user only needs set tilt and azimuth.

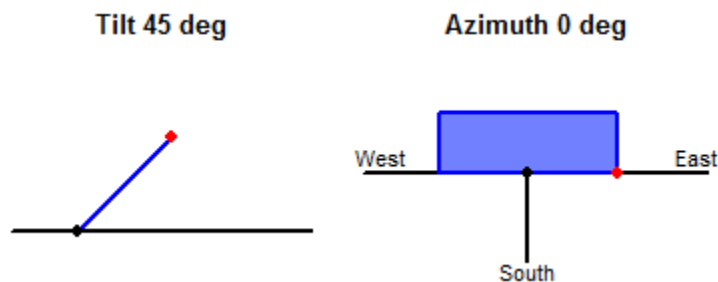


Figure5. 4: fixed mount array

- b. Seasonal tilt adjustment: plane tilt can be adjusted for summer and winter

season.

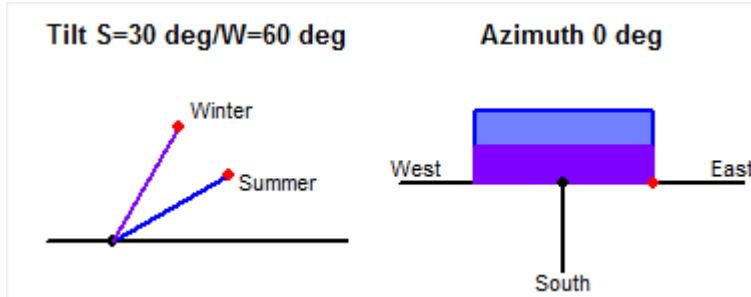


Figure5. 5: Adjustable tilt mounting

g. One axis tracking, vertical axis: solar panel is fixed onto an axis and can rotate with the sun path.

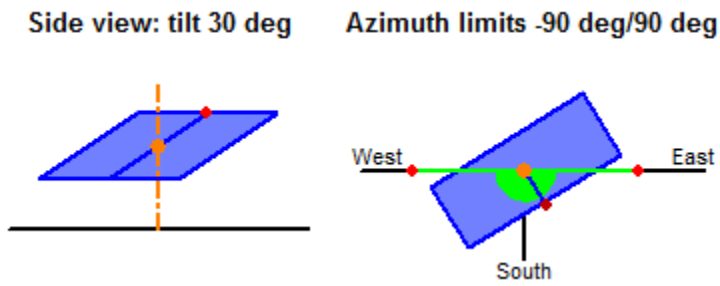


Figure5. 6: vertical axis tracking

e. One axis tracking, horizontal axis E-W: orientation axis is defined normal to the horizontal axis. Stroke limits should be defined from lower limit to upper limit. This configuration is actually not suitable for PV systems.

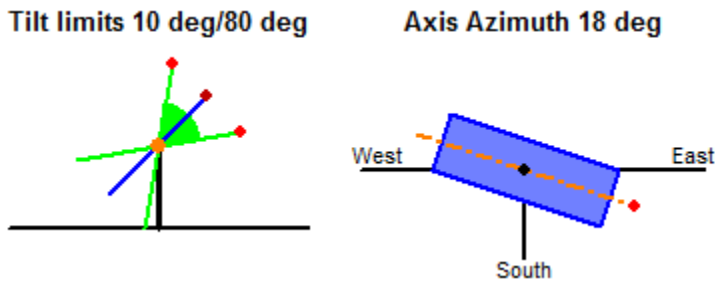


Figure5. 7: one axis tracking

d. Two axis tracking, tilted axis: tilt and azimuth of the axis are needed to be defined.

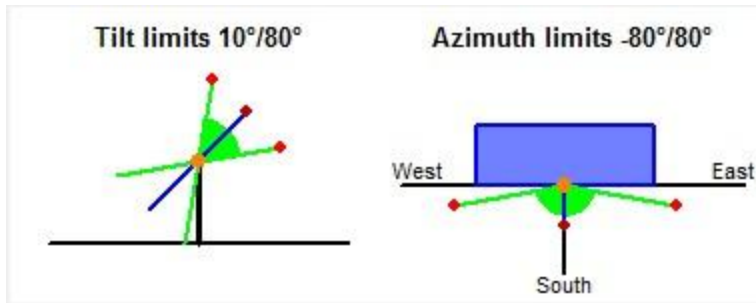


Figure 5. 8: two axis tracking mounting

f. Two axis tracking, horizontal axis N-S east to west: it is the usual setting for horizontal axis tracking systems, using tilt axis with tilt = 0 degree.

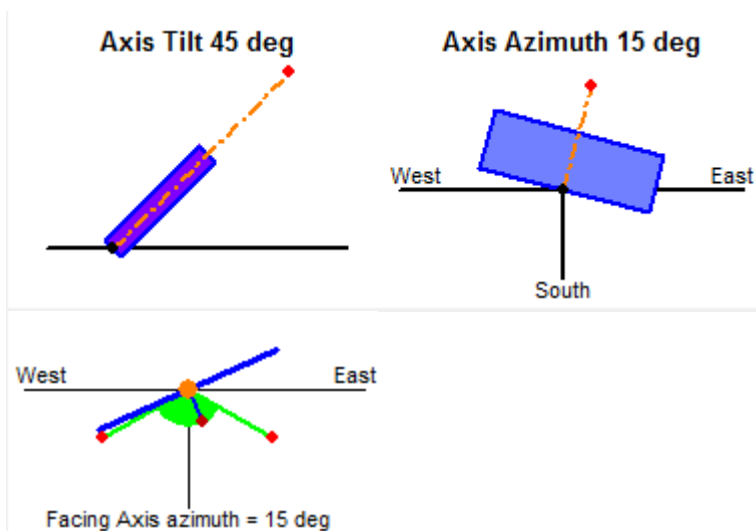


Figure 5. 9: two axis horizontal axis N-S east to west

c. Tracking, two axes: the plane is fixed within a frame and can rotate, tilt and azimuth angle need to be defined with maximum value of -90 degree to 90 degree and -180 degree to 180 degree, respectively. Then user can also choose a frame with north-south axis or a frame with east-west axis.

h. Tracking sun shields: it may yield solutions to the difficult optimization between sun protection and PV production.

For economic and maintenance considerations, here we choose the fixed tilt angle option as simulation model. The optimal tilt angle for fixed mount array is usually the latitude of the location. Since the latitude of Denver is 39.83 degree. The

tilt angle for this project is set to be 40 °.

In PVsyst, by using the plane optimization tool user can also easily find the optimal plane tilt and azimuth.

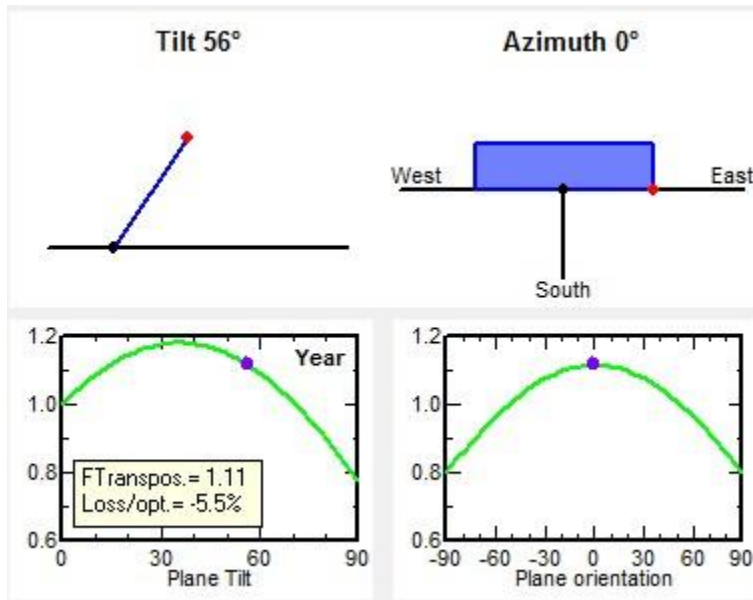


Figure5. 10: plane optimization for yearly irradiation yield

5.4 Stand-alone system sizing

5.4.1 Load analysis

For system configuration, first we need to define the user's need. In stand-alone system, the energy consumption is based on the daily, monthly or yearly use. The daily energy consumption for each load is determined by its power and operating time. In order to get an accurate load demand, the power and operating time must be obtained for each load.

If the system contains AC loads, an inverter is needed to convert DC voltage provided by array or batteries to AC voltages. There are several factors need to be considered when selecting an inverter. First the power output of the inverter should meet the peak watt hour of all AC loads. Usually the inverter is chosen to little larger than the AC loads demand for the possible future load extension. Inverter efficiency

is typically about 80% to 95%. [22]

5.4.1.1 Project assumption of load analysis

The designated location for the example is set to be at Denver, a residential house is constructed with a stand-alone PV system providing its power. The loads are being evaluated by monthly values. The usage of the majority of the loads is thought to be constant during single month. The loads include appliances and media equipments.

The appliances are composed by a refrigerator, a micro-wave oven, a toaster, air conditioner, coffee machine, washing machine and a dryer. First the daily power demand for each of them is obtained. [27] The refrigerator consumes about 1.2 kWh per day. The micro-wave oven has a power rating with 1 kW and operates about 15 minutes each day. So the daily energy consumption for micro-wave oven is 250 Wh. a toaster typically rated at 1150 W and uses for 8 minutes so that it has an energy consumption of 153 Wh. Coffeemaker rates at 800W for 15 minutes per day. The daily energy is 200 Wh. Washing machine has a power rating of 500W and operate twice a week with half an hour each time, the total energy then is 500 a week and 71 Wh per day.

Media equipment includes a TV set, a computer, a satellite dish. The nominal power of TV and satellite dish is 150W and 30W; they are used about 3 hours each day. The summation is 540 Wh one day. The power of a desktop computer is 120W and is used for 2 hours each day. The energy consumption is about 240W.

The power of air conditioner is 1000 W and energy consumption is 3kW for three hours in one day. However, this appliance is only during summer. Because the

total load requirements changes in different time of year, the monthly loads analysis is applied in the project. Next table shows the energy consumption for the household appliances in the month of July.

Table5. 3: AC loads analysis of July:

Load	Number	Power rating (W)	Operating time(hour/day)	Energy consumption (Wh/day)
Fluorescent lamp	4	18	4	288
Fluorescent lamp	4	10	4	160
Refrigerator	1	120	10	1200
Micro-wave Oven	1	1000	0.3	300
Toaster	1	1150	0.2	230
Coffeemaker	1	800	0.25	200
Washing machine	1	500	0.14	71
TV	1	150	3	450
Satellite dish	1	30	3	90
Computer	1	120	2	240
Air conditioner	1	1000	3	3000

Total AC power: 4982 W

Total daily AC energy consumption: 6229Wh

Inverter efficiency 90%

Average daily DC energy consumption: 6921 Wh/day

For the month of July, through the table above it is shown that total AC power requirement is 4982 W and the DC energy demand is 6064 Wh per day. So the inverter should be able to provide AC power of 5 kW. For future load addition considerations, the power rating of inverter should be a little higher than current value with 5.2 or 5.3 kW. Due to the inverter efficiency is 90% the final daily DC energy supply should be 6738 Wh.

The system should be designed to meet each month of the year including the highest loads usage month and lowest insolation month. There is a relationship between loads and insolation for each month and the worst case is that energy consumption is relatively high during low insolation month. The ratio between loads requirement and insolation is called critical design ration, it varies with the load demand and insolation for different months and are given for each month. The critical design month is the month with the highest critical design ratio, which means the system must work and supply enough power to the load under low sunlight conditions. The system components should be designed in the assumption of critical month.

To calculate critical design ratio, besides load consumption the insolation data is also needed. The insolation is represented by peak sun hours (PSH) per day; peak sun hour is the number of hours that receives solar irradiance of $1000\text{W}/\text{m}^2$ during one day from sunrise to sunset. Peak sun hours are given as average daily insolation in the unit of kWh/m^2 . It often gets its maximum value in summer and reaches minimum during December or January in northern hemisphere.

The load is assumed to be seasonally constant during winter, spring and fall. In summer the air conditioner is used and for individual season the energy is considered equal to each other. So the energy consumption for summer which is the month of June, July and August is obtained above, same as the month of July. For other three seasons, the energy use should be the summation of all loads without air conditioner and is 3229 kWh. Considering the inverter efficiency of 90% the final load needs is $3921/0.9=3587$ kWh.

The insolation data can be derived from TMY3 data introduced above. The dataset gives global irradiance for each day and month. Then it is possible to calculate the critical design ratio for each month. Next table shows the critical ratio.

Table5. 4: Critical design analysis

Month	Daily DC energy consumption (Wh)	Insolation(PSH/day)	Critical design ratio
January	3587	2.50	1434.8
February	3587	3.17	1131.5
March	3587	4.66	769.7
April	3587	4.79	748.9
May	3587	6.33	566.7
June	6921	7.27	951.9
July	6921	6.72	1029.9
August	6921	5.99	1155.4
September	3587	5.18	692.4
October	3587	3.68	974.7
November	3587	2.46	1458.1
December	3587	2.08	1724.5

From the critical design ratio given by the form, it is obvious that December has the highest value and therefore December is the critical design month.

The appliances can be entered into the loads datasheet in PVsyst, set December as the sample, the micro-wave oven and coffeemaker are categorized as domestic appliances; toaster is considered as other uses. Next two figure show the loads requirements in January and July:

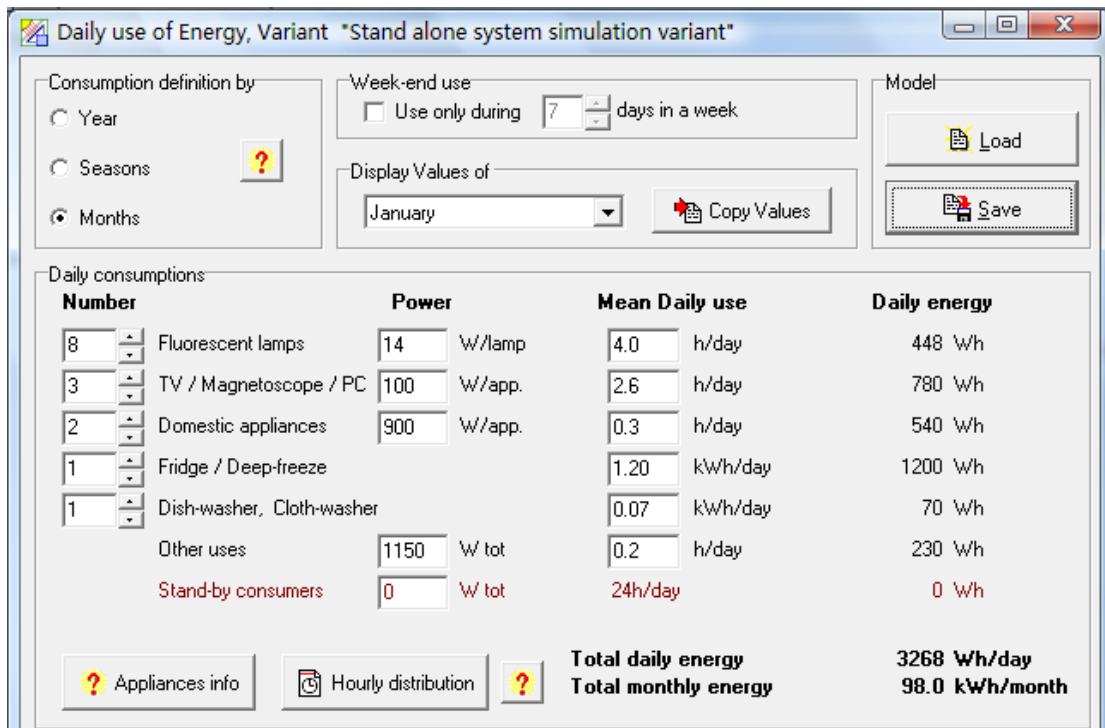


Figure5. 11: domestic appliance power consumption settings for January

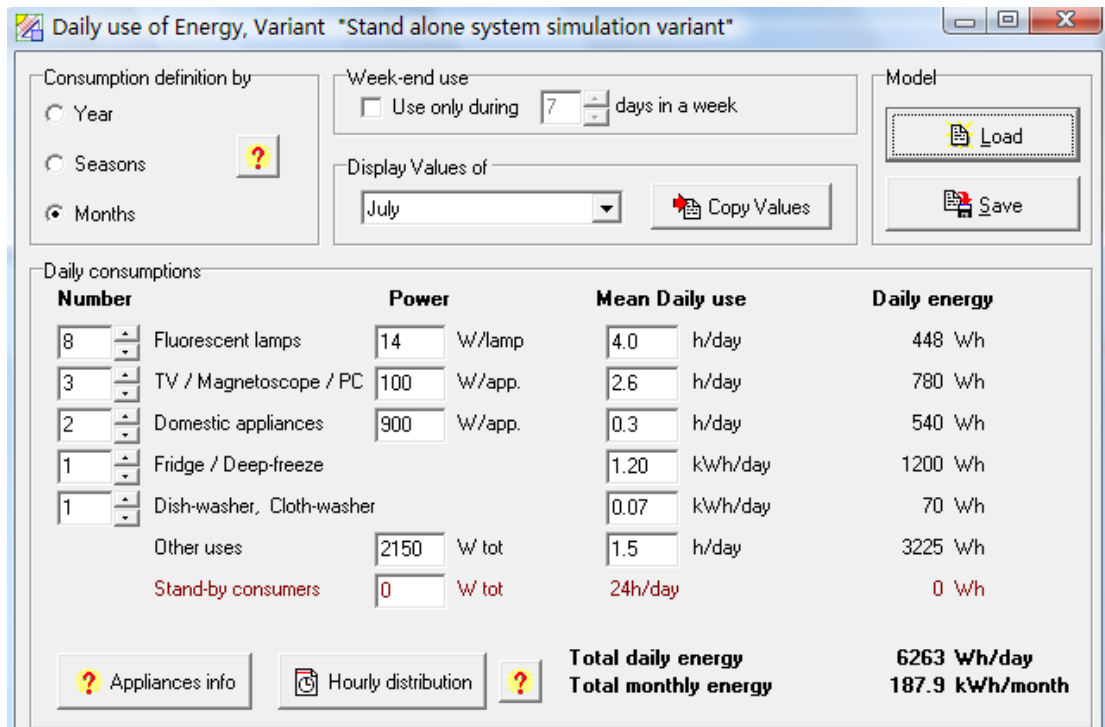


Figure5. 12: loads energy consumption for July

In the loads analysis sheet, the fluorescent lamps with 10W and 18W are thought to be eight identical 14W lamps. The TV set and computer have different

operating time, so it is needed to give the value of average daily use for them, it can be calculated by the following equation:

$$t = \frac{(P_1*t_1+P_2*t_2+\dots+P_n*t_n)}{P_1+P_1+\dots+P_n} \quad (5-1)$$

Where t is the average daily operating time of n loads, p_n is the power rating for each load and t_n is the separate operating time of p_n .

Using the above equation and the load table, the daily usage of TV set, dish and computer are given as:

$$t = \frac{150\text{ W}*3\text{ h}+30\text{ W}*3\text{ h}+120\text{ W}*2\text{ h}}{150\text{ W}+30\text{ W}+120\text{ W}} = 2.6\text{ hours}$$

Similarly, the time of domestic appliance including micro wave oven and coffeemaker is:

$$t = \frac{1000\text{ W}*0.3\text{ h}+800\text{ W}*0.25\text{ h}}{1000\text{ W}+800\text{ W}} = 0.28\text{ hour}$$

Other uses here only means toaster which has an individual operating time of 0.2 hour. But in the season of summer, the other uses includes toaster and air conditioner, thus the operating time is:

$$t = \frac{1150\text{ W}*0.2\text{ h}+1000\text{ W}*3\text{ h}}{1150\text{ W}+1000\text{ W}} = 1.5\text{ hours}$$

PVsyst does not support two digit-numbers after decimal point, so 0.28 hour is rounded to 0.3 hour. That is the reason why the total daily energy consumption appeared on the data sheet is 3268 and 6263 Wh for January and July, a little bit higher than table calculation result.

5.4.2 Array and battery sizing

5.4.2.1 Battery pre-sizing parameters

- 1). Decide the requested autonomy

The requested autonomy is defined as the time period that a battery can

support the loads power consumption without insolation. It is started from a full battery charge state and is given in days. Larger autonomy requires increased battery bank which is more cost and difficult to maintain, but reduces the depth of discharge and is therefore beneficial for the battery.

2). Loss of load probability (LOL probability)

It is the value of the time during one year that PV modules cannot meet the demand of load presented by percentage value, Due to the real insolation condition and system failure, it always exists. During the sizing process, the LOL probability allows for determining PV array size that is needed, for a given battery capacity. LOL probability is decided by autonomy and insolation. In practical, most stand-alone systems have 5% loss of load probability with autonomy of three to five days. The figure below shows factors that affects loss of load probability.

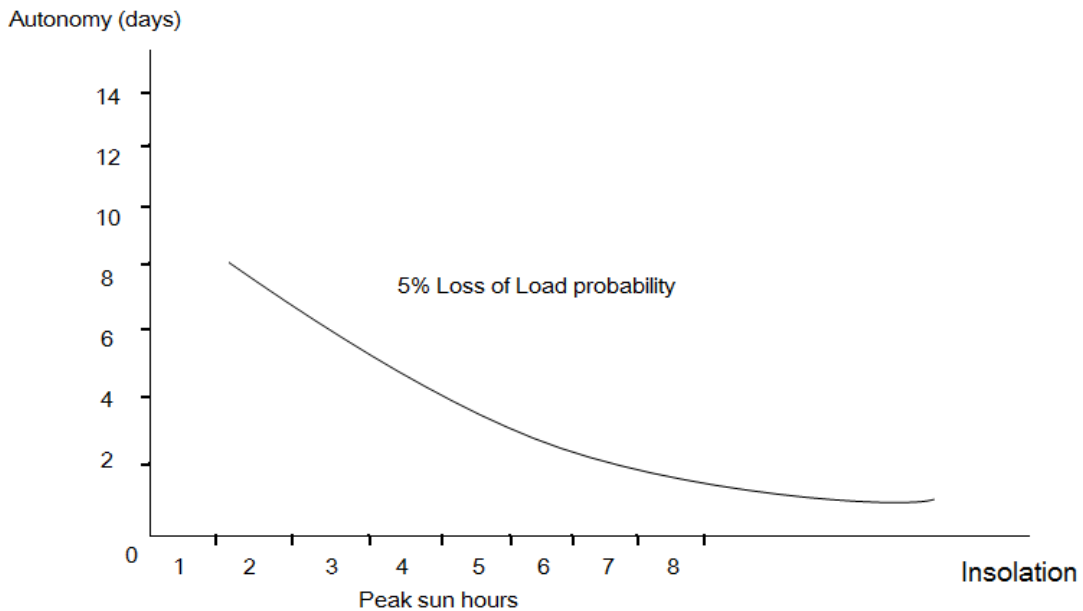


Figure5. 13: Loss of load probability can be roughly determined by insolation and autonomy.

For this project, the autonomy is set to be 4 days and loss of load probability is 5 percent.

3). Battery voltage

Typically the DC voltages for stand-alone system are 12V, 24V or 48V. Higher voltage results in lower current, which can further leads to the decrease of the size of corresponding components including inverter, charger controller and batteries. So the reliability of the system improves. Lower current also reduces the power loss and enhance the efficiency of the system. The figure below shows the relationship between system voltage and current.

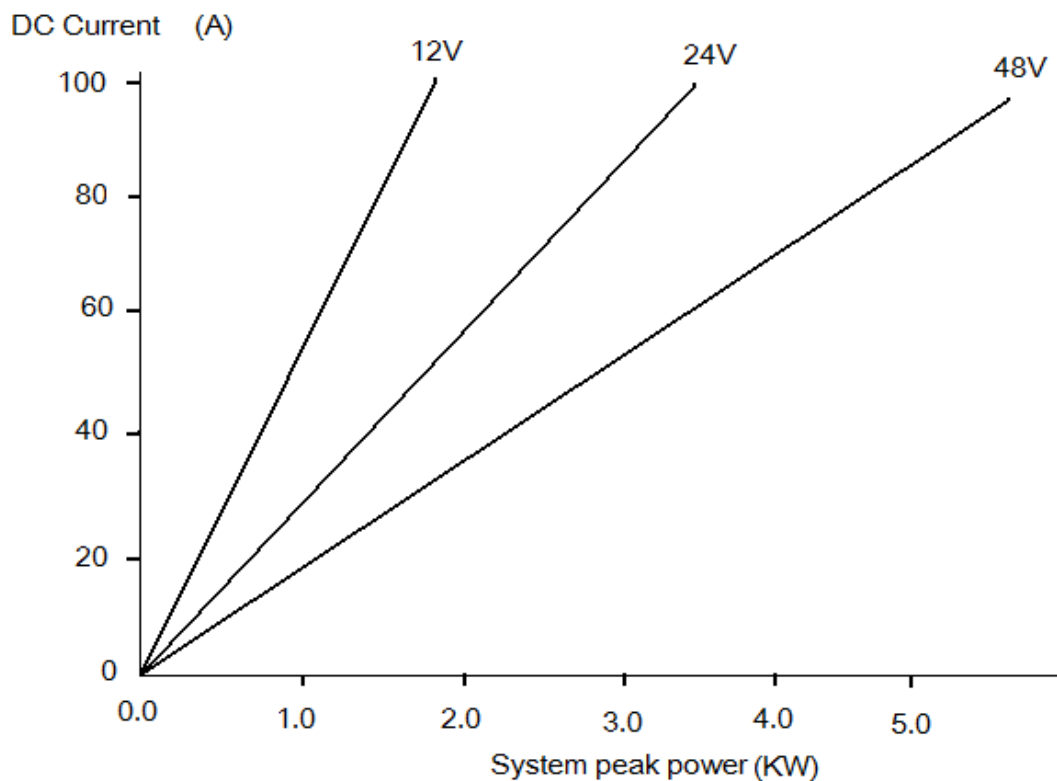


Figure5. 14: DC system voltage and Current

5.4.2.2. Battery sizing

The desired battery output is determined by loads and autonomy and can be calculated through the following equation:

$$B_{out} = \frac{E_{daily} * T_a}{V_{dc}} \quad (5-3)$$

Where E_{daily} is the daily energy consumption and T_a is the autonomy, V_{dc} is DC voltage.

In this system, the daily energy consumption is 6263 Wh, autonomy is 4 days and DC voltage is 48V. So the battery output should be:

$$B_{\text{out}} = \frac{6263\text{Wh} \cdot 4\text{d}}{48\text{V}} = 522\text{Ah}$$

So the battery should have the capacity of 522Ah for the loads to work normally.

In practical use due to some factors the real output will be less than the theoretical calculation. So the battery needs a larger capacity. These factors include depth of discharge, discharge rate and operating temperature. Almost all batteries cannot have a depth of discharge of 100 percent. Once the battery reaches an excessive depth of discharge permanent damage will occur. Usually batteries have a depth of discharge ranging from 20% to 80%. As the most commonly used battery technology, the lead-acid type of battery can have the depth of discharge of 80%.

Temperature also affects battery capacity, the battery capacity is determined under standard test conditions of 25 °C; lower temperature will reduce the battery capacity. Excessive high discharge rate is another factor lowers the battery capacity. The capacity affected by temperature and discharge rate can be drawn into the figure below:

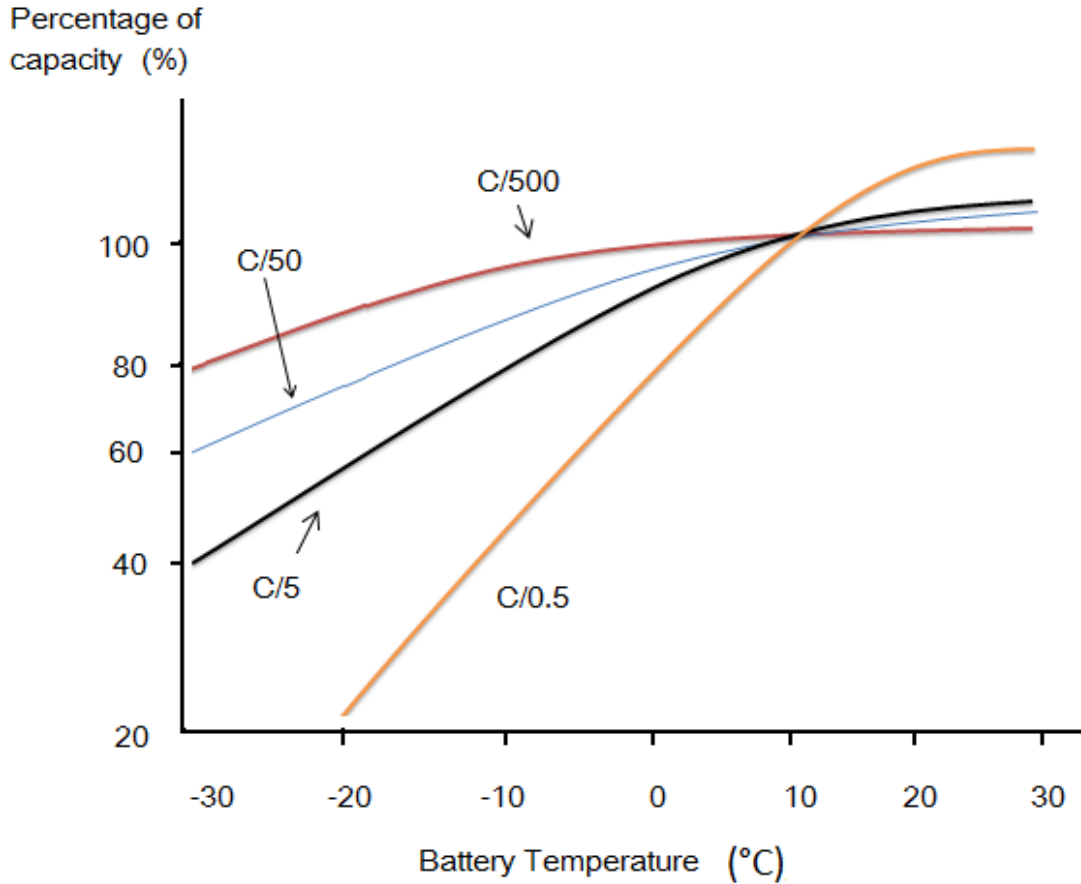


Figure5. 15: battery capacity is affected by discharge rate and temperature

The nominal voltage and rated capacity of the battery is put on the nameplate by manufacturer. In PVsyst these values are given according to the load requirement defined in the previous stage, as well as the loss of load probability and autonomy:

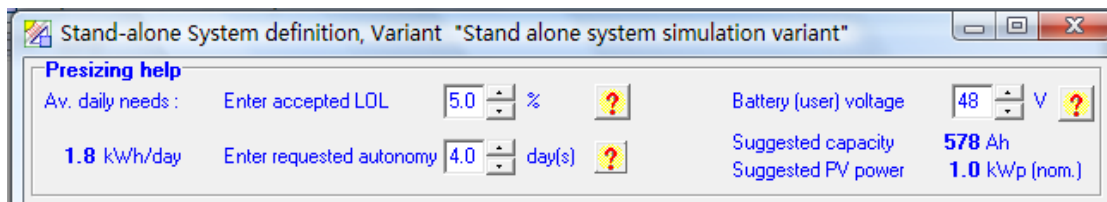


Figure5. 16: Battery basic parameters sizing

To get desired capacity and voltage, batteries need to be connected in series and parallel to form a battery bank. Parallel connection is not ideal because the existence of wiring loss, however, considering the capacity requirement, it is better to limit the parallel connections within three to four strings. Then the battery bank can

be designed according to the DC voltage and capacity. The desired capacity is the summation of the individual capacity of each string; the voltage is the summation of each element constituting the string. For the desired capacity, the number of strings is often not an integer, so the number should be round up to the closest integer. It should be taken into consideration that the final real capacity is not too much than the desired capacity.

The DC voltage of the system should be decided by the load requirements, the power of some appliances exceed 1000W, so a 48V DC voltage is needed to meet the demand of these loads. From figure for the required capacity of 522Ah the suggested capacity is 578Ah. Then a suitable battery set is selected. Through PVsyst numerous kinds of batteries produced by different manufacturers are available. In its data sheet user can view the basic parameters including DC voltage and capacity. In the project a 6V lead-acid battery produced by Surrette is used considering capacity and number of strings. The battery capacity is 291 Ah and voltage is 6V. The weighted operating time for the whole house according to equation () is calculated as:

$$t = \frac{288\text{Wh} \cdot 4\text{h} + 160\text{Wh} \cdot 4\text{h} + 1200\text{Wh} \cdot 0.16\text{h} + 300\text{Wh} \cdot 0.3\text{h} + 230\text{Wh} \cdot 0.2\text{h} + 200\text{Wh} \cdot 0.25\text{h} + 71\text{Wh} \cdot 0.14\text{h} + 450\text{Wh} \cdot 3\text{h} + 90\text{Wh} \cdot 3\text{h} + 240\text{Wh} \cdot 2\text{h} + 3000\text{Wh} \cdot 3\text{h}}{6229\text{Wh}} = 4.02\text{hours/day}$$

In order to get 48V voltage, 8 batteries are connected in series and two strings are connected in parallel to provide 578Ah capacity. Then the total capacity is 582Ah.

Table5. 5: Battery sizing parameter

Daily energy consumption	6229Wh
DC system voltage	48V
Autonomy	4 days
Required battery output	522 Ah
Weighted operating time	4.02 hours
Minimum operating temperature	0 °C
Suggested battery bank capacity	578 Ah
Battery Manufacturer	Surrette
Battery voltage	6V
Battery capacity	291 Ah
Number of batteries in series	8
Number of strings in parallel	2
Total number of batteries	16
Practical battery capacity	582 Ah

The discharge rate of the battery can be obtained directly from PVsyst.

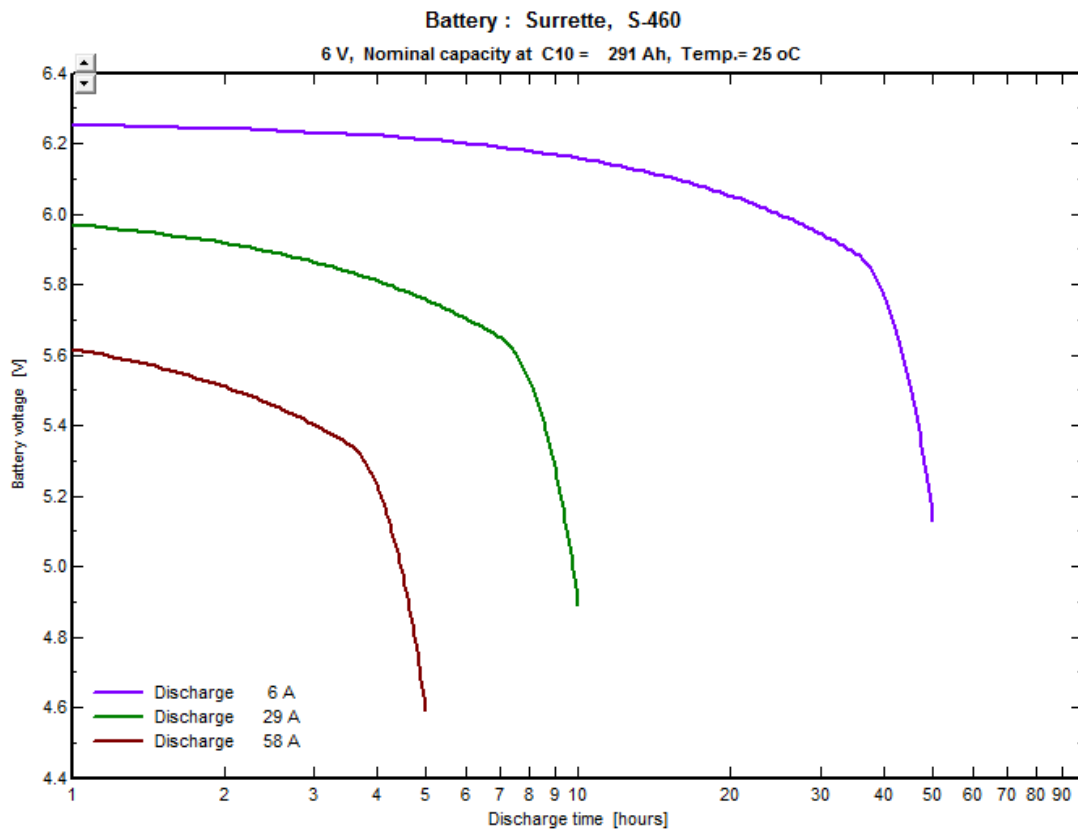


Figure5. 17: battery discharge rate

5.4.2.3 PV array sizing

The array should also be sized properly to provide enough energy to the loads

and for charging the battery. So there is required array output current, first the array is calculated by the energy and DC voltage. However, when considering battery charge, the current should be higher than the original calculation because the battery charging efficiency is always less than 100%. For most batteries the charging efficiency is between 85% and 95% [23], then the final output current is calculated using the following equation:

$$I = \frac{E_{crit}}{\eta_B * V_{DC} * t_{PSH}} \quad (5-4)$$

Where E_{crit} is the daily energy consumption for critical design month, η_B is the battery charge efficiency, V_{dc} is the system voltage, and t_{PSH} is the peak sun hour of the critical design month. The critical design month is December; the battery efficiency is set to be 90%. So from table the current is given by:

$$I = \frac{3587kWh}{0.9*48V*2.08} = 39.9A$$

This means the array should produce at least 39.9A current for loads work normally under peak sun hour conditions. However, similar to battery capacity, the array required output is affected by some factors so it never reaches the theoretical output. These factors include soiling and temperature, in order to get desired array output, it is necessary to increase array size considering these factors.

Soiling is the effect of dust and dirt falls on the surface of the PV array which can cause shade and further reducing the insolation. Most arrays have the soiling factor coefficient of 0.95 under light soiling and 0.9 under heavy condition. Then the rated array output current considering soiling is given by:

$$I_{rated} = \frac{I_{array}}{C_s} \quad (5-5)$$

I_{array} in the above equation is required current and c_s is soiling coefficient. In this case the rated current is then calculated as:

$$I_{\text{rated}} = \frac{39.9\text{A}}{0.95_s} = 42\text{A}$$

Another factor is temperature which affects the voltage output. There is a coefficient of 0.45% drops of voltage for every degree rise from 25 °C. Furthermore, the charging voltage is higher than the required voltage so to get the required voltage it should be multiplied by 1.2 for charging voltage. The array rated voltage can be calculated as:

$$V_{\text{rated}} = 1.2 * V_{\text{SDC}} * \{1 + [C_{\%V} * (T_{\text{max}} - T_{\text{ref}})]\} \quad (5-6)$$

Where V_{SDC} is the DC voltage, $C_{\%V}$ is the temperature coefficient, T_{max} is the maximum module operating temperature, and T_{ref} is the reference temperature.

Then the array voltage should be calculated using above formula:

$$V_{\text{rated}} = 1.2 * 48 * \{1 + [0.0045 * (50 - 25)]\} = 64.08\text{V}$$

Next step is to choose the module and decide the number in series and strings according to the rated voltage and current, which is 64.08V and 42A, respectively. In PVsyst the modules are chosen and arranged to meet the demands. Next table shows the entire array sizing parameters:

Table5. 6: array sizing parameters

Array Sizing	
Average daily DC energy consumption for critical design month	3578Wh/day
DC system voltage	48V
Critical design month insolation	2.08 PSH/day
Battery charging efficiency	90%
Required array output current	39.9A
Soiling factor	0.95
Rated array output current	42A
Temperature coefficient for voltage	0.45%/ °C
Maximum operating temperature	50 °C
Reference operating temperature	25 °C
Rated array operating voltage	64.08V
Module rated voltage	9.8V
Module rated current	7.31A
Number of modules in series	13
Number of modules in parallel	6
Total number of modules	78

In this project the chosen module ND-72 ELU made by Sharp; it has a power of 72W, the maximum power voltage is 9.8V and maximum power current is 7.31A. The array consists of 48 modules with power output of 3456W.

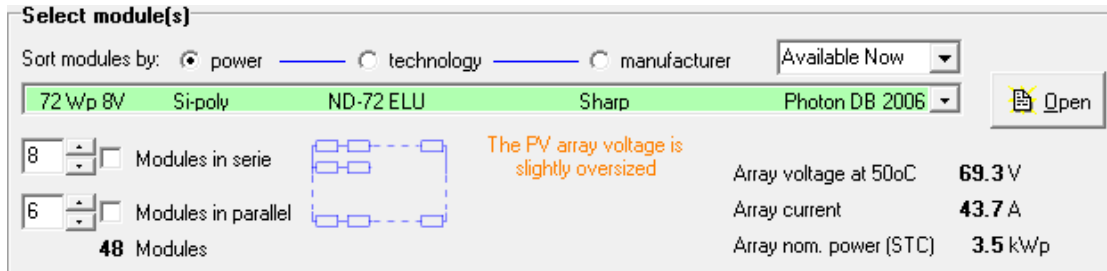


Figure5. 18: choosing PV modules

1) Model parameters

Comprehensive module parameters setting page is provided in the PV module tool window. Similar to the battery setting, in basic data sheet it displays PV modules identifiers from different manufacturers. As mentioned above, ND-72 ELU is considered as the module for this project. The electrical characteristics are measured under standard test conditions. Next table lists the parameters of ND-72 ELU.

Table5. 7: module selection

Module	ND-72 ELU
Manufacturer	Sharp
Nominal power	72Wp
Technology	Polycrystalline silicon
Short circuit current	8.04A
Open circuit voltage	12.43V
Maximum power point current	7.22A
Maximum power point voltage	9.88V
Module area	1.153m ²
Cells area	0.292m ²
Module area efficiency	10.93%
Cells area efficiency	14.53%

Next figure shows the I-V curve of the module. It is slightly different when the series resistance changes.

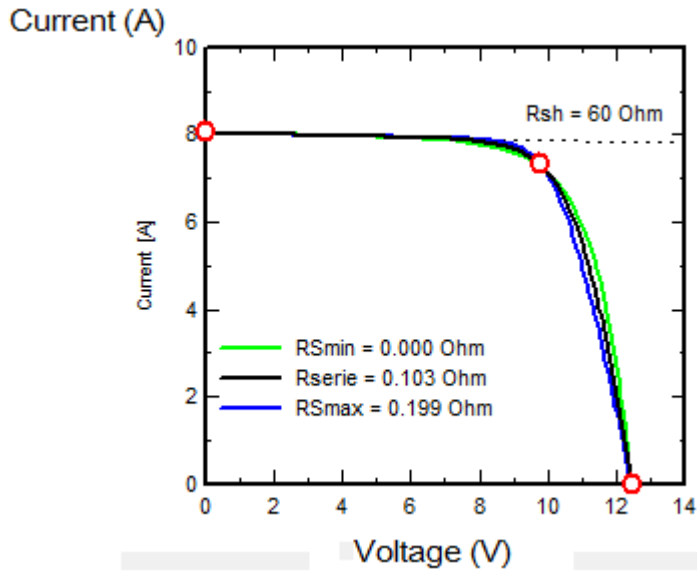


Figure5. 19: I/V characteristics given under irradiance of $1000\text{W}/\text{m}^2$, temperature $25 \text{ }^\circ\text{C}$.

As the conclusion before, irradiance and module temperature mainly affects power output. The performance of the module under different irradiance and temperature is also shown using PVsyst: when comparing irradiance, the module operating temperature is set at $45 \text{ }^\circ\text{C}$, instead of $25 \text{ }^\circ\text{C}$.

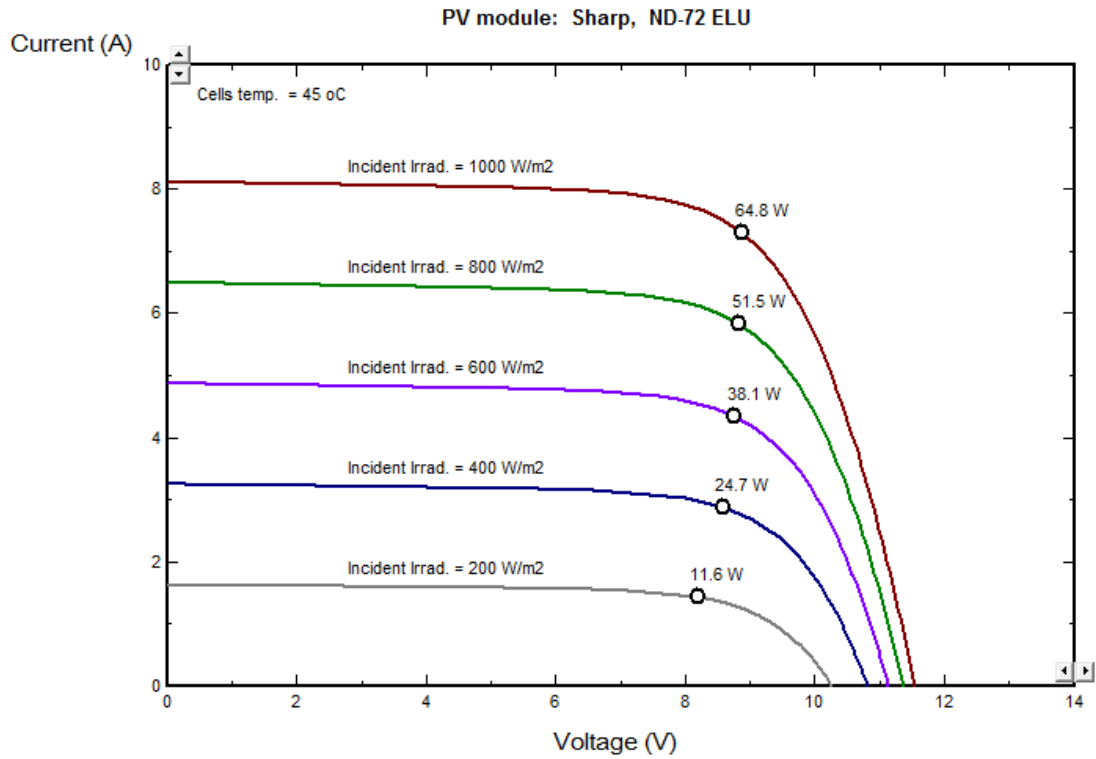


Figure5. 20: ND-72 ELU I-V curve under different irradiance

From the figure it is apparent that the power will increase with the irradiance rises. When comparing the power under different temperature, the default irradiance is 1000W/m^2 .

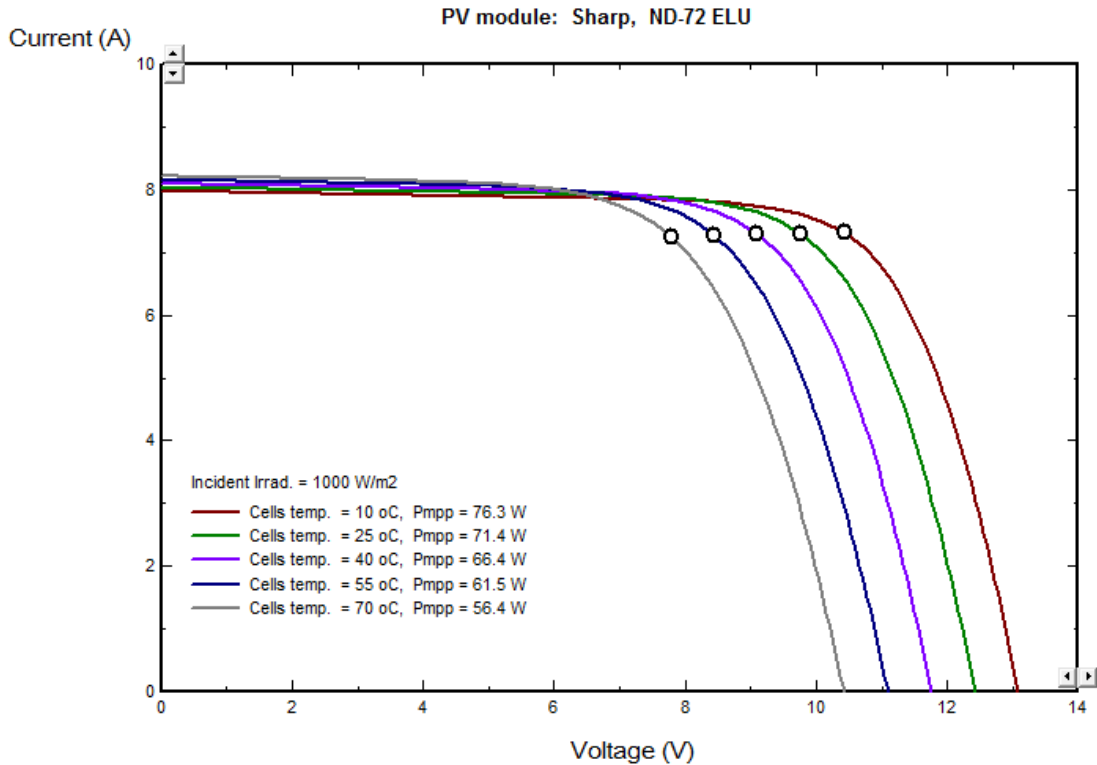


Figure5. 21: PV module behavior with different temperature

From the figure, when the current remains the same for low voltage conditions whatever how much the insolation is. And it begins to drop down when getting close to the maximum power point. High temperature will reduce the power output; it is verified by the curves. When temperature reaches 70 °C, the maximum power voltage is as low as less than 5V. For the reference temperature of 25 °C, the voltage can reach to about 6.5V and makes the maximum power higher.

5.4.3 Charge controllers

Next step is the selection of charge controller which is called regulator in PVsyst. When building a stand-alone system, it is commonly to use a power conditioning unit which integrates inverter, Rectifiers, transformers and DC-DC converters and thus can perform the function of each component. In PVsyst the inverter and maximum power point tracker (MPPT) are part of the charge controller configurations. The most important parameters in charge controller setting is voltage

regulation setpoint, array reconnect voltage setpoint for battery charging, and low-voltage disconnect setpoint, load reconnect voltage setpoint for load management as described in chapter 4.

In table 4.3 some reference voltage regulation setpoints are given depending on the battery type, however these parameters are further optimized according to several factors including controller type and loads [recommended practices for charge controllers Eric P.Usher]. PVsyst can automatically create the voltage regulation setpoints for the predefined system. Similarly to voltage regulation setpoints, the load control setpoints are also based on various kinds of factors including battery maximum depth of discharge and system type. The table below lists the setpoints of the charge controller.

Table5. 8: charge controller setpoints

Charging control setpoints			Load control setpoints		
Voltage regulation setpoints	Per cell	2.25V	Low-Voltage disconnect setpoint	Per cell	1.96V
	Whole system	54V		Whole system	47V
Reconnect voltage setpoint	Per cell	2.18V	Load reconnect voltage	Per cell	2.10V
	Whole system	52.3V		Whole system	50.4V

5.4.3.1 Temperature compensation

The setpoints derived above are based on the temperature of 25 °C. Charge controllers will change these setpoints if the temperature varies because temperature strongly affects the chemical reaction and thus the performance of the battery. When temperature rises, the battery will have a faster charging rate and start gassing earlier. At lower temperature the charging rate becomes slow down. So the battery will be overcharged under high temperature conditions and insufficiently charged in cold

weather if the charge controller uses fixed setpoints. Temperature compensation is introduced to help the battery to be fully charged under hot or cold weather as at 25 °C.

To measure temperature a sensor is installed with the system, small systems uses internal sensors mounted on the battery case for approximating battery temperature. Larger systems or batteries are located at the place with different temperature; an external sensor should be used. They are more accurate since the temperature varies significantly between the ambient environment and inside the controller. Temperature-compensated charge controller adjusts setpoints according to a predefined correction coefficient. For most lead-acid type batteries, this coefficient is -5 mV/ °C/cell.[23] The voltage setpoint at other temperature is computed using the following formula: [22]

$$V_{\text{comp}} = V_{\text{set}} - [C_{\text{Temp}} * (25 - T_{\text{Bat}}) * n_s] \quad (5-7)$$

Where V_{comp} is compensated setpoint, V_{set} is reference temperature setpoint, C_{temp} is compensation coefficient, T_{BAT} is battery temperature and n_s is the number of batteries connected in series. In this simulation, the V_{set} is 54V and N_s is 8, the voltage regulation setpoint at 0 °C can be calculated as:

$$V_{\text{comp}} = 54 - [-0.005 * (25 - 0) * 8] = 55V$$

For the battery operating at 40 °C, the compensated setpoint is

$$V_{\text{comp}} = 54 - [-0.005 * (25 - 40) * 8] = 53.4V$$

5.4.4 Array losses in PVsyst

The array losses plays an important part in reducing the array output, PVsyst takes several types of loss into project simulation consideration including thermal losses, Ohmic losses, module quality losses, mismatch losses, soiling losses and IAM losses. PVsyst gives each of these losses default values so user does not need to set

them, however they can still be changed in particular projects.

1) Thermal losses

The thermal behavior is presented by thermal loss factor U which is given by the following expression:

$$U = U_c + U_v * V \quad (5-8)$$

Where U_c is a constant component with the unit of $W/m^2 \cdot k$ and U_v is the coefficient of the wind velocity V (m/s). They mainly depend on the way of mounting the modules. When using typical meteorological year source, the value of U_c and U_v is given as:

$$U_c = 25 W/m^2 \cdot k, \quad U_v = 1.2 W/m^2 \cdot k/m/s$$

2). Array Ohmic wiring losses

The array wiring losses can be characterized by the resistance R . The program provides a default value for wiring loss of the entire system of 1.5% under the standard test condition. User can modify it for specific situations. The wiring loss result is shown in the figure below:

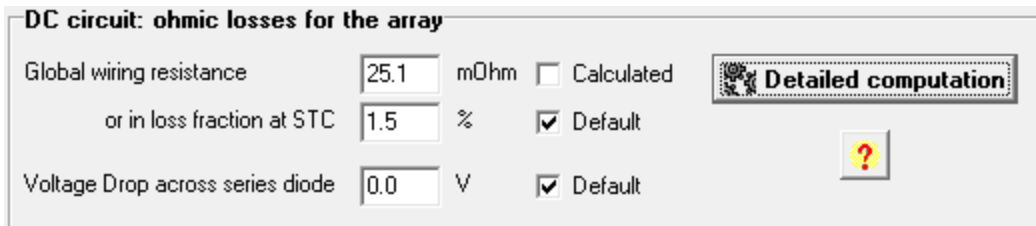


Figure5. 22: wiring loss setting

3). Mismatch loss

Mismatch losses are due to the slightly different characteristics even between the same modules when they are connected together. It is able to show the power loss at the maximum power point as well as the current loss under fixed voltage condition. Through PVsyst a graphic tool is applied to view the effect of adding mismatch loss on the I-V curve compared with ideal one.

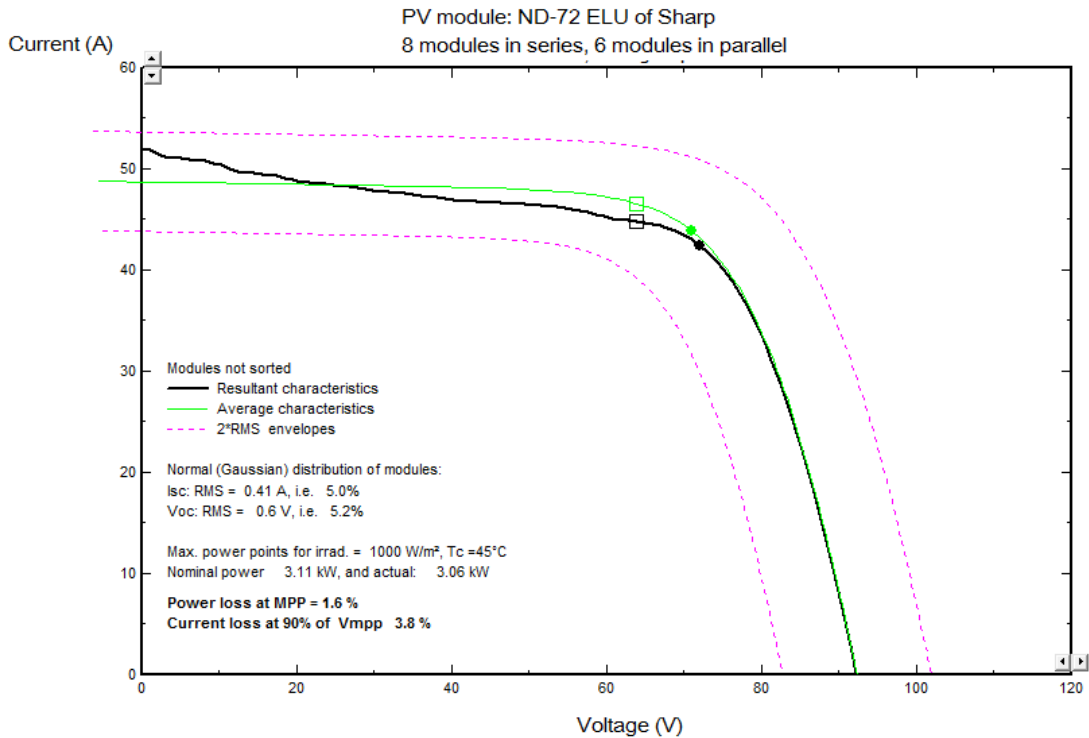


Figure 5. 23: mismatch loss of PV module: ND-72 ELU of Sharp

The curve in green represents the theoretical characteristics, the black one takes mismatch loss into account. There is 2.0% loss at MPP from the figure and the current loss is 3.8%.

4) Soiling loss

Soiling loss is another main factor that affects the power output of PV modules. The influence of soiling loss depends on the location of the modules, the array mounted near industry or urban areas are more likely to become soiled. In PVsyst the soiling loss can be derived using percentage over a year. Usually the soiling loss is 5%. [28].

5) IAM loss

PVsyst defines the loss as the actual incident light when it reaches the surface of the array due to small particles in the air compared with ideal case. It is represented

in equation (4-1). The default value of b_0 is 0.05.

PVsyst gives a synthesized diagram of the losses set above and the results after these losses.

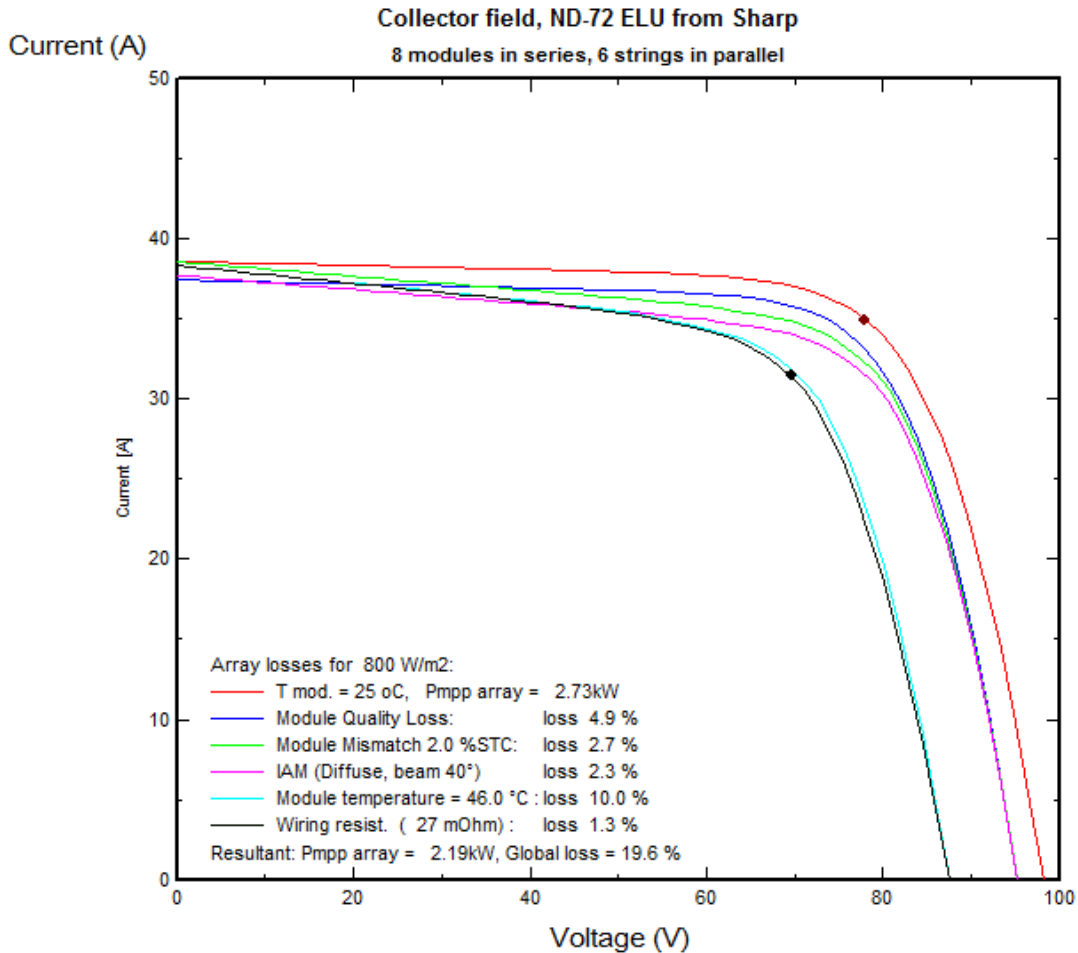


Figure5. 24: array losses effect

This loss effect figure is obtained under 800W/m^2 irradiance instead of standard test condition. The reference condition with irradiance of 800W/m^2 , ambient temperature of $20\text{ }^\circ\text{C}$ and wind speed of 1m/s is called nominal operating cell temperature (NOCT). [29]. When modules are installed in the field, they are often operated at higher temperature and low insolation than standard test conditions. The NOCT is defined as the temperature of the open circuit cell in module. The figure shows that the maximum power is 2.66kW , and each color represents one kind of loss

as shown in the picture. The losses are given by PVsyst in percentage listed in the table below:

Table5. 9: Losses effect

Type of Loss	Quantity of loss (%)
Module quality loss	4.9%
Module mismatch loss	2.7%
IAM loss	2.3%
Module temperature effect	10.0%
Wiring resist	1.3%

The final result is the curve in black and the power output is 2.19kW. So the total loss for this system is $1 - 2.19\text{kW} / 2.73\text{kW} = 19.6\%$.

Chapter six: Grid connected system design

Sizing grid connected photovoltaic system is a relatively simple procedure compared with stand-alone system because the system is connected to the external utility. So if the PV array produces more energy than the loads need, the extra energy can be delivered to utility grids, in the case of PV array cannot meet the loads demand, utility will provide electricity for the loads. Therefore battery bank is not necessary for grid connected systems.

6.1 Grid-connected system sizing

For the convenience of economic analysis the grid-connect system will still based on a building located at Denver as well as the module mounting.

The sizing of grid-connected system involves the loads analysis, module and inverter selection. The load in the stand-alone system project is still available for the grid-connected system, however, there is no need to use battery bank, and the critical design concept will not be used here. So energy consumption in the month of July should be applied for design the project. From chapter 5 the AC loads is 6263 Wh per day and 187.9 kWh each month.

6.1.1 Insolation

According to TMY3 data in table 5.1 and 5.2, the yearly average insolation is 4.57 PSH. That means the daily insolation of $1000\text{W}/\text{m}^2$ is 4.57 hours.

6.1.2 System AC energy needs

The system AC energy is calculated by the following equation:

$$365 * S * P_{\text{DCpeak}} * \eta = E_{\text{ac}} \quad (6-1)$$

Where S in the peak sun hour for the project location, η is the overall system efficiency from PV to AC grid, typically it equals to 75%. [22] P_{DCpeak} represents the peak DC power system rating of 1Wp. Then the E_{ac} can be computed as below:
 $E_{\text{ac}} = 365 * 4.57 \text{ hours} * 1\text{W} * 0.75 = 1.25\text{kWh}$

So 1Wp (DC) installed produces $E_{\text{ac}}=1.25\text{kWh}$ per year for the project. And the AC loads is 187.9 kWh per month derived above, then the yearly consumption is 2286 kWh. Then the required system DC power output will be

$$2254.8/1.25=1.828 \text{ kWp}$$

For module selection, the ND-72 ELU manufactured by Sharp is continued used here. The number of modules in series used is $1828/43 \text{ Wp} = 42.5$ and Rounding up to 43.

6.1.3 Inverter sizing

Most inverters have a recommended array nominal power to inverter nominal power ration ranging from 1.0 to 1.1. The nominal power of the inverter is defined as the output power. When the inverter is sized to match the power of PV array, if the maximum DC power produced by PV array exceeds the input DC limit of the inverter, the inverter will stay at the safe power range by adjusting the operating point on the I-V curve.

According to the DC power needs obtained above, an inverter with nominal power of 2 kWp is selected. The model of the inverter is PVIN02KS made by GE, the main parameters are listed in the table below:

Table6. 1: PVIN02KS main parameter

PV input side		Output AC side	
Minimum MPP voltage	150 V	Grid voltage	230 V
Maximum MPP voltage	450 V	Nominal AC power	2.00 kW
Absolute maximum PV voltage	500 V	Maximum AC power	2.2 kW
		Nominal AC current	8.7 A
		Maximum AC current	10.2 A
		Maximum efficiency	96.0%

After completing the module and inverter sizing, PVsyst gives the system operating conditions and array sizing results:

Tabl 6. 2: Array sizing

Module in series	43
Number of strings	1
Number of modules	43
Module area	17m²
Array nominal power/inverter nominal power ratio	0.92
Array nominal voltage	2.0 kWp

Table 6. 3: operating conditions

Voltage at maximum power point (60 °C)		230V	
Voltage at maximum power point (20 °C)		280 V	
Open circuit voltage (10 °C)		391 V	
Plane irradiance	1116W/m ² (Peak sun hour)	Plane irradiance	1000W/m ² (STC)
Maximum power point current	8.1A	Maximum power point current	7.3A
Short circuit current	9.1A	Short circuit current	8.1A
Maximum operating power	2.0 kW	Maximum operating power	2.0 kW

Next figure shows the inverter I-V curve at the temperature of 60 °C and 20 °C, respectively.

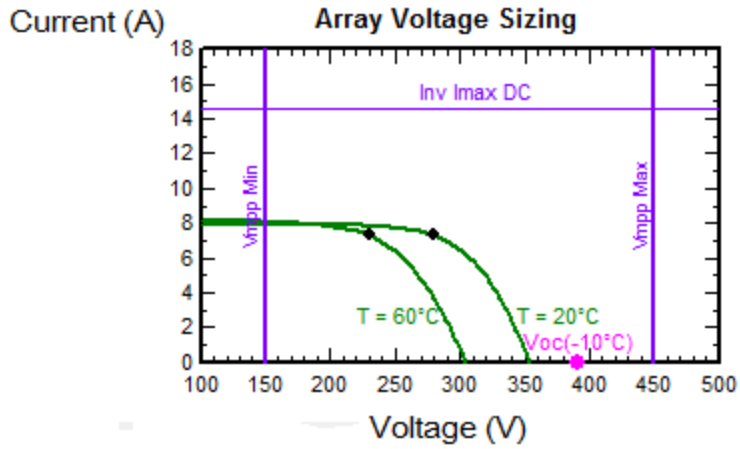


Figure 6. 1: Array voltages setting

The detailed losses are similar to the stand-alone system, however, the Ohmic loss is different, next figure shows the wiring loss parameter setting window:

DC circuit: ohmic losses for the array

Global wiring resistance	561.6	mOhm	<input type="checkbox"/> Calculated	<div style="border: 1px solid gray; padding: 2px; display: inline-block;"> Detailed computation </div> <div style="border: 1px solid gray; padding: 2px; display: inline-block; width: 20px; height: 20px; text-align: center; line-height: 20px;">?</div>
or in loss fraction at STC	1.5	%	<input checked="" type="checkbox"/> Default	
Voltage Drop across series diode	0.0	V	<input checked="" type="checkbox"/> Default	

Figure 6. 2: Array Ohmic loss for grid-connect system

Chapter seven: Simulation using PVsyst

7.1 Simulation process

After completing the system configuration and make sure all the parameters are set properly for the project. Simulation can run in different ways. The simulation dates are based on the meteorological data when defining the project and is limited in a certain period selected by user. There are about fifty variables calculated during simulation, they are classified into several categories according to their characteristics. The simulation process allows performing variables in monthly, daily and hourly values, but hourly results are not available for all variables. For a particular variable that is desired to show the hourly data, user can choose it before simulation and add it into the lists of hourly data storage. Or the user can define the graphs with variables of x and y axis.

The program will firstly simulate the irradiance, including effective global irradiance, array virtual energy at MPP. In the simulation process the factors that affect the final results are calculated simultaneously like diffuse and albedo attenuation factor for irradiance and array temperature for energy at MPP.

The procedures above are the common steps for all kinds of systems, and then PVsyst will do the simulation process and variables according the system type. For stand-alone system, the program will deal with array production, battery and user consumption simultaneously. The current is a function of voltage for each component:

a. PV array: consider the I-V curve of the module; the Ohmic loss, module quality and mismatch loss also affect the current.

b. Battery: voltage characteristics of the battery depend on state of charge, temperature and current.

c. Loads: the current is a function of voltage for the given energy consumption.

After the current is determined, state of charge and battery voltage is calculated at the end of time interval. Besides, the system performance is affected by charge controller.

The variables are mainly PV array behavior and battery operation.

For grid-connected systems, the simulation will take inverter behavior into consideration for different situation:

a. The array maximum power output does not reach the threshold of the inverter, the array is considered as open circuit.

b. The inverter output power is greater than its nominal power; it will either limit the current or cut the inverter input according to the inverter definition.

c. When the MPP voltage reaches the maximum or minimum voltage of the inverter I-V curve, it stays at that point.

d. In normal conditions, the array operates at maximum power point as well as the inverter input energy, the output energy is computed according to its efficiency curve.

For each case above the energy loss is calculated separately. Then for user defined loads, the energy consumption is done. The variables mainly calculated in the simulation and shown in the result are PV array and inverter behavior, energy output and use.

7.2 Results

The simulation results can be displayed comprehensively through PVsyst; it creates a report which includes the main results, the variables are available as monthly values, some of them can be defined as in hourly or daily values before the simulation.

7.2.1 Stand-alone system results

In stand-alone system simulation, the system performance is mainly focused on battery characteristics, array output and energy usage. The stand-alone system is described in chapter 5; the meteorological data for the location of Denver is listed in the table:

Table7. 1: Meteorological and irradiation data

	Horizontal global irradiation (kWh/m ²)	Horizontal diffuse irradiation (kWh/m ²)	Ambient temperature (°C)	Wind velocity (m/s)	Incident global irradiation (kWh/m ²)	Incident diffuse irradiation (kWh/m ²)
January	77.6	22.88	0.79	3.8	133.1	28.43
February	88.7	31.03	-0.05	3.5	128.6	34.60
March	144.4	42.56	6.13	4.4	180.1	44.92
April	143.6	60.54	5.83	5.3	154.2	59.05
May	196.1	73.09	15.49	3.8	192.3	69.06
June	218.0	62.98	23.10	3.4	205.1	58.44
July	208.2	68.17	22.27	3.0	198.9	63.80
August	185.7	61.18	22.61	4.5	192.4	59.45
September	155.3	48.51	19.16	4.1	181.8	50.05
October	114.2	34.81	10.04	3.8	157.9	38.95
November	73.9	29.16	2.9	4.2	117.3	34.05
December	64.4	21.54	1.43	3.2	114.6	26.76
Year	1670.2	556.45	10.88	3.9	1956.2	567.56

Table7. 2: Battery bank performance:

	Average battery voltage	SOCmean	EffbatI %	EffbatE %
January	50.7	0.818	91.2	83.2
February	50.8	0.853	92.0	89.3
March	51.0	0.875	90.5	84.2
April	50.8	0.851	91.3	92.7
May	51.3	0.891	86.3	78.1
June	51.4	0.900	85.2	78.6
July	51.2	0.889	87.2	83.2
August	51.2	0.888	87.5	82.8
September	51.4	0.901	83.2	76.8
October	50.8	0.844	92.1	90.9
November	50.4	0.770	93.4	88.2
December	50.6	0.811	93.1	94.8
Year	51.0	0.858	89.3	84.9

SOCmean: average state of charge

EffbatI: battery current charge/discharge efficiency

EffbatE: battery energy charge/discharge efficiency

The battery voltage is affected by temperature; it rises with increasing temperature and drops down when temperature decreases. The battery state of charge also reduces in low temperature.

Table 7.3 shows the system energy production and consumption:

Table7. 3: system energy production and consumption

	E array (kWh)	E avail (kWh)	E user (kWh)	E load (kWh)	I user (Ah)
January	160.0	266.6	101.3	101.3	1970.6
February	153.3	273.5	91.5	91.5	1766.2
March	210.7	381.5	101.3	101.3	1947.4
April	190.2	337.9	98.0	98.0	1887.0
May	226.2	408.6	101.3	101.3	1937.5
June	210.4	426.7	187.9	187.9	3675.2
July	233.8	410.0	194.2	194.2	3784.4
August	225.4	403.1	194.2	194.2	3792.3
September	209.1	385.7	98.0	98.0	1881.4
October	187.3	337.0	101.3	101.3	1954.0
November	138.2	243.5	98.0	98.0	1905.7

December	133.5	225.7	101.3	101.3	1971.2
Year	2278.0	4099.8	1468.4	1468.4	28472.9

E array: effective energy at the output of the array

E avail: produced available solar energy

E user: energy supplied to the user

E load: energy need of the load

I user: current supplied to the user in Ah.

From the table above the energy produced by PV array is sufficient to meet the demand of the loads for the entire year, for the design is based on the critical operating condition month. And the capacity for the month from June to August is higher than other months because of the use of air conditioner.

The loss diagram gives a detailed illustration of the quality of the system design by defining the main sources of loss. The loss diagram can be shown as a whole year or individual month. The loss calculation begins with the array nominal energy which is derived from global effective radiation and array MPP efficiency at standard test condition. Then different kind of loss is taken into consideration according to system type. There are common losses exist, while in stand-alone system the diagram gives detailed battery use illustration. Each loss is defined as a percentage value of the previous energy.

Some losses are impossible to calculate accurately, for instance the Ohmic loss in stand-alone system is obtained using the relation $P_{Loss}=R \cdot I^2$. In practical the array resistance modifies the array operating point and the whole circuit equilibrium, so more accurate calculation will simulate the system with and without the resistance, and compare the difference. However this method also causes some error. The loss

diagram for the stand-alone project is shown in figure

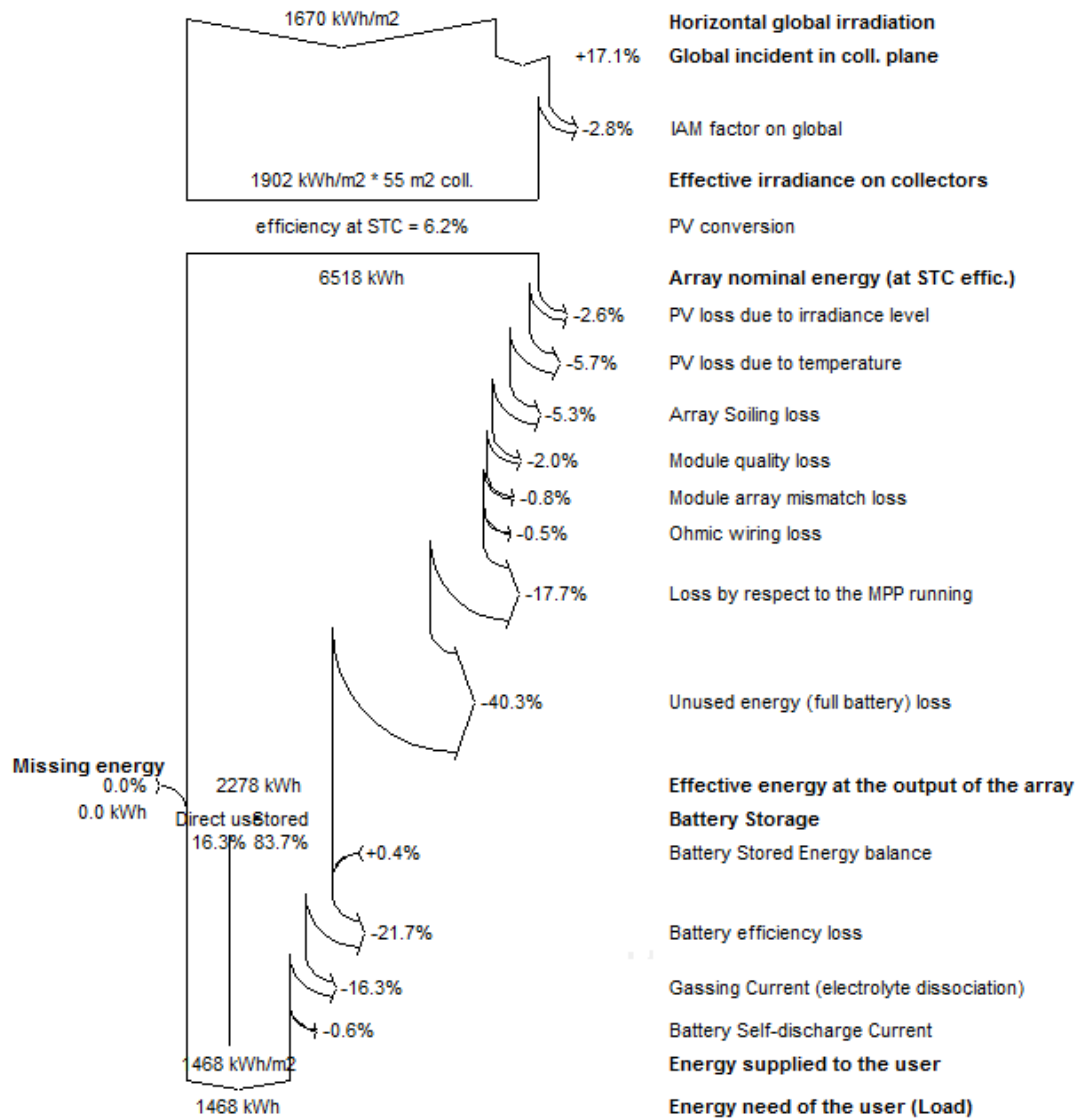


Figure7. 1: loss diagram of stand-alone system

The array nominal energy is 6518 kWh, and then it calculates different kinds of losses according to the values set in the loss configuration. The design is on the critical month and therefore the battery has to be selected with enough capacity to meet the loads needs and autonomy, so the unused energy loss in the diagram takes large amount. And at last the energy to the loads is 1468 kWh indicates that the whole system has an efficiency of 22.5%.

The results can be shown in the form of graphs divided into different kinds for display such as: meteorological and irradiation data, PV array behavior, battery operation and system operating conditions. Each of them has further detailed information as results.

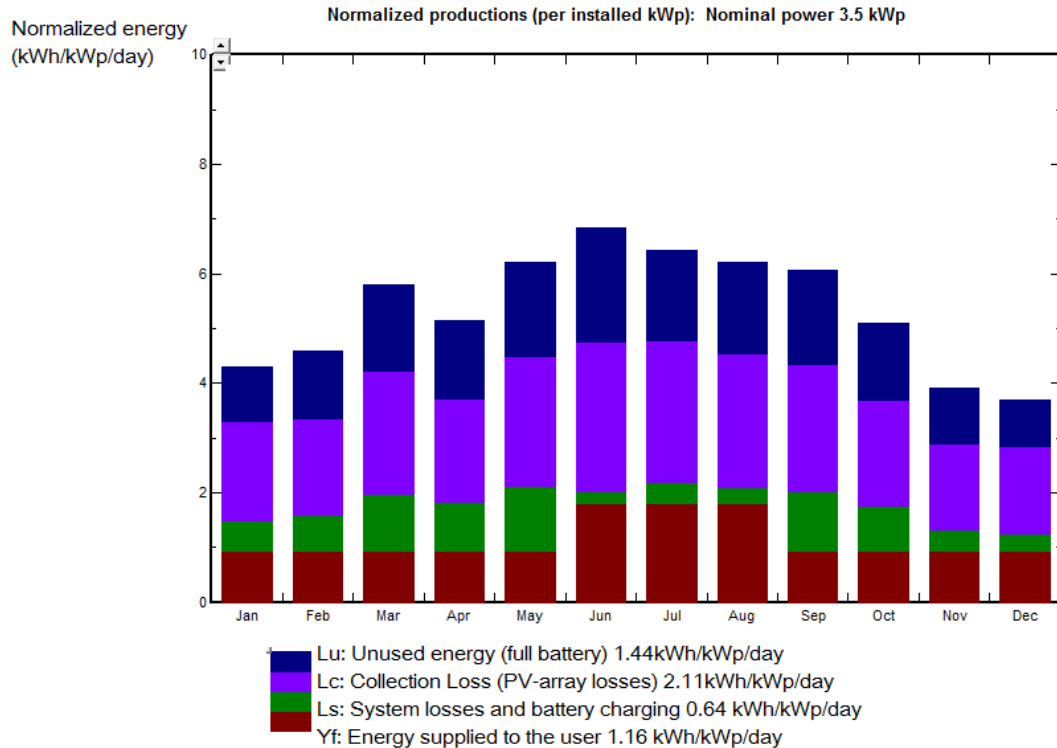


Figure7. 2: normalized productions of the stand-alone system

7.2.2 Grid-connected system simulation results

The simulation process and results of grid-connected system are similar to stand-alone system, however, instead of battery bank, an inverter analysis is run by the program.

Table7. 4: Inverter performance

	EoutInv (kWh)	EffinvR (%)	InvLoss (kWh)	IL Oper (kWh)
January	226.8	94.5	13.09	13.09
February	212.2	94.4	12.64	12.62
March	277.9	94.4	16.48	16.46
April	226.0	93.8	14.86	14.86
May	262.9	94.2	16.32	16.31
June	263.4	94.3	15.93	15.93
July	256.9	94.2	15.96	15.96
August	256.8	94.4	15.32	15.30
September	255.5	94.6	14.69	14.66
October	243.5	94.6	13.96	13.93
November	194.7	94.5	11.47	11.46
December	193.3	94.2	11.81	11.80
Year	2869.9	94.3	172.52	172.39

EoutInv: available energy at inverter output

EffinvR: inverter efficiency

InvLoss: global inverter losses

IL Oper: inverter loss during operation

The energy produced by PV array is delivered into the inverter and then becomes AC power. The energy and the inverter output increases with the irradiation collected by PV panels. The efficiency stays nearly the same throughout the whole year. The loss variation is similar to energy output.

The loads energy consumption of the grid-connected project is displayed below.

Table7. 5: Energy yield of grid-connected system

	E Avail (kWh)	E Load (kWh)	E User (kWh)	E_Grid (kWh)	SolFrac
January	177.4	194.2	56.11	177.4	0.289
February	165.5	175.4	54.96	165.5	0.313
March	217.1	194.2	67.10	217.1	0.346
April	175.6	187.9	64.77	175.6	0.345
May	197.8	194.2	74.74	197.8	0.385
June	199.3	187.9	72.86	199.3	0.388
July	190.5	194.2	74.66	190.5	0.384
August	196.7	194.2	69.72	196.7	0.359
September	197.2	187.9	66.15	197.2	0.352
October	190.9	194.2	59.85	190.9	0.308
November	149.8	187.9	51.49	149.8	0.274
December	149.0	194.2	52.19	149.0	0.269
Year	2206.8	2286.0	764.48	2206.8	0.334

E Avail: available solar energy

E Load: energy need of the user

E User: energy supplied to the user

E_Grid: energy injected to the grid

SolFrac: solar fraction ($E_{\text{User}}/E_{\text{Load}}$)

The table above shows that the not all energy produced by PV array are used by loads, some of them are transmitted into power grid, however, the rest of the energy is not enough for the loads needs so the grid also need to supply power to the loads. The reason is that at daytime the array produce more energy than loads need so the extra energy should be delivered into grid instead of storing in battery bank as stand-alone system, while in the evening the user's needs rises to a high level but the

array stop working and there is no battery to support the system, so the grid needs to power the system.

The efficiency of the system is shown in table 7.6:

Table 7. 6: System efficiency

	EffArrR (%)	EffSysR (%)
January	5.17	3.82
February	5.16	3.80
March	5.00	3.69
April	4.97	3.62
May	4.54	3.24
June	4.54	3.17
July	4.56	3.30
August	4.56	3.30
September	4.62	3.37
October	4.86	3.61
November	5.10	3.70
December	5.10	3.71
Year	4.83	3.51

EffArrR: Array Efficiency: Array energy/rough area

EffSysR: System efficiency: inverter output energy/rough area

The array efficiency trends is opposite compared with the energy production, it is higher at winter months and lower in the summer, the reason is high temperature in summer will reduce the module performance. The PV module which is made by polycrystalline has a lower efficiency than single crystalline, but the cost is less expensive.

The loss diagram of the system:

Loss diagram for "Denver_GridConnected_Project" - year

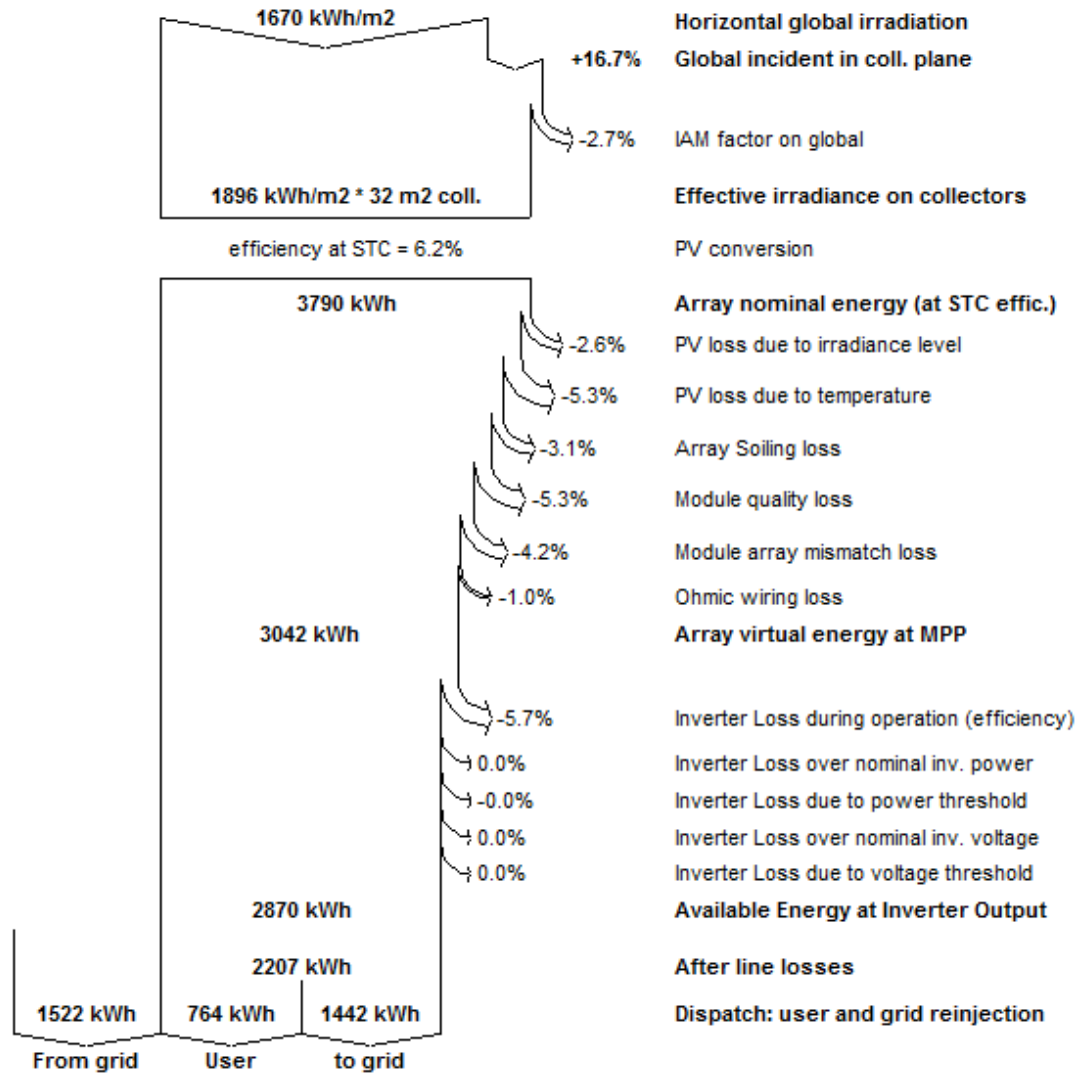


Figure 7. 3: loss diagram of grid-connected system

The loss diagram contains all the losses that may exist in the whole process, the loss factors are summarized according to each procedure; the final energy produced by the array is 2207 kWh. However, due to the loads distribution, only 764 kWh is used by the loads and 1442 kWh is transferred into grid. In peak hours the grid will provide 1522kWh for the loads running normally.

The normalized productions graph is shown below:

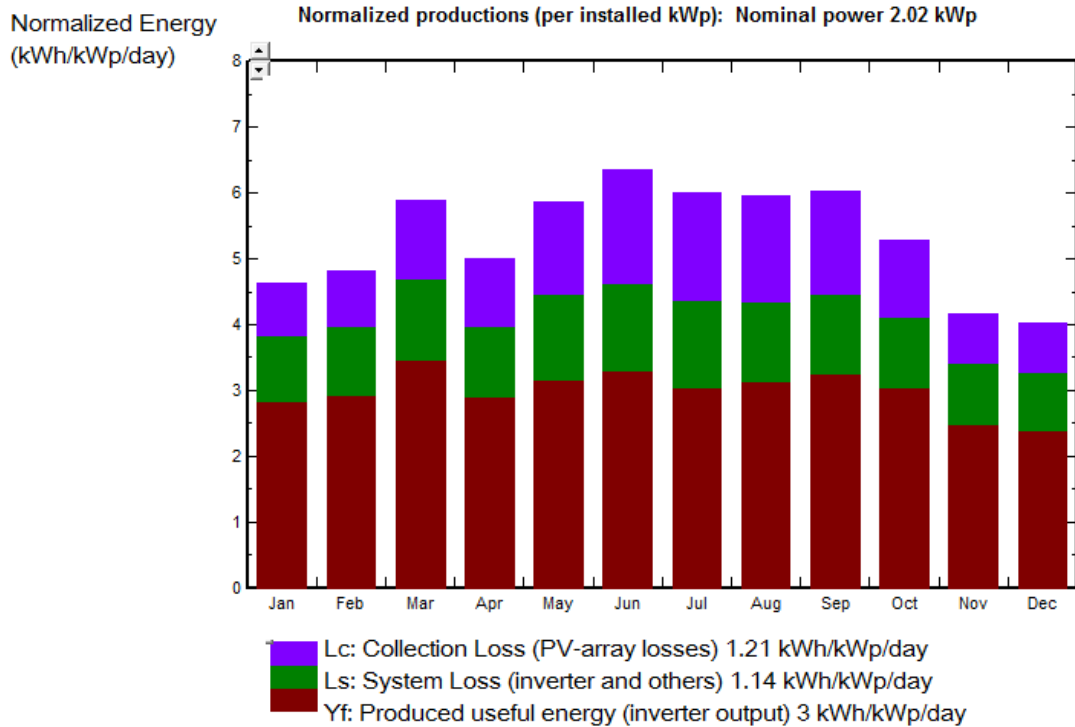


Figure 7. 4: Grid-connected system normalized production

The above figure is a graphical expression of the system energy yields. It shows the system losses including PV array loss and other losses, the inverter output energy are also shown at the bottom of the histogram.

In figure 7.2 and 7.4, the yield energy is expressed as kWh/kWp/day, it is an indicator related to the incident energy on the collector, and normalized by array nominal installed power at standard test conditions for the convenience of comparison between different systems. Next two tables show this normalized system performance for both stand-alone system and grid-connected system.

Table7. 7: Stand-alone system normalized performance coefficients

	Yr (kWh/m ² /day)	Lu	Lc	Ya (kWh/kWp/day)	Ls	Yf (kWh/ kWp/d ay)	PR
January	133.06	1.178	2.798	1.24	0.548	0.95	0.220
February	128.57	1.329	3.008	1.33	0.639	0.95	0.206
March	180.13	1.763	3.844	1.68	1.021	0.95	0.162
April	154.21	1.440	3.306	1.49	0.888	0.95	0.184
May	192.33	1.855	4.093	1.80	1.166	0.95	0.152
June	205.07	2.133	4.806	1.98	0.218	1.81	0.265
July	198.88	1.757	4.233	1.86	0.370	1.81	0.282
August	192.38	1.706	4.102	1.80	0.292	1.81	0.292
September	181.79	1.853	4.043	1.75	1.071	0.95	0.156
October	157.92	1.515	3.346	1.47	0.802	0.95	0.186
November	117.32	1.104	2.578	1.13	0.387	0.95	0.242
December	114.59	1.045	2.451	1.07	0.300	0.95	0.256
Year	1956.25	1.558	3.554	1.55	0.642	1.16	0.217

Yr: reference system yield, is the ideal array yield without any loss. It represents the one kWh incident energy produces the array nominal power.

Ya: array yield, the array daily output

Yf: system yield, the system daily useful energy

Lc: collection loss, it is equal to $Y_r - Y_a$ and is the array losses including thermal, wiring, module quality, mismatch and IAM losses.

Ls: System loss which is the battery inefficiencies in stand-alone system.

PR: performance ratio, $PR = Y_f / Y_r$, it is the global system efficiency.

For stand-alone system, unused energy (Lu), the energy cannot supply to the user because full battery.

Table7. 8: Grid-connected system normalized performance coefficients

	Yr (kWh/kWp/day)	Lc	Ya (kWh/kWp/day)	Ls	Yf (kWh/kWp/day)	PR
January	143.70	0.797	2.30	0.999	2.84	0.612

February	134.86	0.833	2.39	1.051	2.93	0.609
March	182.38	1.174	2.92	1.235	3.47	0.591
April	150.23	1.025	2.48	1.080	2.90	0.580
May	181.78	1.396	3.91	1.303	3.16	0.540
June	190.69	1.738	3.15	1.322	3.30	0.519
July	186.18	1.640	2.98	1.319	3.05	0.507
August	184.75	1.607	2.96	1.206	3.15	0.528
September	181.00	1.566	2.99	1.207	3.26	0.540
October	163.85	1.167	2.62	1.065	3.05	0.578
November	125.21	0.764	2.07	0.933	2.48	0.593
December	124.49	0.734	1.99	0.898	2.38	0.594
Year	1949.12	1.206	2.65	1.135	3.00	0.562

Chapter eight: Economic analysis

PV systems are often considered as a clean energy solution which is friendly to environment; however, on the other hand, PV systems are also valuable in financial issues. With effective design and operation, a PV system may pay back its investment and have further profit. Some PV systems have lower cost than other type of generations. To decide the cost and value of a PV system, an economic analysis is conducted by designers.

8.1 Cost analysis

A cost analysis involves both the cost and value. The financial cost is not the only factor though. Other factors include lifetime, availability, practicality and ease of use all contribute to the feasibility of a system. So the cost analysis will take as many factors into consideration as possible although some of them are difficult to quantify. When analyzing PV systems a life-cycle cost [22] is usually used. It is the total cost of all expenses from the design of the system until the end of its life. It gives the detailed fees for every stage of the system installation and operation. Some factors are easy to quantify like the price of system components while others are not and can only be estimated such as system installation cost.

It is better to do life-cycle cost analysis before the system design because through the results designer can get a depth of understanding of how to choose the system type, do the configurations and select appropriate components. So the purpose of getting maximum value and minimum costs can achieve. Sometimes this is done after the system installation, the advantage of doing analysis after the project is that the cost of system installation and components are determined so the results are more accurate than pre-analysis. And the exact experience can be used for future work such as replacement.

8.1.1 Initial costs

Financial costs include initial costs, maintenance costs, repair costs and replacement costs. At the end of a system life salvage value is considered.

Initial cost involves the stage of design, engineering, devices and installation of the PV system. The prices of equipments are obtained from manufacturer or sellers. Labor costs for design, engineering and installation should be estimated. The different cost between a system that is installed by self and a system that requires professional installation should also be noticed. Other charges may come from the transportation of the devices. Then the total cost is thought to be the initial cost at the beginning of life of the system.

8.1.2 Maintenance costs

Maintenance costs are created during the operation period of the system; it includes system monitoring, cleaning, insurance, property taxes and operator salaries. The fuel for hybrid system and replacement costs is not included. Maintenance costs appear periodically during the life of the PV system so they can be summarized as an annual fee.

8.1.3 Energy costs

The energy cost is the input energy costs used to produce electricity in an electric generation. The fuel type depends on the generators. For PV system, the cost solar radiation does not exist.

8.1.4 Repair and replacement costs

If one or several of the system components is damaged or malfunction, it has to be repaired to continue work normally. In most times it is hard to predict which part of the system will have failure, so the repair costs are often estimated a value and added together with replacement cost. The repair budget may include the fuses, mounts and modules renovate expenses. Replacement cost is the cost of changing a new device instead of an old one which has a shorter life than the entire PV system design life. For instance, in stand-alone system, the batteries usually can use for three to five years, while the whole system is designed to run 15 to 20 years. So the batteries will need to be replaced for several times during this period.

8.1.5 Salvage value

The salvage value is the money value of the PV system at the end of its life. Usually a 20% value of the original price of the system movable components is set for salvage value. [22] This number can be adjusted according to specific system condition.

8.2 Life-cycle cost analysis

To calculate the life-cycle cost analysis, all kinds of cost should be added together and subtract the salvage value at last. The result can be expressed as follows:

$$LCC = I + M_{PV} + E_{PV} + R_{PV} - S_{PV} \quad (8-1)$$

Where LCC is the life-cycle cost, I is the initial cost, M_{PV} is the maintenance cost, E_{PV} is the energy cost, R_{PV} is the repair and replacement cost and S_{PV} is the

salvage value. Then the life-cycle cost of stand-alone system and grid-connected system can be calculated by using the formula.

For stand-alone system, the prices of system components and other fees are listed in the table below, based on a 20 year life usage:

Table8. 1: Life-cycle costs of stand-alone system

Initial costs	Battery	Price
	Surette S-460 (16)	\$4880
	PV Module	Price
	Sharp ND-72 ELU (48)	\$22848
	Charge controller	price
	Xantrex	\$124
Maintenance costs		\$1000
Repair and replacement costs	Battery bank replacement	\$14640
	Charge controller replacement	\$124
Salvage value		-\$2785
Life cycle costs		\$40831

The single battery price for Surette S-460 is 305 dollars, in the stand-alone system the battery bank consists of 16 batteries so the price is $305 \times 16 = 4880$ dollars. The price for one piece of Sharp ND-72 ELU module is 476 dollars, 48 modules are used in the project with a price of 22848 dollars. The maintenance cost for each year is estimated for 50 dollars each year and 1000 dollars for 20 years. The designed battery life time is 5 years, and they need to be replaced at the year of 5, 10 and 15. The charge controller should be replaced at the year of 10. The salvage value is estimated about 10% of system initial cost which is 2785 dollars. So the total life

cycle cost will be 40831 dollars.

The life cycle cost of grid-connected system is similar. In the initial costs inverter are instead of battery bank. Next table shows the items:

Table8. 2: life cycle costs of grid-connected system:

Initial costs	PV Module	Price
	Sharp ND-72 ELU (28)	\$13328
	Inverter	Price
	GE PVIN02KS	\$1954.34
Maintenance costs		\$1000
Repair and replacement costs	Inverter replacement	\$2000
Salvage value		-\$1528
Life cycle costs		\$16754.34

Comparing the results, the grid-connected system is less cost than stand-alone system because batteries are not used. However, grid-connected system will need to connect with grid utilities and limits the practical application of grid-connected system. Although stand-alone system costs more, it will be an ideal choice for remote areas for its independence.

In practical use, the performance of a photovoltaic system will be affected by real weather, load usage and other unpredictable events, the economic analysis is then not accurate, and so to better evaluate the system cost and investment, we use software called System Advisor Model to do the economic analysis. System Advisor Model is designed to do the construction and evaluation of renewable energy project and industry which is developed by NREL. The built model can calculate the cost of the electricity based on the information of project location, technology type and financial option.

8.3 Economic evaluations by using SAM (System Advisor Model)

The current version of System Advisor Model can only provide grid-connected type system analysis. To get started for a new system, there are some input pages with different topics for user to configure. They are climate, financing, annual performance, PV system costs, PVWatts solar array and electric load. As the same grid-connected system, the climate conditions is still set at Denver, SAM can automatically search and get the weather information after the user chooses the location of the project.

8.3.1 Financing settings

The input variables of financing settings include analysis period, inflation rate and real discount rate. The analysis period is the life of the project, we set it 20 years. Inflation rate is the annual rate of change of prices, typically based on a price index. SAM uses the inflation rate to calculate the value of costs in years two and later of the project. Real discount rate is a measure of the time value of money expressed as an annual rate. It is used to calculate the present value of dollar amounts in the project. The values of these rates are set in the figure below:

General	Taxes and Insurance
Analysis Period <input type="text" value="20"/> years	Federal Tax <input type="text" value="28.00"/> %/year
Inflation Rate <input type="text" value="2.50"/> %	State Tax <input type="text" value="7.00"/> %/year
Real Discount Rate <input type="text" value="10.80"/> %	Property Tax <input type="text" value="0.00"/> %/year
Nominal Discount Rate <input type="text" value="13.57"/> %	Sales Tax <input type="text" value="0.00"/> %
Salvage Value	Insurance <input type="text" value="0.00"/> %
Net Salvage Value <input type="text" value="10.00"/> % of Installed Cost	
Present Value <input type="text" value="\$ 2,233.76"/>	

Figure8. 1 Financing setting page

The salvage value is still set to be ten percent of the initial cost. Besides, SAM also lists some tax options including federal and state tax.

8.3.2 Annual system performance

Annual system performance contains system degradation and availability. System degradation represents the system annual output reduction due to the aging equipments. If the degradation rate is one percent, the power output of the system from the year two will be 99% of the previous year. The availability accounts for downtimes due to forced and scheduled outages. The default value of 100% for photovoltaic systems results in no reduction in output.

8.3.3 PV system costs

A PV system cost gives user access to define the installation and operation costs of the photovoltaic project. The cost is further divided into direct cost and indirect cost. Direct cost represents the expense of the system components while indirect cost is mainly the fees that are difficult to get a specific value. For grid-connected system the direct costs are module and inverter, balance of system and installation costs. An indirect cost is classified as engineer, procure and construct which is the cost of as design and construction. Also we need to decide the operation and maintenance costs, it can be input in three ways: fixed annual, fixed cost by capacity, and variable cost by generation. The total initial costs and maintenance cost is shown in the figure below:

Direct Capital Costs						
Module	1 units	1.8 kWdc/unit	1.828 kWdc	\$ 2.31	\$/Wdc	\$ 4,222.68
Inverter	1 units	1.4 kWac/unit	1.40756 kWac	\$ 0.72	\$/Wac	\$ 1,013.44
Balance of System, Fixed	\$ 0.00	\$ 1.31	\$/W	\$ 0.00	\$/m2	\$ 2,394.68
Installation, Fixed	\$ 0.00	\$ 1.06	\$/W	\$ 0.00	\$/m2	\$ 1,937.68
Contingency					0 %	\$ 0.00
Total Direct Cost						\$ 9,568.48

Indirect Capital Costs				
	% of Direct Cost	Non-fixed Cost	Fixed Cost	Total
Engineer, Procure, Construct	0 %	\$ 0.00	\$ 1,400.00	\$ 1,400.00
Project, Land, Miscellaneous	0 %	\$ 0.00	\$ 0.00	\$ 0.00
Sales Tax of	0 %	applies to 100 % of Direct Cost		\$ 0.00
Total Indirect Cost				\$ 1,400.00

Total Installed Costs	
Total Installed Cost	\$ 10,968.48
Total Installed Cost per Capacity (\$/Wdc)	\$ 6.00

Figure 8. 2 PV system costs setting page

Operation and Maintenance Costs		
First Year Cost		
Fixed Annual Cost	Value Solved	200.00 \$/yr
Fixed Cost by Capacity	Value Solved	25.00 \$/kW-yr
Variable Cost by Generation	Value Solved	0.00 \$/MWh

Figure 8. 3 Operation and maintenance costs

From the figure, it is concluded that the total initial cost is \$10968.48.

8.3.4 Solar array inputs

The system inputs define the size of the system, derate factor and array orientation, these items are the same as they are made before.

8.3.5 Electric load

Similar to the array settings, the load in SAM should follow the results obtained in previous chapter.

8.4 economic results

On the result page, SAM provides table and graphs for cash flow and energy usage. The main parameters include cash flow year, energy, and operating and maintenance costs.

Table8. 3 Results of the PV system simulation

Year	Energy(kWh)	Energy value (\$)	Fixed operating and maintenance annual (\$)	Fixed operating and maintenance (\$)	Operating costs (\$)
1	3751	900.29	200	45.7	245.7
2	3732	918.18	205	46.84	251.84
3	3714	936.43	210.12	48.01	258.14
4	3695	955.04	215.38	49.21	264.59
5	3677	974.02	220.76	50.44	271.21
6	3658	993.38	226.28	51.71	277.99
7	3640	1013.12	231.94	53	284.94
8	3622	1033.26	237.74	54.32	292.06
9	3604	1053.80	243.68	55.68	299.36
10	3586	1074.74	249.77	57.07	306.85
11	3568	1096.10	256.02	58.5	314.52
12	3550	1117.89	262.42	59.96	322.38
13	3532	1140.10	268.98	61.46	330.44
14	3515	1162.76	275.7	63	338.7
15	3497	1185.87	282.59	64.57	347.17
16	3479	1209.44	289.66	66.19	355.85

17	3462	1233.48	296.9	67.84	364.74
18	3445	1258	304.32	6954	373.86
19	3428	1283	311.93	71.28	383.21
20	3410	1308.50	319.73	73.06	-1360.69
					4522.86

The table above shows the energy and maintenance cost for each year during the 20 year lifetime of the system. The power output gradually drops due to the aging of the system. The fixed operating fees is becoming higher each than before because of the inflation. On the twentieth year the negative cost is due to the salvage value. The initial install cost calculated before is 10968.48 dollars, the operating and a maintenance cost is 4522.86 dollars. So the total cost for this grid-connected system should be 15491.34 dollars. This result is less than the cost analysis derived before, because the price of module and inverter may be from a different source. Next figure shows the costs in different kinds.

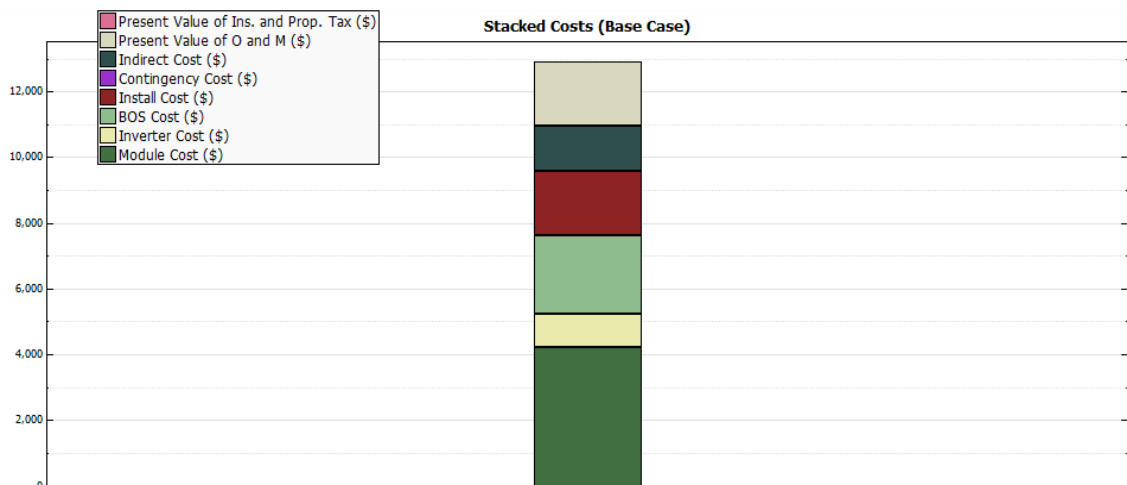


Figure8. 4 The total cost of a PV system

From the figure above, we can see that the system components including module, inverter and other BOS costs take main part of the total costs. After the installation is completed, the yearly operating and maintenance cost only take

relatively small part of the total costs.

Chapter nine: Conclusion

Photovoltaic technology has been thought as one of the main renewable energy source in the near future. The research of photovoltaic systems is developing fast in recent years with the increasing concern of traditional fossil fuel and environmental issues. Some applications have been put into use in several countries and more are in planning and building. Although it is developing fast, the electricity generated by solar energy still only takes a small percentage in the world's energy distribution. So the prospect of photovoltaic system is enormous.

Geographical information system can be used in the pre-feasible study of a photovoltaic system design. With the meteorological data collected from different ways the analyzers can get immediate weather information and long term climate conditions in order to determine whether solar energy solution is available. GIS can further provide terrain and topography data for the type selection of the system. In mountainous areas, the shading effects cannot be neglected. By using GIS designers can get an idea of how the shadings affect the system. Usually for photovoltaics systems solar resource distribution maps are generated for research. They can be yearly, monthly or seasonally. Through GIS analysis it is better for the preliminary stage such as site selection and some mounting parameters.

Choosing the type of system depends on the location. Stand-alone system is used for remote areas or the areas away from the grid. For this kind of system, because solar radiation is not available during night time, it is necessary to install a battery bank for the loads otherwise the loads will not work. The sizing of a stand-alone system mainly depends on the loads energy consumption. The battery bank capacity determination is affected by some other factors like autonomy and in the case of damage of PV array. For a designed area, to guarantee the system can meet the loads demand, critical design month is used for sizing the system. It is the worst case scenario in all months. Since the system is designed to meet the energy consumption in this month, it will work normally all over the year.

The sizing of grid-connected system is not complicated as stand-alone systems because it is interactive with the grid and if there is failure of the PV system the loads can still be powered by grid utility. While in the case of the energy produced by PV array exceeds loads demand, the system can transmit extra energy into power grid. So the battery bank is not used in grid-connected any more. Both of the systems have wide range of applications like transmission tower beacons, street and security lighting and water pumping.

The photovoltaic simulation software of PVsyst is used to get a comprehensive study of the PV systems. It can build the different projects as the user's requirement. In this study the stand-alone system and grid-connected system are built at the location of Denver, Colorado. The climate data is obtained from the typical meteorological year 3 developed by NREL. The system components and sizing are designed and calculated according to common household energy

consumption. The advantage of PV system compared with other kind sources is that after the initial investment there is no other costs except equipment replacements. And usually the system is designed to run at least 20 years. But the initial cost is rather high and for stand-alone systems the battery need to be replaced every five to seven years.

In the project design there is still some work can be improved, for example, the near shading effects are not considered in the building. The shading effects not only affect solar radiation in mountainous areas, some objects like trees and buildings also have similar influence. In stand-alone system project, in order to meet the critical design demand, the PV array and battery bank is designed with large production and capacity, so it will produce extra energy which cannot be stored in the battery and thus the costs more and waste of energy. It should be solved by better coordinate the loads demands and battery bank.

Reference:

- [1] NREL GIS, Solar Maps, U.S. Solar resource maps, <http://www.nrel.gov/gis/solar.html>
Last access 3-20-2011
- [2] Stuart R. Wenham, Martin A. Green, Muriel E. Watt and Richard Corkish, “applied PHOTOVOLTAICS” Second edition, Earthscan, 2007
- [3] C. Honsberg, Solar Electric Systems, University of Delaware, ECE Spring 2008,
http://www.cis.udel.edu/~honsberg/Eleg620/02_Solar_radiation.pdf Last access 4-1-2011
- [4] **Murat Kacira, Mehmet Simsek, Yunus Babur and Sedat Demirkol**, Determining optimum tilt angles and orientations of photovoltaic panels in Sanliurfa, Turkey, [Renewable Energy](#) , [Volume 29, Issue 8](#), July 2004, Pages 1265-1275
- [5] Solar power astronomy, http://www.mpoweruk.com/solar_power.htm last access 4-5-2011
- [6] Solar radiation estimation and site analysis, <http://www.pyresources.com/en/location.php>
last access 4-7-2011
- [7] RETScreen ENGINEERING & CASES TEXTBOOK, PHOTOVOLTAIC PROJECT ANALYSIS

- [8] B. Y. H. Liu and R. C. Jordan, The Interrelationship and Characteristic Distribution of Direct, Diffuse, and Total Solar Radiation. *SOLAR ENERGY* 4, 1-19 (1960).
- [9] Scharmer, K., and J. Greif. 2000. European Solar Radiation Atlas: fundamentals and maps, Ecole des Mines de Paris, Paris. <http://catalog.ensmp.fr/Files/ESRA11res.pdf> last access 5-10-2011
- [10] M. ˇ Súrı and J. Hofierka, “A new GIS-based solar radiation model and its application to photovoltaic assessments,” *Trans. GIS*, vol. 8, no. 2, pp. 175–190, Apr. 2004.
- [11] M. ˇ Súrı, T. Huld, and E. D. Dunlop, “PV-GIS: A web based solar radiation database for the calculation of PV potential in Europe,” *Int. J. Sustainable Energy*, vol. 24, no. 2, pp. 55–67, Jun. 2005.
- [12] <http://re.jrc.ec.europa.eu/pvgis/solres/solrespvgis.htm> last access 1-19-2011
- [13] Marcel S ˇ u ´ ri , Thomas A. Huld, Ewan D. Dunlop, Heinz A. Ossenbrink , “Potential of solar electricity generation in the European Union member states and candidate countries”, *Solar Energy* 81 (2007) 1295–1305
- [14]T. G. Farr *et al.*, “The shuttle radar topography mission,” *Rev. Geophys.* vol. 45, no. RG2004, pp. 1–33, 2007 [Online]. Available: <http://www2.jpl.nasa.gov/srtm/> last access 4-9-2011
- [15] http://www.soda-is.com/eng/services/linke_turbidity_info.html last access 4-15-2011
- [16] L.Wald, M. Albuissou, G. Czeplak, B. Bourges, R. Aguiar,H. Lund, A. Joukoff, U. Terzenbach, H.-G. Beyer, and E. P. Borisenko, , J. Greif and K. Scharmer, Eds., *European Solar Radiation Atlas (ESRA)*, 4th ed. Paris, France: Presses de l’Ecole des Mines de Paris, 2000, Scientific Advisors: R. Dogniaux and J. Page.
- [17] “Meteorological data collection, processing and analysis,” in *Methodology of the Mars Crop Yield Forecasting System*, F. Micale and G. Genovese, Eds. Luxembourg: Office for Official Publications of the European Communities, 2004, vol. 1.
- [18]T. Huld, M. ˇ Súrı, and E. D. Dunlop, “Geographical variation of the conversion efficiency of crystalline silicon photovoltaic modules in Europe,” *Prog. Photovoltaic: Res. Appl.*, accepted for publication.
- [19]R. Meyer, S. Lohmann, C. Schillings, and C. Hoyer, “Climate statistics for planning and siting of solar energy systems: Long-term variability of solar radiation derived from satellite data,” in *Solar Energy Resource Management for Electricity Generation From Local to Global Scale*, E. D. Dunlop, L. Wald, and M. ˇ Súrı, Eds. New York: Nova, 2006, pp. 55–68.

- [20] PVsyst contextual help, User's guide, www.PVsyst.com last access 1-20-2011
- [21] Duffie, W. Beckman. Solar Engineering of thermal processes. John Wiley and Sons, Inc., New York, 2006.
- [22] Jonathan F. Gosse, Peter A. Zurlis, James M. Clarke "Photovoltaic Systems" National Joint Apprenticeship and Training Committee for the Electrical Industry, 2007
- [23] James P. Dunlop, P.E. Batteries and Charge Control in Stand-Alone Photovoltaic Systems Fundamentals and Application, January 15, 1997
- [24] NREL DC-AC derate factor
http://www.nrel.gov/rredc/pvwatts/changing_parameters.html last access 4-29-2011
- [25] National Solar Radiation Data Base, 1991- 2005 Update: Typical Meteorological Year 3,
http://rredc.nrel.gov/solar/old_data/nsrdb/1991-2005/tmy3/ last access 5-15-2011
- [26] http://rredc.nrel.gov/solar/old_data/nsrdb/1991-2005/tmy3/usTMYmaps3medium.gif
last access 4-29-2011
- [27] Average Power *Consumption* of Household Appliances,
<http://www.absak.com/library/power-consumption-table> last access 5-17-2011
- [28] Kimber, A. Mitchell, L. Nogradi, S. Wenger, H. PowerLight Corp., Berkeley, CA The Effect of Soiling on Large Grid-Connected Photovoltaic Systems in California and the Southwest Region of the United States , May 2006
- [29] <http://pvcrom.pveducation.org/MODULE/NOCT.htm> last access -5-23-2011
- [30] Hofierka J., Huld T., Cebecauer T., d'z' d'z'ri M., 2007. Open Source Solar Radiation Tools for Environmental and Renewable Energy Applications, International Symposium on Environmental Software Systems, Prague, 2007.
- [31] M., Kenny, R.P., Dunlop E.D., 2005. Estimating PV Performance Over Large Geographical Regions. Presented at the 31st IEEE Photovoltaic Specialists Conference and Exhibition, 3-7 January 2005, Coronado Springs Resort, Lake Buena Vista, Florida, USA
- [32] Dunlop E.D., Huld T.A., Ossenbrink H.A., 2006. Geographical Aspects of Solar Electricity Generation in Europe. In Dunlop E. D., Wald L., Suri M. (Eds.), Solar Energy Resource Management for Electricity Generation from Local to Global Scale. Nova Science Publishers, New York.
- [33] Kenny R.P., Huld T., Iglesias S., 2006. Energy rating of PV modules based on PVGIS irradiance and temperature database. Proceedings of the 21st

European Photovoltaic Solar Energy Conference and Exhibition, 4-8 October 2006, Dresden, Germany (preprint)

- [34] Dunlop E.D., Albuissou M., Wald L, 2006. Online data and tools for estimation of solar electricity in Africa: the PVGIS approach. Proceedings of the 21st European Photovoltaic Solar Energy Conference and Exhibition, 4-8 October 2006, Dresden, Germany (preprint, presentation)
- [35] Dunlop E.D., 2006. A GIS-Based System for Performance Assessment of Solar Energy Systems over Large Geographical Regions. Solar 2006 Conference: Renewable Energy, key to climate recovery, 7-13 July 2006, Denver CO, USA. (preprint)
- [36] Edwards R.A.H., d'z' d'z'ri M., Huld M.A., Dallemand J.F., 2005. GIS-Based Assessment of Cereal Straw Energy Resource in the European Union. Proceedings of the 14th European Biomass Conference & Exhibition. Biomass for Energy, Industry and Climate Protection, 17.-21. October 2005, Paris (preprint, presentation).
- [37] Dunlop E., 2005. Putting PV on the map ? internet tools for solar resource assessment in Europe. Renewable Energy World, March-April 2005, Earthscan/James & James.
- [38] Huld T.A., d'z' d'z'ri M., Dunlop E. D., 2003. GIS-based Estimation of Solar Radiation and PV Generation in Central and Eastern Europe on the Web. Proceedings of 9th EC-GI&GIS Workshop, A Coruña (Spain), 25-27 June 2003
- [39] d'z' d'z'ri M., 2002. Modeling and Cartographic Presentation of the Global Irradiation. In Feranec, J. Pravda J., eds. Proceeding of the workshop "Aktivity v kartografii 2002", Bratislava (Slovak Cartographic Society and Institute of Geography SAS), 31.10.2002, pp. 126-133
- [40] d'z' d'z'ri M., Dunlop E. D., Jones A. R., 2002. GIS-based inventory of the potential photovoltaic output in Central and Eastern Europe. Proceeding of the international conference "Photovoltaics in Europe. From Photovoltaic Technology to Energy Solutions", 7.-11.10.2002, Rome (Italy), pp. 1039-1042